MINISTRY OF PUBLIC WORKS

MINISTERE DES TRAVAUX PUBLICS

MINISTRY OF HIGHER EDUCATION

MINISTERE DE L'ENSEIGNEMENT SUPERIEUR

Ecole Nationale Supérieure des Travaux Publics

UNIVERSITÀ DEGLI STUDI DI PADOVA

DEPARTEMENT OF CIVIL ENGINERING

DEPARTEMENT DE GENIE CIVIL

DEPARTEMENT OF CIVIL, ARCHTECTURAL AND ENVIROMENTAL ENGINEERING

INFLUENCE OF RIGID AND NON-RIGID SLABS ON THE STRUCTURAL BEHAVIOR OF TALL BUILDINGS WITH IRREGULAR PLAN
CASE STUDY: G+5 STOREY BUILDING IN YAOUNDE MIMBOMAN

A thesis submitted in partial fulfilment of the requirement for the degree of Masters of Engineering (MEng) in Civil Engineering

Curriculum: Structural Engineering

Presented by:

KAM NOULA Steve Emmanuel

Student number: 15TP20962

Supervised by:

Prof. Carmelo MAJORANA

Co-supervised by:

Dr. Eng. Guillaume Hervé POH'SIE

Eng. Guiseppe CARDILLO

ACADEMIC YEAR: 2019/2020

DEDICATION

TO MY BELOVED PARENTS

AKNOWLEDGEMNTS

First of all, I thank the Almighty God for giving me the courage, strength and patience to complete this modest work. This work would not have been completed without the combined efforts of individuals who contributed directly and/or indirectly to its realization. I wish to express my sincere thanks and gratitude to:

- The President of the jury ;
- The Examiner of this jury for accepting to bring his criticisms and observations to ameliorate this work ;
- My supervisors Prof. Eng. Carmelo MAJORANA, Dr Eng. Guillaume Hervé POH'SIE, and Eng. Guiseppe CARDILLO for all the guidance and advices they provided me with, during this thesis work ;
- Professors George NKENG and Carmelo MAJORANA for all their academic and administrative support during these five years spent at ENSTP in the MEng program in partnership with University of Padua in Italy ;
- The vice-director of ENSTP, Dr M. BWEMBA Charles Loic for his perpetual help and advices during our sojourn in this school ;
- Prof. Michel MBESSA, the head of department of Civil Engineering for his tutoring and valuable advices ;
- All the teaching staff of ENSTP and University of Padua for their good quality teaching and the motivation they developed in us to continue our studies ;
- My family and more specially my father NOULA Camille and my mother BOUGA TCHUENKAM Carole, for the education and financial support during all these years;
- The group MATRICE for the presence since level one;
- All my classmates and all my friends who were a source of motivation and tenacity. As a team, together we have been able to achieve more.

GLOSSARY

ABBREVIATIONS

3D	Three Dimensional
CM	Centre of Mass
CR	Centre of Rigidity
EC	Eurocode
ETABS	Extended Three-dimensional Analysis Of Building Systems
FEMA	Federal Emergency Management Agency
IBC	International Building Codes
RC	Reinforced Concrete
SLS	Serviceability Limit State
SSI	Soil Structure Interaction
ULS	Ultimate Limit State
VLLRS	Vertical Lateral Load Resisting Systems

SYMBOLS

A	Area of the cross section
A_c	Area of the concrete cross section
A_s	Area of the lower steel reinforcement section
A_s'	Area of upper steel reinforcement section
$A_{s,max}$	Maximum steel reinforcement section area
$A_{s,min}$	Minimum steel reinforcement section area
A_{sw}	Cross sectional area of the shear reinforcement
D	Plate rigidity
E	Youngs modulus
$F_{ed,sup}$	Design support reaction
G_{1k}	Structural load of the building
G_{2k}	Non-structural load apply on the building
J_{cr}	Moment of inertia of the uncracked section
M_{ED}	Soliciting bending moment
M_{RD}	Resisting moment
Q_k	imposed load
S_e	Elastic response spectrum
T	Period of the structure with fixed base
T_B	Lower limit of the period of the constant spectral acceleration branch
T_C	Upper limit of the period of the constant spectral acceleration branch
T_D	Value defining the beginning the constant displacement response range of the spectrum
T_k	Period of vibration of mode k

V	Reduction factor
V_{ED}	Design shear value
V_{Rd}	Resisting shear
V_{rdc}	Shear capacity of concrete
ag	Design ground acceleration
b	Width of the element
b_t	Mean width of the tension zone
b_w	Smallest width of the cross section in the tensile area
c	Concrete cover
d	Effective height of the section
d_r	Design inter-storey drift
e_x	Eccentricity along x axis
e_y	Eccentricity along x axis
e_a	Accidental eccentricity
e_o	Structural eccentricity
f_{cd}	Design resisting strength of the concrete
f_{ctm}	Tensile strength of the concrete
f_{yd}	Design yielding strength of the steel
f_{yk}	Characteristic yield strength
f_{ywk}	Design yield strength of the shear reinforcement
gk	Permanent load applied on the building
h	Structure height or the effective structure height
h_i	Height of the level i
l	Span length of the beam
lo	Effective length of the element
m	Mass of the structure
q	Behavior factor
S	Soil factor
$s_{l,max}$	Maximum longitudinal spacing
$s_{t,max}$	Maximum transversal spacing
$S_d(T1)$	Design spectral acceleration
$S_e(t)$	Elastic response spectrum

$C_{dur,add}\,dd$	Add reduction of minimum cover for use of additional protection
$\Delta C_{dur,st}$	Reduction of minimum cover for use of stainless steel
ΔCdur,v	Additive safety element
α	Angle between shear reinforcement and axis of design element
α_{cw}	Coefficient of interaction between compressive stresses
a_g	Design ground acceleration
a_i	Shifting distance
α_x	Grashof coefficient in x direction
α_y	Grashof coefficient in y direction

b	Width of the element
b_t	Mean width of the tension zone
b_w	Smallest width of the cross section in the tensile area
cc	Concrete cover
c_{min}	Minimum concrete cover
$c_{min,b}$	Minimum cover due to bond requirement
$c_{min,dur}$	Minimum cover due to environmental conditions
d	Effective height of the section
d_r	Design inter-storey drift
f_{cd}	Design resisting strength of the concrete
f_{ctm}	Tensile strength of the concrete
ϕ_{lmin}	Minimum diameter of the longitudinal bars
f_{yd}	Design yielding strength of the steel
f_{yk}	Characteristic yield strength of steel
f_{ywd}	Design yield strength of the shear reinforcement
h	Structure height or the effective structure height
h	Storey height
hi	Height of the level i
i	Gyration radius of the uncracked concrete section
j	Index denoting the mode of vibration
k	Stiffness of the fixed base structure
φ_{ef}	Effective creep ratio
k	Number of modes taken into account
l_0	Effective length of the element
λ_{lim}	Limit value of slenderness
m	Mass of the structure
n	Relative normal force
n_∞	Long term coefficient of homogenization
n_0	Short term coefficient of homogenization
q	Behaviour factor
$\rho 1$	Shear reinforcement ratio
r_m	Moment ratio
s	Stirrup spacing
S	Soil factor
σ_c	Stress in concrete
Scl$x$	Maximum longitudinal spacing
σ_{cp}	Stress due to axial forces
Sr	Recovery area of column
σ_s	Stress in steel
v1	Reduction coefficient of shear crack
ω	Mechanical reinforcement ratio

x	Neutral axis
ξ	Viscous damping ratio
z	Inner lever arm
γ	Specific weight
ν	Poisson's ratio
Ψ_E	Combination coefficient for variable action
θ	Angle of concrete compression struts to the beam axis
λ	Slenderness

ABSTRACT

The main objective of this work was to study the effect of slab rigidity on the seismic response of a tall irregular building. In other to achieve this goal, an evaluation of the performance of the structure with rigid and flexible slabs was done. A literature review was carried out to highlight how slabs are classified based on rigidity and the diaphragm role slabs play in the transfer of lateral loads to the vertical lateral load resisting systems, followed by the effect of structural irregularities on buildings. The methodology adopted consisted first in the presentation of the case study which is a G+5 storey hotel building followed by the design two most used types of slabs in Cameroon (hollow-block slabs and two-way slabs) for this structure. The case study designed with the hollow-block slab was then analysed and designed under static and dynamic loads according to the European standards. The rigid and flexible slabs were then modelled on the case study giving a total of two models. The models were subjected to the 1995 Kobe earthquake accelerogram using the software ETABS (Extended Three-dimensional Analysis of Building Systems) version 18. The results of the seismic response are presented and compared for the two models in terms of vibration period, maximum story displacement, inter-story drift, base shear and torsional moments. It was observed that for the vibration period, maximum story displacement and inter-story drift, the structure with flexible slab gives higher values compared to the structure with rigid slab. For the base shear and torsional moment, the rigid slab structure has higher values compared to the flexible slab structure. It was also observed that, the response of the structure for the observed parameters are always greater along the y-axis compared to the x-axis. Later on the effect of soil structure interaction on the rigid and flexible slab model was also observed for three parameters; period, storey displacements and base shear. The results obtained for the models with SSI showed that SSI increases the overall flexibility of the structure. All these results show that the slab in-plane rigidity has an effect on the seismic response of buildings although for structures with rigid and flexible slabs with moment resenting frames as vertical lateral load resisting systems, the effects are slightly different. Furthermore, when taking into consideration SSI the effects of slab in-plane rigidity may be greater or smaller depending on the parameter observed but the difference between the effects of rigid and flexible slabs on the structure are slightly different as for the structure with fixed base.

Keywords: Rigid slabs, flexible slabs, period of vibration, story displacement, inter-story drift, base shear, torsional moment

RESUME

L'objectif principal de ce travail était d'étudier l'effet de la rigidité d'une dalle sur la réponse séismique d'un grand bâtiment irrégulier en plan. Pour atteindre cet objectif, une évaluation des performances de la structure avec dalle rigide et flexible a été faite. Une revue de littérature a été faite pour présenter comment les dalles son classifiés selon leur rigidité et le rôle de diaphragme que joue la dalle dans le transfert des charges latérales aux éléments porteurs verticaux suivi des effets de l'irrégularité structurelle sur le bâtiment. La méthodologie adoptée a consisté dans un premier temps a consistait dans un premier temps à concevoir un cas d'étude qui est un bâtiment R+5 conçue pour un hôtel suivi par le dimensionnement des deux types des dalles les plus utilisés au Cameroun (dalle a hourdis et dalle pleine a 2 sens porteur) pour ce bâtiment. Le cas d'étude conçu avec la dalle a hourdis a ensuite été dimensionnée sous l'effet des charges statique et dynamique suivant les Normes Européen. La dalle rigide et la dalle flexible ont ensuite été modélisé sur ce cas d'étude a l'aide du logiciel ETABS (Extended Three-dimensional Analysis of Building Systems) version 18 donnant un total de deux modèles. Le bâtiment a été soumis, à l'aide du logiciel ETABS 18, à l'accelerogram du tremblement de terre de Kobe de 1995. Les résultats de l'analyse séismique sont ensuite présentés et comparé pour les deux modèles en termes de période de vibration, déplacement latérale, déviation inter-étage, effort tranchant à la base et moment torsionel. Il a été observé que pour la période de vibration, déplacement latérale et la déviation inter-étage la structure avec la dalle rigide donne de plus grande valeurs comparé à la structure à dalle rigide. Pour l'effort tranchant par étages et moment torsionel, la structure à dalle rigide à de plus grande valeurs comparé à la structure à dalle flexible. Il a aussi été observé que la réponse de la structure selon les paramètres observés sont toujours plus grands selon l'axe y compare à l'axe x. Ensuite l'effet de l'interaction sol structure sur les modelés a dalle rigide et a dalle flexible a été observé sur trois paramètre ; la période de vibration, déplacement latéral et les efforts tranchants par étages. Les résultats obtenus pour les modèles avec interaction sol structure (ISS) ont montrés que l'ISS augmentait généralement la flexibilité de la structure. Ces résultats nous montrent que la rigidité de la dalle a un effet sur la réponse séismique des bâtiments même si pour les structures à ossatures poutre-poteau la différence des effets des dalles rigide et non rigide sont minimes.

Mots clés: Dalle rigide, dalle flexible, de période de vibration, déplacement latérale, déviation inter-étage, de l'effort tranchant à la base et moment torsionel

LIST OF FIGURES

LIST OF TABLES

TABLE OF CONTENTS

GENERAL INTRODUCTION

In the analyses of multi-storey buildings subjected to lateral loads, a common assumption is that the floor system undergoes no deformation in its own plane. In current practice, horizontal diaphragms are typically assumed to be rigid, thus in reinforced concrete buildings the in-plane flexibility of the floor diaphragms is often ignored for simplicity in practical design. However, this assumption is found to create certain discrepancy in lateral load distribution. This discrepancy occurs in the floors systems (horizontal diaphragms) which typically function as deep beams with short spans, and have very high stiffness and strength in comparison with other structural components. The seismic response of buildings subjected to earthquake ground motion depends not only on the characteristics of its vertical lateral force resisting systems, such as braces and moment resisting frames, but also on horizontal lateral force resisting elements, which typically consist of floor diaphragms.

A study which was done by Sashi K.Kunnah and Nader Panahshahi and Andrei M.Reinhorn on 1991 shows that the in-plane deflections of floor slabs impose a larger demand on strength and ductility of flexible frames than predicted values using the assumption of rigid or elastic slabs .Another study which was done by S.H JU and M.C Lin on 1999 shows that for the buildings without shear walls, the rigid-floor model is accurate as the flexible model even for irregular floor systems and this is observed since the in-plane stiffness of the slab is much larger than the out-of-plane column stiffness and for the buildings with shear walls, the rigid-floor and flexible-floor analyses can differ greatly due to the very large lateral stiffness of the shear wall system, the in-plane stiffness of the slab is relatively insignificant, and the slab in-plane deformation cannot be ignored.

This study is therefore important in that it aims to evaluate the effects of the rigid and flexible slab assumptions on a structure with the moment resisting frame as the lateral load resisting system, and compare these effects in other to verify that the rigid slab assumption is accurate for these type of buildings taking in to account the effect of soil structure interaction. To attain this objective, the work is divided in three chapters. The first chapter is about the state of the art and will permit to have a better understanding of all the concepts related to in-plane slab rigidity, tall building and structural irregularity. The second chapter entitled methodology will present the steps adopted to achieve the objective of this work. Finally, at chapter three the results are going to be interpreted and a comparison of the results for rigid and flexible slab assumption will be presented.

CHAPTER 1: LITTERATURE REVIEW

In the analysis of multi-storey buildings subjected to lateral loads, a common assumption is that the floor system undergoes no deformation in its own plan that is they behave like rigid diaphragms. The rigidity of the slab particularly affects the way the slab transfers lateral loads to the vertical resisting systems. All the seismic codes generally accept that in most cases the floor diaphragms may be modelled as fully rigid without in-plane deformability. Even though a rigid floor diaphragm is a good assumption for seismic analysis of the most buildings, several building configurations may exhibit significant flexibility in floor diaphragms. The lateral loading due to earthquakes also particularly affects tall buildings and irregular buildings. For tall buildings the effect of wind must also be taken into account since wind loads compared to seismic loads have the governing effect in tall buildings design meanwhile for irregular buildings, the seismic loads have the governing effect. This chapter will start by briefly presenting some research already done on floor diaphragm flexibility and some code provisions which can be used to classify a slab as rigid or non-rigid. This will be followed by the description of slabs, particularly rigid and non-rigid slabs with a brief overview on their diaphragm functions and the role they play in the transfer of lateral loads to the vertical load resisting systems. We will equally talk about tall buildings and structural irregularity. For tall buildings, particular attention will be given on how they are affected by wind loads and for irregular structures, attention will be given on the effect of seismic loads.

1.1. Research and code provisions on floor diaphragm rigidity

Throughout the past years, some researches have already been done to have a better understanding of the behaviour of flexible floor diaphragms. Also some modern seismic codes set certain qualitative criteria, while some others set quantitative criteria. This section is going to present some researches and some codes

1.1.1. Research

Muto (1974) used a beam with bending and shear deformation effects to simulate the behaviour of flexible floors in buildings.

Jain (1984) also used this beam including flexible and shear deformation effects to generate a solution to find the flexible-floor effect under the dynamic analysis.

Saffarini and Qudaimat (1992) analyzed 37 reinforced concrete buildings to compare the difference between static rigid floor and flexible-floor analyses. They found that the rigid-floor assumption is accurate for buildings without shear walls, but it can cause errors for building systems with shear walls. The quantitative investigation of the difference between the

flexible-floor and rigid-floor analyses of buildings with shear walls was not found in their study and appears to be absent in the literature.

Ju and Lin (1999) investigated the difference between rigid floor and flexible-floors. They found that the rigid-floor assumption can cause errors for building system with shear walls. A quantitative investigation was made and an error formula was generated using the regression analysis of the rigid-floor and flexible-floor analyses from 520 rectangular, U-shaped, and T-shaped buildings. The effect of opening in slab was not found in their study and appears to be absent in the literature.

Busu and Jain (2004) investigate the influence of floor diaphragm flexibility in asymmetric buildings. They investigate the effect of torsional code provisions in asymmetric buildings. They concluded that torsional effects may be quite significant in buildings with a flexible floor diaphragm (in semi-rigid structures specially). In such buildings, neither the floor diaphragm flexibility nor the torsional response can be ignored. Moreover, ignoring either accidental torsion or torsional amplification may cause significant differences in design forces.

1.1.2. Code provisions

According to Moeni & Rafezy, 2011 all the seismic codes generally accept that in most cases the floor diaphragms may be modelled as fully rigid without in plane deformability. Even though a rigid floor diaphragm is a good assumption for seismic analysis of the most buildings, several building configurations may exhibit significant flexibility in floor diaphragms. In these configurations, some codes such as the UBC-97, IRAN SESMIC CODE-THIRD EDITION, FEMA-273 set a certain a quantitative criteria related to the shape of the diaphragm, while some others like; EC8, NZS4203, GSC-2000 set a qualitative criteria relating the in-plane deformation of the diaphragm with the average drift of the associated storey. The UBC-97, IRAN SESMIC CODE-THIRD EDITION and the EC8 are going to be developed in this section.

1.1.2.1. Uniform Building Code [UBC, 1994]

According to the UBC a floor diaphragm is considered flexible for the purposes of distribution of storey shear and torsional moment when the maximum lateral deformation of the diaphragm ($\Delta_{flexible}$) is more than twice the average storey drift of the associated storey (Δ_{story}). The deflection in the plane of the floor diaphragm shall not exceed the permissible deflection of the attached elements. Permissible deflection shall be that deflection which permits the attached element to maintain its structural integrity under the individual loading and continue to support the permissible loads formulas. In other word a floor diaphragm is rigid when it follows the condition stated in equation 1.1 and a floor diaphragm is flexible when it follows the condition stated in equation 1.2.

$$\frac{\Delta_{flexible}}{\Delta_{story}} \geq 2 \quad (1.1)$$

$$\frac{\Delta_{flexible}}{\Delta_{story}} \geq 2 \quad (1.2)$$

Where:

$\Delta_{flexible}$ is lateral deformation of the diaphragm

Δ_{story} is the average storey drift of the associated storey

1.1.2.2. Iran seismic code-third edition (2800)

Floor diaphragms shall be classified as either flexible or rigid. Flexible when the maximum lateral deformation of the diaphragm along its length is more than half the average inter-storey drift of the storey immediately below, rigid when this lateral deformation of the diaphragm is less than half the average inter-storey drift of the associated storey. The inter-storey drift and diaphragm deformations shall be estimated using the seismic lateral forces. In other word a floor diaphragm is rigid when it follows the condition stated in equation 1.3 and a floor diaphragm is flexible when it follows the condition stated in equation 1.4.

$$\frac{\Delta_{diaph}}{\Delta_{interstorey}} < 0.5 \quad (1.3)$$

$$\frac{\Delta_{diaph}}{\Delta_{interstorey}} > 0.5 \quad (1.4)$$

Where:

Δ_{diaph} is lateral deformation of the diaphragm

$\Delta_{interstorey}$ is the average inter-storey drift of the storey immediately below

1.1.2.3. Euro code 8 [EC8, 1994]

When the floor diaphragms are sufficiently rigid in their plane, the masses and the moments of inertia of each floor may be lumped at its center of gravity. The seismic design shall cover the verification of reinforced concrete (RC) diaphragms in the following cases of Ductility Class “H” structures:

- Irregular geometries or divided shapes in plan, recesses, re-entrances
- Irregular and large openings in the slabs
- Irregular distribution of masses and or stiffness
- Basements with walls located only in part of their perimeter, or only in part of the ground floor area.

In these cases, action effects in RC diaphragms may be estimated by modelling them as deep beams on yielding supports or plane trusses. When the floor diaphragms of the building may be taken as being rigid in their planes, the masses and the moments of inertia of each floor may be lumped at the center of gravity. The diaphragm is taken as being rigid, if, when it is modelled with its actual in-plane flexibility, its horizontal displacements nowhere exceed those resulting from the rigid diaphragm assumption by more than 10% of the corresponding absolute horizontal displacements in the seismic design situation.

1.2. Slabs

A slab is an important structural element which is constructed to create flat and useful surfaces such as floors, roofs, and ceilings. It is a horizontal structural component, with top and bottom surfaces parallel or near so. Commonly, slabs are supported by beams, columns (concrete or steel), walls, or the ground. Slabs play a crucial role in transferring lateral loads to the vertical load resisting system.

1.2.1. Diaphragm role of slab

A diaphragm can be defined as horizontal or sloped system acting to transmit lateral forces to the vertical resisting elements such as shear walls, braced frames and moment resistant frames. According to Eurocode, structural elements such as slabs, roofs, decks can be defined as diaphragm when they are continuous and homogeneous, of specific thickness and constant in plane stiffness From the definition of diaphragms, we realize that slabs play the role of diaphragms in buildings that is; in the same way as diaphragms, slabs play a crucial role in transferring lateral loads to the vertical load resisting system. So a slab is a diaphragm but diaphragm is not necessarily a slab because there are many other different types of materials and structural elements that play the role of diaphragms in buildings such as composite steel deck with concrete, on-top steel deck (roof deck) and plywood sheathing to state just these ones.

A diaphragm can be visualized as a wide horizontal beam with components at its edges termed chords designed to resist tension and compression chords are similar to the flanges or a vertical beam as seen in figure 1.1.

Figure 1.1. Deep beam action of diaphragm (Taranath, 2013)

Diaphragm's crucial role is in collecting and transferring translation or rotational forces which result from the distribution of the shear base to the lateral resisting vertical system as for instance shear walls or frame systems. The joints or connections between the diaphragm and the lateral resisting solution system remain constant as well as the distance between them. In addition, diaphragms tie the structure together collectively so that it acts as a single entity during an earthquake. The robustness and redundancy of a structure is highly dependent on the performance of the diaphragms.

1.2.2. Classification of slabs

There are many different types of slabs which can be classified based on different characteristics. Four major properties which can be used to classify slabs are Rigidity, load distribution, material used and the Support system.

1.2.2.1. Based on the rigidity

Rigidity in slabs is mostly concerned about the in-plane rigidity of the slab that is, the ability of the slab to resist in-plane deformation under the action of lateral forces. Based on rigidity, slabs can be classified into 3 categories; rigid slabs, flexible slabs and semi-rigid slabs.

a. Rigid slabs

Rigid slabs are those that possess the strength and stiffness to distribute the lateral forces to the lateral force resisting frames in proportion to the relative stiffness of the vertical lateral-load resisting system (VLLRS) without significant deformation in the slab. Under the action of lateral loads, these slabs undergo a uniform translational displacement and no in-plane deformations as illustrated in figure 1.2(b).

b. Flexible slabs

Flexible slabs are those in which the distribution of the lateral force is independent of the relative stiffness of the lateral force-resisting frames and also undergoes in-plane deformation under the effect of lateral forces. A slab is considered flexible if;

- It distributes horizontal forces to VLLR elements independent of their relative rigidities
- It distributes horizontal forces to VLLR elements based on tributary areas
- Slab deflection is significantly large compared to that of VLLR elements (see figure 1.2(c))

c. Semi-rigid slabs:

A semi-rigid slab is one that distributes lateral forces in proportion to the stiffness of the slab and the relative stiffness of the lateral-force-resisting frames but also undergoes an in-plane deformation under the effect of lateral forces. Semi-rigid slabs are often analysed using the

analogy of a beam on elastic supports where the beam represents the stiffness of the slab and the elastic supports represent the stiffness of the lateral-force-resisting frames.

The rigidity of a slab can be evaluated using equation 1.5.

$$D = \frac{m^2 E h^3}{12(m^2 - 1)} \tag{1.5}$$

Where: $m = {}^{1}/_{v}$

v is the poison's ratio
E is the young modulus
h is the slab thickness

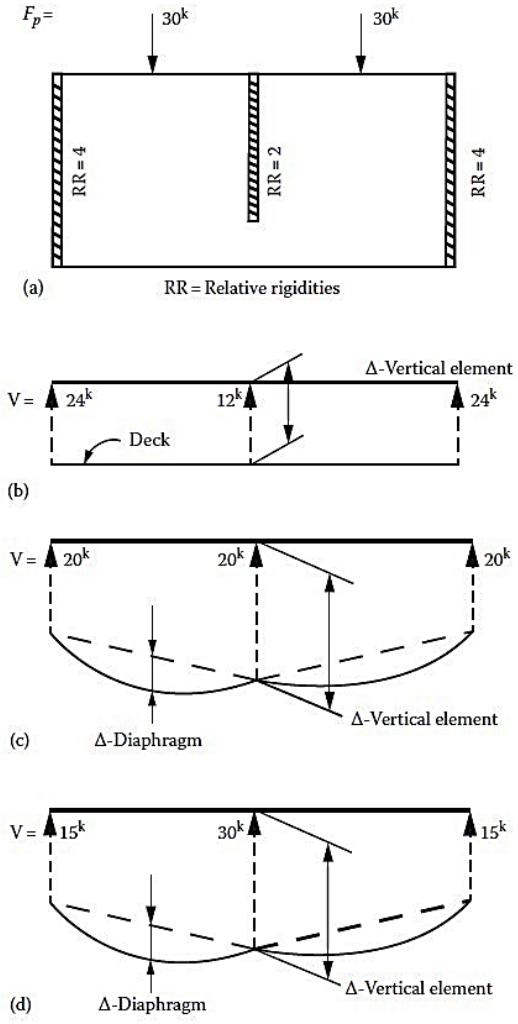

Figure 1.2. Relative effects of diaphragm stiffness. (a) Schematic plan, (b) rigid diaphragm, (c) semi-rigid diaphragm, and (d) flexible diaphragm (Taranath, 2013).

Figure 1.2 illustrates the behaviour of rigid, semi-rigid and flexible diaphragms under the effect of an external lateral force F_p. These behaviours can be assimilated to slabs since a slab is a diaphragm. Figure 1.2(a) shows a schematic plan of a diaphragm supported by three VLLR elements with different relative rigidities. In Figure 1.2(b) we can observe a rigid diaphragm behaviour, with the lateral force distributed to the VLLR element according to their

relative rigidities. The resultant force received by each VLLR element is denoted as V with V of the of the middle VLLR element being the smallest since it has the smallest relative rigidity. It is also observed the diaphragm undergoes a uniform displacement (Δ-vertical elements) and no in-plane deformation.

Figure 1.2(c) illustrates a semi-rigid diaphragm behaviour with the diaphragm undergoing a lateral displacement (Δ-Vertical elements) which is greater in the middle (since the VLLR element in the middle has the smallest relative rigidity) and an in-plane deformation (Δ-Diaphragm). The distribution of the lateral force to the VLLR element is done irrespective of the relative rigidities of the VLLR elements but instead, similarly to a beam with three supports. Flexible diaphragm behaviour is illustrated in Figure 1.2(d) it is observed that the diaphragm undergoes the same lateral displacement end the same in-plane deformation as for the semi-rigid diaphragm condition. As for the distribution of the lateral load to the VLLR elements it is done according the tributary areas of each VLLR element. Therefore, the force received by the middle frame is greater than that of the two others since it has the largest tributary area.

From the above classification of slabs based on the rigidity, it should be understood that a slab cannot be made as rigid or non-rigid but instead, when a structure is subjected to lateral loads its structural behaviour is observed the slabs can be classified as rigid or non-rigid by observing parameters such as the in plane deformation of the slab and the distribution of lateral loads to the VLLRS. Obviously, there are some factors affecting slab rigidity such as the presence of openings in the slab and the span to depth ratio of the slab.

1.2.2.2. Based on the load distribution

Slabs can distribute loads either in one direction or two and based on the sense of distribution, slabs can be classified into two that is one way slabs and two way slabs.

a. One way slabs

These are slabs supported by beams on two opposite sides to carry the load along one direction. When the ratio of the shorter span to the longer span follows the condition in equation 1.6, the slab is considered as one-way slab. Here the slab will bend in one direction that is in the direction along its shorter span. However minimum reinforcement known as distribution steel is provided along the longer span above the main reinforcement to distribute the load uniformly and to resist temperature and shrinkage stresses. Main bars are cranked to resist the formation of stresses. As an example, all the Cantilever slabs are generally one way slab.

$$\frac{Shoter\ span\ (b)}{Longer\ span(l)} \leq 0.4 \tag{1.6}$$

b. Two way slabs

A two-way slab is one supported by beams on all the four sides and the loads are carried by the supports along both directions. In two-way slab, the ratio of the shorter span to the longer span follows the condition in equation 1.7. The slabs are likely to bend along both the directions to the four supporting edges and hence distribution reinforcement is provided in both the directions. To resist the formation of stresses, distribution bars are cranked at both the ends in two -way slab. These types of slabs are used in constructing floors of multi-storey building.

$$\frac{Shoter\ span\ (b)}{Longer\ span(l)} \geq 0.4 \tag{1.7}$$

An illustration of one-way and two-way slabs is presented in figure 1.3

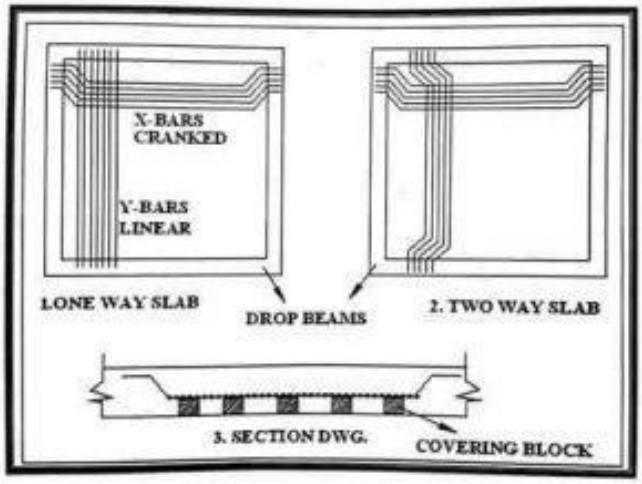

Figure 1.3. One way and two way slabs (https://civilread.com)

1.2.2.3. Based on the materials used

Slabs can be classified according to the number of different materials used for its implementation and also based on the type of material used. When a slab is made up of two or more different materials, it called a composite. Composite slabs generally comprise reinforced concrete cast on top of profiled steel or wood decking, which acts as formwork during construction and external reinforcement at the final stage. We denote two types of composite slabs: and timber concrete slabs.

On the other hand for slabs predominantly composed of one material, we have concrete slabs, steel slabs and wooden slabs.

1.2.2.4. Based on the support system

Support systems are simply the structural elements which carry the slab and receive the loads from the slab to transfer them to the ground. Based on this slabs can be classified in to three:

- Slabs directly supported by columns such as flat slabs
- Slab supported by beams and columns such as conventional slabs and hollow block slabs
- Slabs directly supported by the grounds such as slabs on grade

1.2.3. Types of slabs

There are many different types of slabs and in the following paragraphs we are going to outline these slabs, describe them and give some of their advantages and disadvantages.

1.2.3.1. Conventional slabs

These are slabs which are supported on beams and columns with the thickness of the slab been small compared to the depth of the beam. Here the load transfer is from that slab to the beam and then to the column. Conventional slabs have a square shape and a thickness that varies between 10cm to 15cm. Reinforcement is provided in conventional slab and the bars which are set in horizontal are called Main Reinforcement Bars and bars which are set in vertical are called Distribution bars.

1.2.3.2. Flat slabs

The flat slab is a reinforced concrete slab supported directly by concrete column or caps. Flat slab doesn't have beams so it is also called a beam-less slab. Here loads are directly transferred to columns. Flat slabs have a minimum thickness of 20cm. They are generally used in parking decks, commercial buildings, hotels or places where beam projections are not desired.

There are four different types of concrete flat slabs (see figure1.4.) that is; slab without drop and column without column head, slab with drop and column without column head, slab without drop and column with column head and slab with drop and column with column head

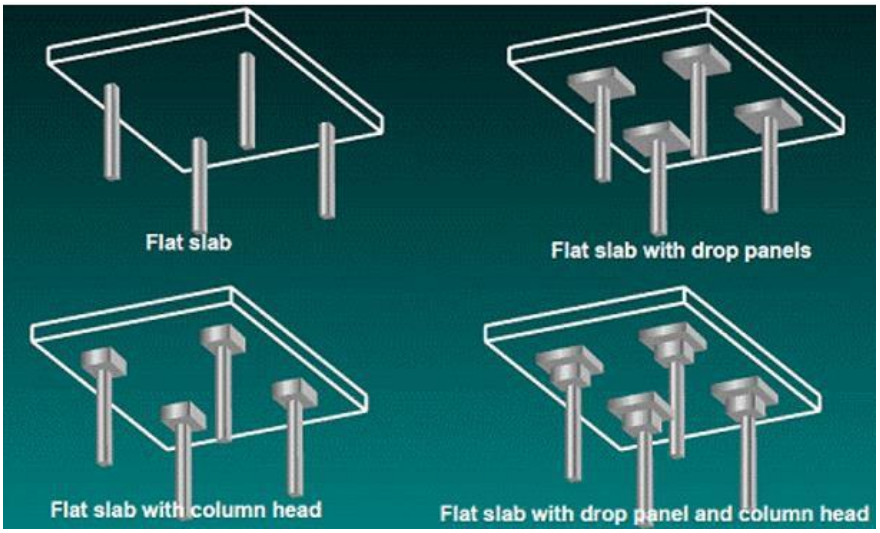

Figure 1.4. Types of flat slabs (https://civilread.com)

1.2.3.3. Hollow core slabs

Hollow core ribbed slabs derive their name from the voids or cores which run through the units as seen in figure 1.5. The cores can function as service ducts and significantly reduce the self-weight of the slabs, maximizing structural efficiency. The cores also have a benefit in sustainability terms in reducing the volume of concrete used. Units are generally available in standard 1200 mm widths and in depths from 110mm to 400 mm. There is total freedom in the length of units. These type of slabs are pre-cast and are used where the construction has to be done fast. The hollow core ribbed slabs have between four and six longitudinal cores running through them, the primary purpose of the cores being to decrease the weight, and material within the floor, yet maintain maximal strength. To further increase the strength, the slabs are reinforced with 12 mm diameter steel strand, running longitudinally. This is one of the types of concrete slabs. Hollow core ribbed slabs have excellent span capabilities, achieving a capacity of 2.5 KN/m2 over a 16 m span. The long-span capability is ideal for offices, retail or car park developments. Units are installed with or without a structural screed, depending on requirements. Screed is a concrete material in which we use small broken stones as aggregates instead of 20mm aggregates.

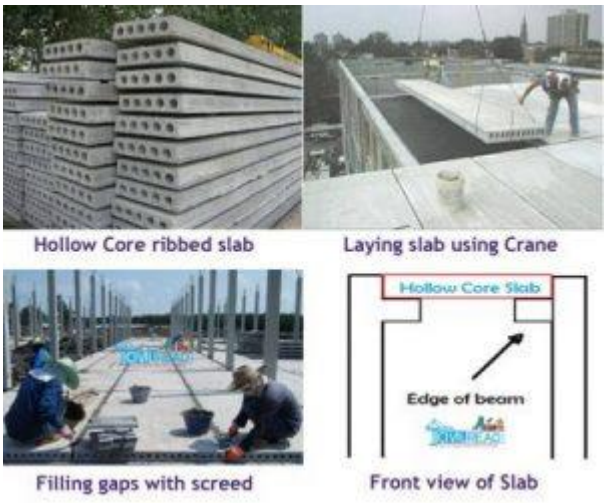

Figure 1.5. Hollow core ribbed slab (civilread.com)

1.2.3.4. Hardy slabs (Hollow block slab)

Hardy slabs are constructed using hardy bricks and reinforced concrete. Hardy bricks are hollow bricks made up of concrete of dimension 50x20x16 in Cameroun. These blocks are used to fill portions of the slab where there will not be concrete. Hardy slabs reduce the amount of concrete to be used and hence the self-weight of the slab is reduced. These slabs generally have a thickness of 20cm to 25cm. they have the disadvantage of not being economic on small spans and are difficult to repair. An illustration of hollow block slabs is presented in figure 1.6.

Figure 1.6. Presentation of a hollow block slab (Mbangue, Douala)

1.2.3.5. Waffle slabs

Waffle slab is a reinforced concrete roofs or floors containing square grids with deep sides. This kind of slab is majorly used at the entrance of hotels, Malls, Restaurants for good pictorial view and to install artificial lighting as seen in figure 1.7 (a) and (b). The concrete waffle slab is often used for industrial and commercial buildings while wood and metal waffle slabs are used in many other construction sites. It is usually used where large spans are required (for example auditorium and cinema halls) to avoid many columns interfering with space. The main purpose of employing this technology is for its strong foundation characteristics of crack and sagging resistance. Based on the shape of Pods (PVC trays) waffle slabs are classified into two types: Triangular pod system and Square pod system.

Waffle slabs are able to carry heavier loads and span longer distances than flat slabs as these systems are light in weight, but they require strict construction supervision and skilled labour.

(a) (b)

Figure 1.7. Waffle slabs (a) (https://civilread.com) (b) Hotel Mont Fébé Cameroun

1.2.3.6. Composite slabs

Commonly, it is constructed from reinforced concrete cast on top of profiled steel decking. The decking acts as formwork and working area during the construction phase, and it also acts as external reinforcement during service life of the slab. For a steel decking of thickness between 50-60mm, the span of the slab can reach up to 3m. However, if the steel decking thickness is increased up to 80mm, slabs with span of 4.5m can be constructed. An example of a steel concrete composite slab is shown in figure 1.8.

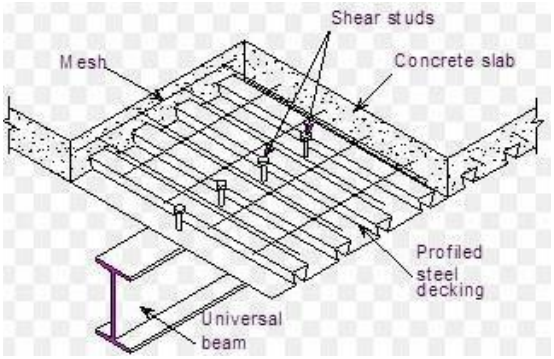

Figure 1.8. Presentation of composite slabs (theconstructor.org/practical-guide/concrete-)

1.2.3.7. Slabs on grades

The slab which is cast on the surface of the earth is called a ground slab as shown in figure 1.9. Generally, slabs on grades are classified into three types as follows:

a. Slab on ground

It is the simplest type of slab on grade which is composed of stiffening concrete beams constructed around perimeter of the slab, and has a slab thickness of 100mm. It is suitable for stable ground which is mostly composed of sand and rock and not influenced by moisture, and soils that undergo slight movement due to moisture.

b. Stiffened raft slab

It is similar to slab on ground apart from stiffening beams which are set in channels through the middle of the slab. Consequently, it creates a kind of supporting grid of concrete on the base of the slab. Soil with moderate, high amount, and severe movement due to moisture.

c. Waffle raft slab

It is constructed entirely above the ground by pouring concrete over a grid of polystyrene blocks known as 'void forms'. Waffle raft slabs are generally suitable for sites with less reactive soil, use about 30% less concrete and 20% less steel than a stiffened raft slab, and are generally cheaper and easier to install than other types. These types of slabs are suitable only for very flat ground.

Figure 1.9. Slab on grade (www.civilsapshot.com)

1.3. Tall buildings

In this section an overview will be done on the history of tall buildings and on the lateral stability systems for tall buildings.

1.3.1. History of tall buildings

The definition of tall building is ambiguous in design practice. We normally define building below eight stories as low-rise buildings. For building with 8 and 20 storeys it is called mediate-rise building. For building over 20 storeys it is called tall building. However, with the fast development of modern construction technology, increasing number of supertall buildings was built and is going to be built. Therefore, the above definition is not accurate.

The Council on Tall Buildings and Urban Habitat (CTBUH) has released a study on the world's 20 tallest buildings projected to be built by 2020 presented in table 1.1. From this table, it can be seen that the definition of tall building is based on the comparisons to the height of other buildings, at present, people can hardly call a 20-story building as a tall building any more, if it is to be compared to the buildings listed in table 1.1. However, from a structural engineer' point of view, the first priority in design consideration for a tall building would be the lateral stability system, as its design and structural analysis are mainly affected by the lateral loads such as wind or earthquake. Therefore, we can define a structure as a tall building when its lateral stability is the first priority in the design.

Table 1.1. List of tallest buildings in the world (https://civilread.com)

	Building and localisation	Height
1	Kingdom Tower, Jeddah	1000 m
2	Burj Khalifa, Dubai	828 m
3	Ping An Finance Center, Shenzhen	660 m
4	Seoul Light DMC Tower, Seoul	640 m
5	Signature Tower, Jakarta	638 m
6	Shanghai Tower, Shanghai	632 m
7	Wuhan Greenland Center, Wuhan	606 m
8	Makkah Royal Clock Tower Hotel, Makkah	601 m
9	Goldin Finance 117, Tian Jin	597 m
10	Lotte World Tower, Seoul	555 m
11	Doha Convention Center and Tower, Doha	551 m
12	One World Trade Center, New York City	541 m

In the case of Cameroon which is a less developed country, the tallest building is the one of the BEAC (Bank of Central African States) with a height of 89m and 18 storeys constructed in 1987. This building is irregular in plan and in elevation as can be seen in figure 1.10**.** A list of the ten tallest buildings in Cameroon is presented in Table 1.2.

Table 1.2. List of tallest buildings in Cameroon (www.emporis.fr/statistics/tallest-buildings)

	Building	Height	Localisation
1	BEAC Headquarters	89m	Yaounde
2	Ministerial building number 1	89m	Yaounde
3	Ministerial building number 2	68m	Yaounde
4	SNI Headquarters	66m	Yaounde
5	Charles de Gaulle building	62.7m	Douala
6	Hotel la Falaise	62.7m	Douala
7	CARAT Residence	62.7m	Douala
8	ONCPB Building	62.7m	Douala
9	Cauris building	62.7m	Douala
10	Rue de trieste building	62.7m	Douala

Figure 1.10. Bank of Central African States in Yaounde (neoindependance.canalblog.com)

1.3.2. Lateral stability systems for tall buildings

From a structural engineer's point of view, the key feature of the tall building is its lateral stability structural system. The development of structural system for tall buildings can be divided into certain stages in the history. They are developed from rigid frame, bracing system, shear wall system to tube, core-outrigger, and diagrid structures. The following paragraphs are going to talk about the three basic lateral load resisting systems which are, the moment resisting frame (MRF) system, the bracing system and the shear wall system.

1.3.2.1. Moment resisting system

A moment-resistant frame is the engineering term for a frame structure with no diagonal bracing in which the lateral forces are resisted primarily by bending in the beams and column mobilized by strong joints between columns and beams. Moment-resistant frames provide the most architectural design freedom.

1.3.2.2. Braced system

Braced frames act in the same way as shear walls however, they generally provide less resistance but better ductility depending on their detailed design. They provide more architectural design freedom than shear walls. There are two general types of braced frames: conventional concentric and eccentric.

In the concentric frame, the center lines of the bracing member meet the horizontal beam at a single point. In the eccentric-braced frame, the braces are deliberately designed to meet the

beam some distance apart from one another. The short piece of beam between the ends of the braces is called a link beam.

1.3.2.3. Shear walls

Shear walls are designed to receive lateral forces from diaphragms and transmit them to the ground. The forces in these walls are predominately shear forces in which material fibres within the wall try to slide pass one another. To be effective, shear walls must run from the top of the building to the foundation with no offsets and a minimum of openings.

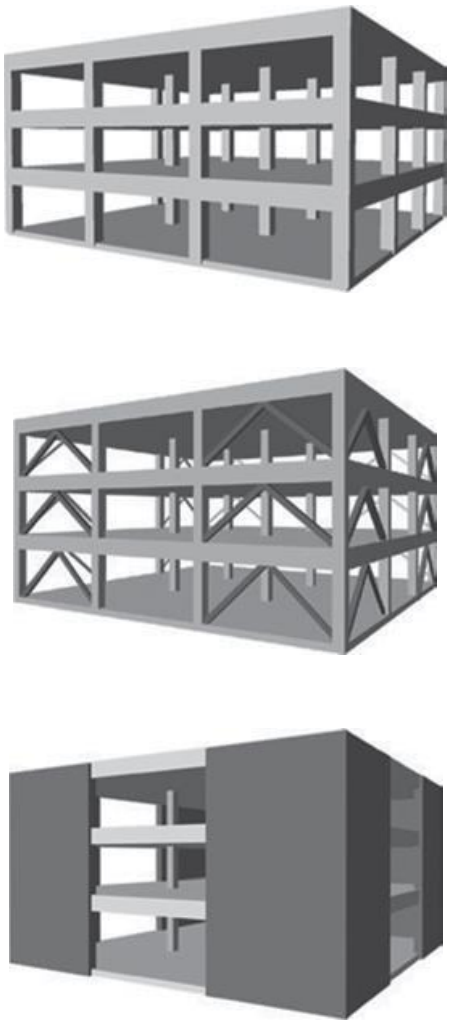

(a) (b) (c)

Figure 1.11. The three basic lateral load resisting systems (a) moment resisting fames (b) braced system (c) shear walls (FEMA-454, Designing for Earthquakes)

1.3.3. Wind loads on tall buildings

The lateral loading due to wind or earthquake is the major factor that causes the design of high-rise buildings to differ from those of low-to-medium-rise buildings. For buildings up to about ten stories and of typical proportions, the design is rarely affected by wind loads. Above this height, however, the increase in size of the structural members, and the possible

rearrangement of the structure to account for wind loading incurs a cost premium that increases with height and advances in methods of analysis.

Tall building structures have become more efficient and lighter and consequently, more prone to deflect and even to sway under wind loading. This served as a spur to research, which has produced significant advances in understanding the nature of wind loading and in developing methods for estimation. These developments have been mainly in experimental and theoretical techniques for determining the increase in wind loading due to gusting and the dynamic interaction of structures with gust forces. To understand wind action on tall buildings is important for an engineer. Compared to seismic loading, wind load is the governing load in tall building design in most instances for lateral stability system design. This is due to the longer natural period of the tall building, which results in a smaller earthquake response compared to low rise building. However, it depends on the location and importance of the building, sometimes a necessary check needs to be performed. While designing the Shanghai Tower, in order to compare the influences of wind load and earthquake action on the structural member design, the base reactions of 100-year wind load, frequent earthquake (50-year return period) and moderate earthquake (475-year return period) are analysed. It is found that the structural responses under wind load is larger than those under frequent earthquake, but is smaller than those under moderate earthquake

1.4. Structural Irregularity

An Irregular structure is one in which either mass or stiffness and geometric regularity is not uniform throughout the structure. These are structures in which the position of the center of mass does not coincide with the position of the center of rigidity. Throughout the history of buildings complex shapes have always been present mostly due to aesthetic reasons and for tall buildings these complex shapes should be studied carefully. A structure can be irregular in plan (horizontal irregularity) and in elevation (vertical irregularity) which can further be classified into four other types as shown in figure 1.12. In the case of Cameroun most buildings are irregular in plan which make them particularly vulnerable to seismic loads.

1.4.1. Major effects of configuration irregularities

Irregularity in buildings causes two majors effects: stress concentrations and torsion.

1.4.1.1. Stress concentrations

Irregularities tend to create abrupt changes in strength or stiffness that may concentrate forces in an undesirable way resulting in stress concentration. Stress concentration occurs when large forces are concentrated at one or a few elements of the building, such as a particular set of beams, columns and walls. These few members may fail and by the chain reaction damage or even bring down the whole building.

This effect can be caused both by both horizontal and vertical stiffness irregularities. The short-column phenomenon is an example of stress concentration created by vertical dimensional irregularity in the building design. In plan, a configuration that is most likely to produce stress concentrations is the re-entrant corner condition as exemplified in the buildings with plan forms such as L or a T. The vertical irregularity of the soft or weak story types can produce dangerous stress concentration along the plane discontinuity.

1.4.1.2. Torsion

Configuration irregularities in plan may cause torsional forces to develop, which contribute a significant component of uncertainty to an analysis of building resistance, and are the most frequent cause of structural failure. Torsional forces are created in a building due to the eccentricity between the center of mass and the center of rigidity. This eccentricity originates either in the lack of symmetry in the arrangement of the perimeter-resistance elements or in the plan configuration of the building, as in the re-entrant corner discussed earlier. Torsional moment is generated whenever the center of gravity of the lateral forces fails to coincide with the center of rigidity of the vertical resisting elements provided that the diaphragm is sufficiently rigid to transfer torsion. The magnitude of the torsional moment that is required to be distributed to the vertical resisting elements by a diaphragm is determined by the sum of the moments created by the physical eccentricity of the translational forces at the level of the diaphragm from the center of rigidity of the resisting elements (MT = Fp e ; where e = distance between CM and CR) and the accidental torsion of 5%. The accidental torsion is an arbitrary code requirement equivalent to the story shear acting with an eccentricity of not less than 5% of the maximum building dimension at that level. The torsional distribution by the more rigid floor diaphragms to the resisting elements is assumed to be in proportion to the stiffness of the elements and its distance from the center of rigidity.

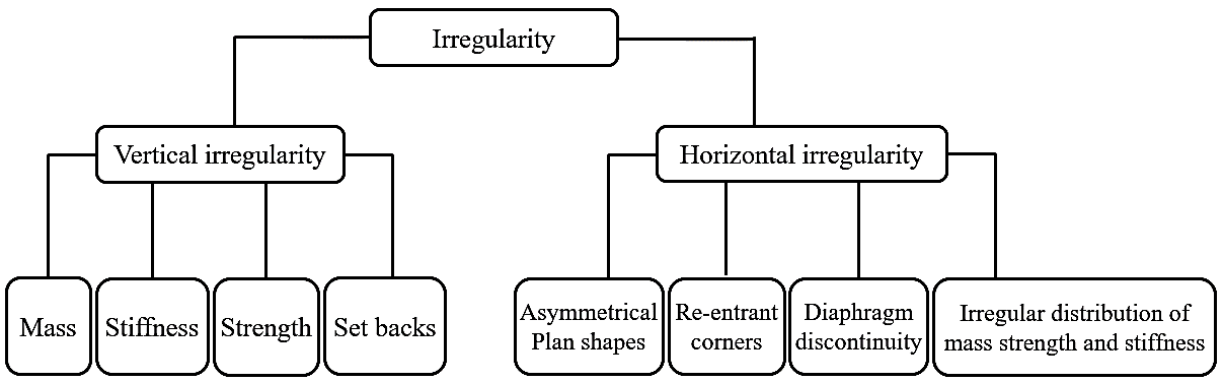

Figure 1.12. Classification of irregularity (Varadharajan et al, 2011)

1.4.2. Irregularity in plan

It is defined as an uneven distribution of stiffness in the plan of a structure resulting in the torsional response of the structure when subjected to external charges. Horizontal irregularity can be internal or external. Internally it is generally due to the difference in slab thickness from one side of the building to the other. External irregularity is concerned about the shape of the building in plan such as U-shaped, H-shaped and Z-shaped buildings as seen in figure 1.13. Structures with plan irregularity quite often suffer severe damage in earthquake events because the response of the structure is not only translational, but also torsional.

Below is a serious configuration condition due to horizontal irregularity that has the potential of seriously impacting the seismic performance of a building.

1.4.2.1. Re-entrant corners

The re-entrant corner is the common characteristic of building forms that, in plan, assume the shape of L, T, H, or a combination of these shapes (see figure 1.14). Invariably these forms result in torsion due to eccentricity of center of mass and center of rigidity as shown schematically in figure 1.15.

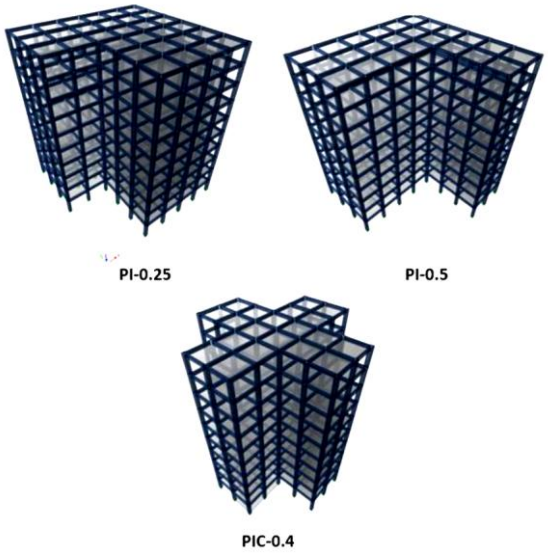

Figure 1.13. 3D view of models having irregularity in plan (JCEU, Volume 7, Issue 6: 87-94)

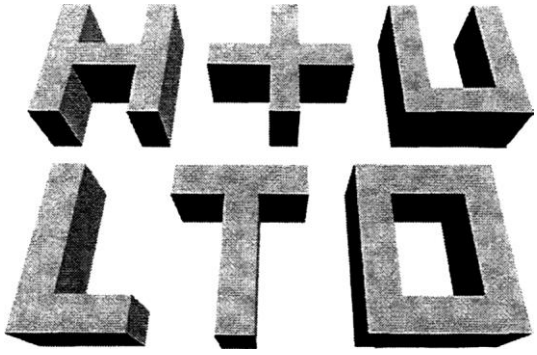

Figure 1.14. Re-entrant corner plan forms

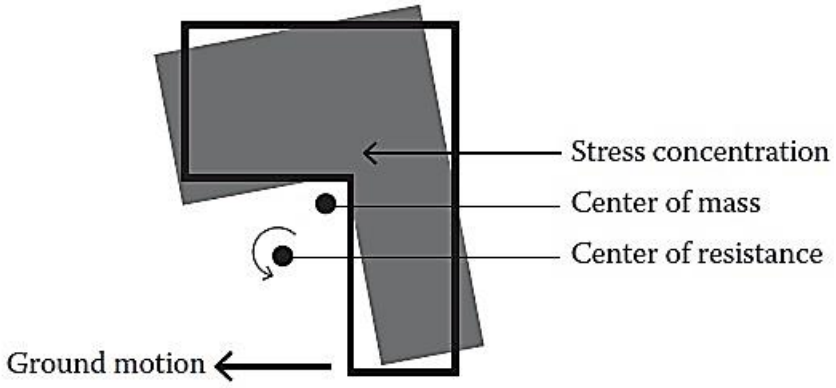

Figure 1.15. Torsion due to eccentricity of center of mass and center of resistance.

There are two problems created by these shapes. The first is that they tend to produce differential motions between different wings of the building that, because of stiff elements that tend to be located in this region, result in local stress concentrations at the re-entrant corner or notch. The second problem of this form is the torsion caused because the center of mass and the center of rigidity do not geometrically coincide for all possible earthquake directions. The result is rotation. The resulting forces are very difficult to analyse and predict. The magnitude of the forces and the severity of the problems will depend on the following points:

- The characteristics of the ground motion
- The mass of the building
- The type of structural systems
- The length of the wings and their aspect ratios (length to width proportion)
- The height of the wings and their height depth ratios

Re-entrant corner plan forms are however the most useful set of building shapes for urban sites, particularly for residential apartments and hotels. This is because large plan areas may be accommodated in relatively compact form yet still provides a high percentage of perimeter rooms with access to air and light.

There are two basic alternative approaches to the problem of re-entrant corner forms, we can structurally separate the building into simpler shapes using separation joints or to tie the building together more strongly with elements positioned to provide a more balanced resistance (see figure.1.16). If the decision is made to use separation joints, the structurally separated entities of the building must be fully capable of resisting vertical and lateral forces on their own, and their individual configurations must be balance horizontally and vertically. To design a separation joint, the maximum drift of the two units must be calculated so as to avoid the two individual structures to lean toward each other simultaneously. Therefore, the dimension of the separation space must allow for the statistical sum of the building deflections.

Several considerations arise if it is decided to instead tie the building together. Collectors at the intersection can transfer forces across the intersection area, but only if the design allows for these beam-like members to extend straight across without interruption. Since the portion of the wing that typically distorts the most is the free end, it is desirable to place stiffening elements at that location. The use of splayed rather than right-angle re-entrant corners lessens the stress concentration at the notch (see figure.1.17) This is analogous to the way a rounded hole in a steel plate creates less stress concentration than a rectangular hole or the way a tapered beam is structurally more desirable than an abruptly notched one.

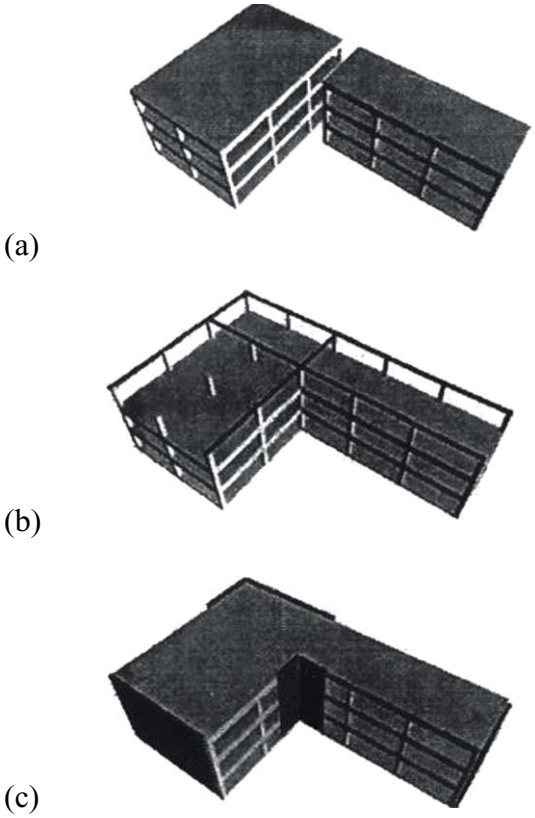

Figure 1.16. Solutions for the re-entrant corner condition (a) separation of building (b)strengthening notch (c) adding stiff elements at notch

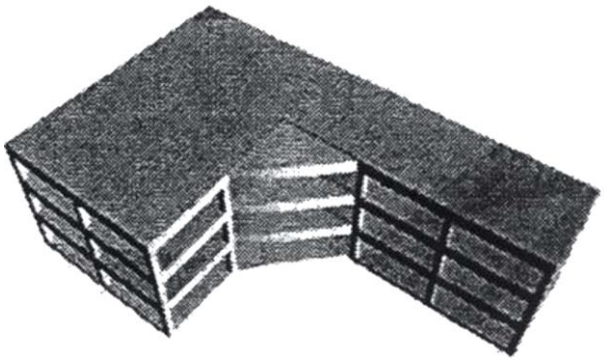

Figure 1.17. Relieving the stress on the re-entrant corner by using splays

1.4.3. Irregularity in elevation

It is defined as the uneven distribution of mass and/or stiffness along the height of a multi-storey structure due to geometrical set-backs changing the floor plan between the adjacent floors. During a seismic event, the result can be a soft story mechanism. Stepped buildings, inverted-T buildings and U-shaped buildings are examples of buildings with vertical irregularities as shown in figure 1.18.

Below is a serious configuration condition due to vertical irregularity that has the potential of seriously impacting the seismic performance of a building.

1.4.3.1. Soft and weak stories

The term weak story has commonly been applied to buildings whose ground-level story is less stiff than those above. The building code distinguishes between soft and weak stories. Soft stories are less stiff, or more flexible, than the story above while weak stories have less strength. A soft or weak story at any height creates a problem since the cumulative loads are greatest toward the base of the building. A discontinuity between the first and second floor tends to result in the most serious condition. The way in which severe stress concentration is caused at the top of the first floor is shown in the diagram sequence in figure 1.19. Normal drift under earthquake forces that is distributed equally among the upper floors is shown in figure 1.19(a). With a soft story, almost all the drift occurs in the first floor and stress concentrate at the second-floor connections (figure 1.19(b)). This concentration over stresses the joints along the second-floor line leading to distortion or collapse (figure.1.19(c)).

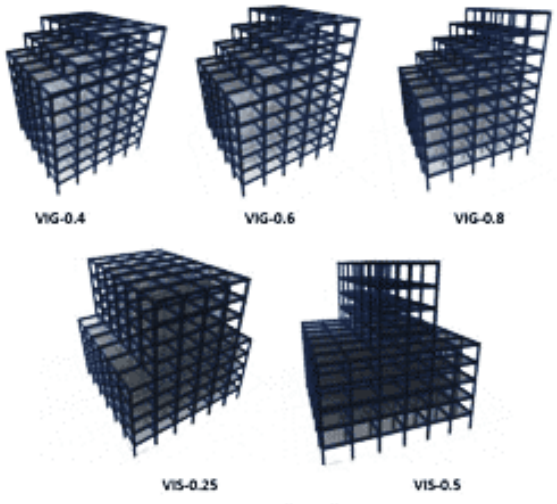

Figure 1.18. 3D of models having irregularity in elevation (JCEU, Volume 7, Issue 6: 87-94)

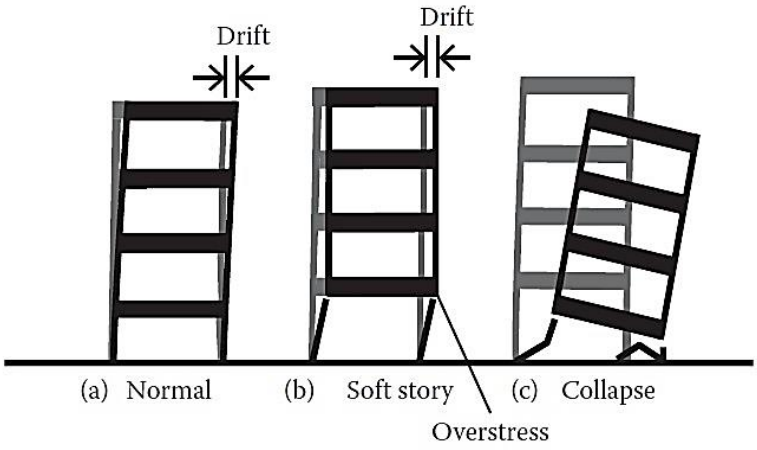

Figure 1.19. Soft story mechanism (Bungale S. Taranath, 2017)

Three typical conditions illustrated in Figure.1.20 create a soft first story. The first condition shown in figure1.20 (a) is where the vertical structure between the first and second floor is significantly more flexible than that of the upper floors. This discontinuity most commonly occurs in a frame structure in which the first-floor height is significantly taller than those above, resulting in a large discrepancy in stiffness. The second form of soft story shown in figure.1.20 (b) is created by a common design concept in which some of the vertical framing elements do not continue to the foundation but rather are terminated at the second floor to increase the openness at ground level. This condition creates a discontinuous load path that results in an abrupt change in stiffness and strength at the plane of change. Finally, the soft story may be created by an open first floor that supports heavy structural or non-structural walls above (see figure.1.20(c)). This situation is most serious when the walls above are shear walls acting as major lateral-force-resisting elements.

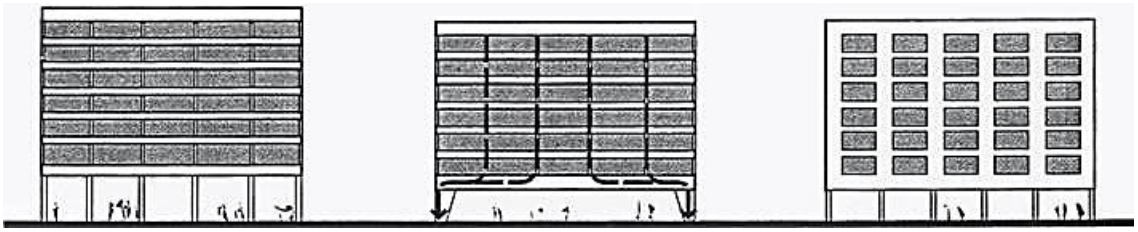

(a) (b) (c)

Figure 1.20. Soft story mechanism (Bungale S. Taranath, 2017)

The best solution to the soft and weak story problem is to avoid the discontinuity through architectural design. There may, however, be good programmatic reasons why the first floor should be more open or higher than the upper floors. In these cases, careful design must be employed to reduce the discontinuity. Some conceptual methods for doing this are shown in figure.1.21. Not all buildings that show slender columns and high first floors are soft stories. For a soft story to exist, the flexible columns must be the main lateral-force-resistant system.

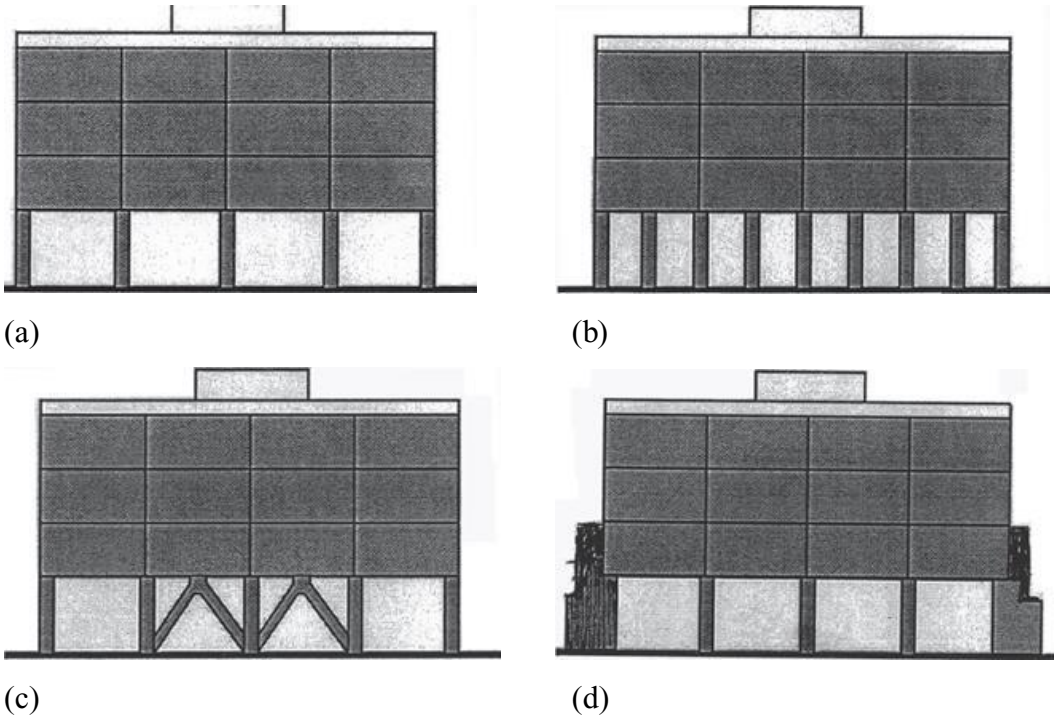

Figure 1.21. . Design solutions for soft-story condition: (a) soft-story condition, (b) add columns, (c) add bracing d) add external buttresses (Bungale S. Taranath, 2017)

Conclusion

In this first chapter, particular interest was given in understanding the basic concepts related to slab rigidity, tall buildings and structural irregularity. It is found that based on rigidity, slabs can be classified into rigid, flexible and semi-rigid slabs; depending on how they transfer lateral loads to the VLLRS and deform under effect of lateral loads. As for tall buildings they are defined relative to the location and even time due to the rapid evolution of the technology which varies from a lot from place to place. The most damaging effect on tall buildings is caused by wind. For irregular structures, they can be exhibit vertical or horizontal irregularity and the most damaging effect on these structures are caused by earthquakes.

In the case of our building we are going to concentrate our analysis on the seismic effects since the building is more irregular than tall. The analysis will be done on a C-shaped G+5 storey building in Yaoundé and the methodology that will be adopted is presented in the next chapter.

CHAPTER 2: METHODOLOGY

Introduction

The principal objective of the methodology is to clarify how the study will be conducted in order to attain the objectives set. In this work the first step consist in the site recognition, data collection, presenting the norms used and the considered loads acting on the structure followed by presentation of the tools of numerical modelling and a detailed description the modelling of the structure. To continue, the static design methodology o the slabs, beams and column will be presented followed by the procedure to represent SSI. Finally, the parameters such as period of vibration, storey displacement, inter-storey drift ratio, story shear and torsional moment used as the analysis criteria are going to be brought forth to be explained and the effect of SSI will also be observed.

2.1. Site recognition

The site recognition will be carried out from documentary research whose essential goal is to know the location of the site, the climate, the hydrology and socio-economic parameters in the region.

2.2. Site visit

The site visit will be done in two phases, the first phase for the observation of the site and the second for data collection.

2.3. Data collection

The data collected are those related to the geometry and those related to the structure. These data will be taken from different plans available where we can identify the sections and positions of structural element and the characteristics of materials used.

2.4. Actions and combination of actions

The norms that will be used for the design of elements are the Eurocode 0, basis of structural design Eurocode 1, actions on structure, Eurocode 2, design of concrete structures, Eurocode 7, geotechnical design and Eurocode 8 design for earthquake resistance. These European standards define the actions and the combination of actions for the design.

2.4.1. Actions

Different types of actions can be applied on a structure. This analysis is focused on a building structure and the different kinds of actions which are considered are permanent actions, imposed actions and seismic action.

2.4.1.1. Permanent actions

This kind of actions is constituted by the self-weight of structural and non-structural elements. The weight of the structural elements is obtained by multiplying the specific weight of concrete by the section of the elements. The self-weight of the non-structural elements are extracted form Eurocode 1.

2.4.1.2. Imposed actions

Imposed actions are those arising from occupancy. It includes the normal use by people, the furniture and moveable objects and others. According to the Eurocode 1, different use categories of areas exist. Therefore, those ones are presented in the table A1 of the annex A. Based on these different categories the different values of loads recommended by this norm are presented in the table A2 of the Annex A.

2.4.1.3. Seismic action

These are actions due to earthquake ground motions and according to the Eurocode 8, the reference method for determining the seismic effect is the modal response spectrum analysis using the linear elastic model of the structure and the design response spectrum.

Seismic actions are going accounted in the analysis by the definition of an elastic response spectrum defined in the Eurocode 8 by the following expressions:

$0 \leq T \leq T_B$: $$S_e(t) = a_g.S\left[1 + \frac{T}{T_B}(\eta 2.5 - 1)\right] \quad (2.1)$$

$T_B \leq T \leq T_C$: $$S_e(t) = a_g.S.\eta 2.5 \quad (2.2)$$

$T_C \leq T \leq T_D$: $$S_e(t) = a_g.S.\frac{T_C}{T} \quad (2.3)$$

$T_D > T$: $$S_e(t) = a_g.S.\eta 2.5\left[\frac{T_C T_D}{T^2}\right] \quad (2.4)$$

Where:

$S_e(t)$ is the elastic response spectrum

T is the vibration period of a linear single degree of freedom system

a_g is the design ground acceleration on type A ground

T_B is the lower limit of period of the period of the constant spectral acceleration branch

T_C is the upper limit of the period of the constant spectral acceleration branch

T_D is the value defining the beginning the constant displacement response range of the spectrum

S is the soil factor that depends on the ground type

η is the correction factor given by $\eta = \sqrt{10/(5+\xi)}$

ξ is the viscous damping ratio

The general shape of the elastic response spectrum defined by the Eurocode 8 is presented in figure 2.1.

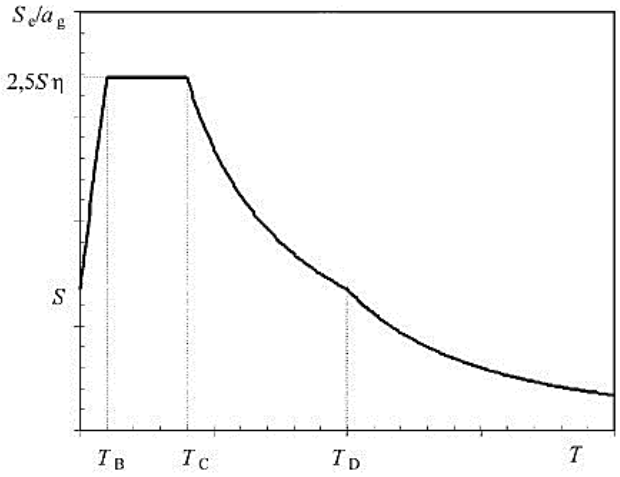

Figure 2.1. Shape of the elastic response spectrum (EC8 Part 1)

This elastic spectrum depends on many inputs notably the ground type, the importance class of the buildings, the peak ground acceleration of the region and the damping ratio of the structure which are going to be described in the following paragraphs.

The ground type has a great influence on the seismic waves when it travels on the soil so it can modify his spectra. Eurocode 8 considers seven different ground types, accounting by a ground factor S, depending on their mechanical properties (average value of propagation velocity of S waves, Standard penetration test blow count and undrained shear strength of the soil or cohesive resistance). These different ground types are presented in the table A3 of the annex and the variation of the elastic spectrum in function of the ground type is presented in figure 2.2.

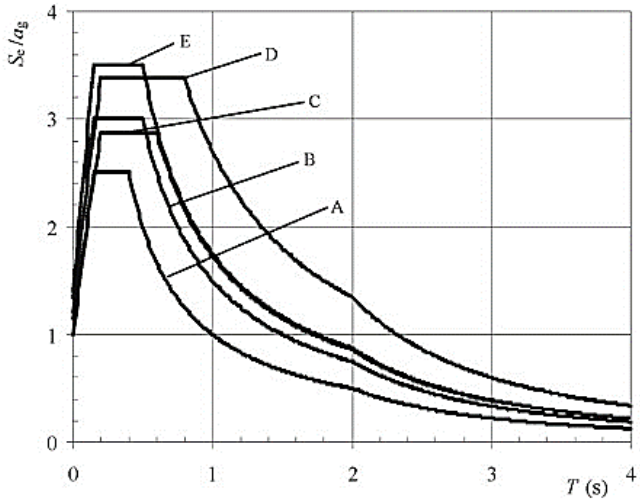

Figure 2.2. Shape of the elastic response spectrum for different ground type

The importance class permits the classification of the building considers the consequence of the collapse for human life, on their importance for public safety and civil protection in the immediate post-earthquake, on the social and economic consequences of collapse. Each class is characterized by an importance factor $\gamma 1$. There are four classes of building as presented in table A4 of the annex.

Peak ground acceleration values are generally available for different hazard zone in the national annex, usually through a hazard map. This value has to be corrected by the importance factors corresponding to the importance class of the buildings.

The damping ratio depends on the material used and the structural type of the building. For a concrete building, the Eurocode 8 uses a default damping ratio ξ of 5%. The correction factor is obtained by equation 2.5.

$$\eta = \sqrt{\frac{10}{5+\xi}} \tag{2.5}$$

$$for\ \xi = 5\%$$

2.4.2. Combination of actions

A combination of actions defines a set of values used for the verification of the structural reliability for a limit state under the simultaneous influence of different actions. In the case of a building, they are defined by:

The fundamental combination, used for the Ultimate Limit State (ULS) associated with collapse or other similar forms of structural failure is expressed in equation 2.6.

$$\sum_{j\geq 1} \gamma_{G,j} G_{k,j} + \gamma_{Q,1} Q_{k,1} + \sum_{i\geq 1} \gamma_{Q,i} \Psi_{0,i} Q_{k,i} \quad (2.6)$$

Where the coefficients $\gamma_{G,j}$ and $\gamma_{Q,i}$ are partials factors which minimize the action which tends to reduce the solicitations and maximize the one which tends to increase it. The recommended values preconized by the Eurocode 0 for the structural and Geotechnical (STR and GEO) verifications are:

$\gamma_{G,jsup}$ =1.35

$\gamma_{G,jinf}$ =1

$\gamma_{Q,1}$ =1.50 Where unfavourable (0 where favourable)

$\gamma_{Q,i}$ =1.50 Where unfavourable (0 where favourable)

The characteristic combination for rare and quasi permanent loading used for non-reversible serviceability limit states is expressed in equation 2.7. This Equation is to be used in the verifications of the allowable stress and deflections.

$$\sum_{j\geq 1} G_{k,j} + Q_{k,1} + \sum_{i\geq 1} \Psi_{0,i} Q_{k,i} \quad (2.7)$$

The seismic combination used for the ultimate and serviceability limit state is expressed in equation 2.8.

$$\sum_{j\geq 1} G_{k,j} + E + \sum_{i\geq 1} \Psi_{2,i} Q_{k,i} \quad (2.8)$$

Ψ is the combination factor that is function of the category of the building. The recommended values by the Eurocode 0 are presented in the table A6 of the annex.

With:

$G_{k,j}$ is the characteristic value of the permanent action j

$Q_{k,1}$ is the characteristic value of the leading variable action 1

$Q_{k,i}$ is the characteristic value of the accompanying variable action i

E is a combination of the effects of the horizontal components of the seismic action

The inertial effects of the design seismic action shall be evaluated by taking into account the presence of the masses associated with all gravity loads appearing in the following combination of actions in equation 2.9.

$$G_{1k} + G_{2k} + \Psi_{E,i} Q_k \quad (2.9)$$

Where:

$\Psi_{E,i}$ is the combination coefficient for variable action defined by equation 2.10

$$\Psi_{E,i} = \varphi . \Psi_{2,i} \quad (2.10)$$

Where φ is a combination factor that is function of the storey occupancy. The recommended values of the Eurocode 8 are presented in table A5 of the annex.

Figure 2.3. Interface of the software ETABS 18

2.5. Static design methodology

The static analysis of the building is done by the definition of the concrete cover, the design and the verification of a portion of slab, one horizontal element and one vertical element which are going to be considered as representative of the other elements of the structure.

2.5.1. Durability and concrete cover to reinforcement

To ensure the required design working life of the structure (see table A7 of the annex), it is necessary to protect each structural element against the environmental action. For concrete structures, the Eurocode 2 ensured this protection by the definition of a concrete cover taking into account the structural class of the structure and the exposure class. This concrete cover is defined as the distance between the surface of the reinforcement closest to the nearest concrete surface and the nearest concrete surface (figure 2.4).

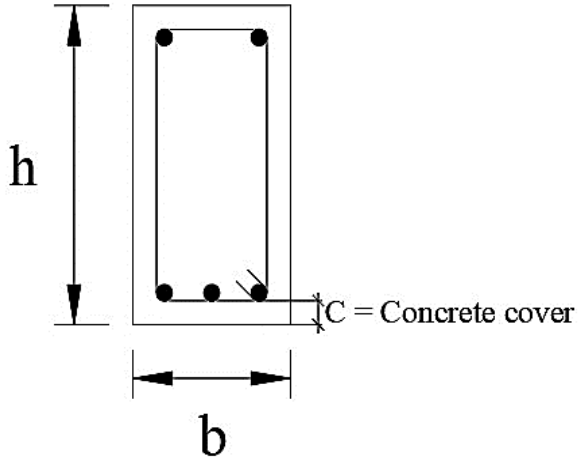

Figure 2.4. Illustration of the concrete cover

The nominal value of the concrete cover is defined as a minimum cover C_{min} plus an allowance in design for deviation. The minimum cover C_{min} is define by equation 2.11.

$$C_{min} = max\left(C_{min,b}; C_{min,dur} + \Delta C_{dur,\gamma} - \Delta C_{dur,st} - \Delta C_{dur,add}; 10\right) \quad (2.11)$$

With:

$C_{min,b}$ is the minimum cover due to bond requirement, equal to the diameter of the bars or the equivalent diameter in the case of bundled bars

$\Delta C_{dur,\gamma}$ is the additive safety element with a recommended value of 0 mm

$\Delta C_{dur,st}$ reduction of minimum cover for use of stainless steel

$\Delta C_{dur,add}$ is the add reduction of minimum cover for use of additional protection

$C_{min,dur}$ is the minimum cover due to environmental conditions obtain from the table A8 of the annex A in function of the exposure and the structural class of the building

The nominal value of the concrete cover is expressed by equation 2.12.

$$C_{nom} = C_{min} + \Delta C_{dev} \quad (2.12)$$

Where:

C_{min} is the minimum concrete cover

ΔC_{dev} is the allowance in design for deviation with a recommended value of 10 mm

2.5.2. Design of slabs

In this section we are going to design two different types of slabs: a hollow block slab and a two-way slab supported by beams which are the most used types of slabs in Cameroon.

2.5.2.1. Two-way slab supported by beams

The design of this type of slab consist of finding the proportion of charges acting on the slab in the x and y direction. For this we are going to use the method of Grashoff.

a. Preliminary design of slab

The preliminary design is done according to the deflection condition in equation 2.13.

$$h > \frac{L}{25} \quad (2.13)$$

From which we have:

$$h_t > \frac{L_{max}}{25}$$

With: $L_{max} = \max\left(L_{max,x}\ ;\ L_{max,y}\right)$

Where:

h_t is the thickness of slab

$L_{max,x}$ is the length of longest span

b. Grashoff method

For a reinforced concrete slab of dimension $l_x \times l_y$ carrying loads along the x and y axes, the method of Grashoff used to have the proportion of charges is as follows:

The surface loads acting on the slab are considered on for a 1m strip of slab. The loads acting on the 1m strip of the slab are brought back to linear loads (q) by multiplying the surface loads by the width of the strip which is 1m (equation 2.14). The above procedure is done in the x and y directions and illustrated in figure 2.5.

$$q = (G_1 + G_2 + Q_k) \times 1\ m \tag{2.14}$$

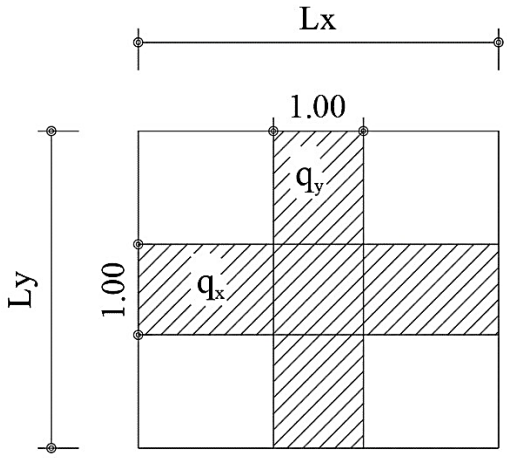

Figure 2.5. Illustration of Grashoff's method

The proportion of loads acting along the x and y axes (q_x and q_y) are calculated using the equation of Grashoff (equations 2.15 and 2.16)

$$q_x = \frac{l_y^4}{l_y^4 + l_x^4} q \tag{2.15}$$

$$q_y = \frac{l_x^4}{l_y^4 + l_x^4} q \tag{2.16}$$

Where:

q_x: proportion of loads acting on the slab along the x-axis

q_y: proportion of loads acting on the slab along the y-axis

l_x: Dimension of slab along the x-axis

l_y: Dimension of slab along the y-axis

With the value of q_x and q_y the 1m strip of slab is designed along the x and y axes respectively. The design is like that of a beam subjected to a uniformly distributed linear load.

c. Ultimate Limit State Design

The ULS design of this element will be done for the bending moment and the shear force solicitations since there is not axial force on the element.

i. Bending moment design

For the longitudinal reinforcements, knowing the solicitation curve, the steel reinforcement is compute for a rectangular section with the height h, the width b and the effective depth d as shown in figure 2.6.

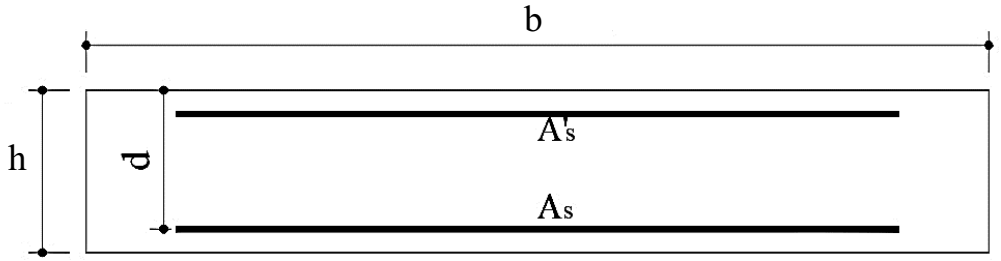

Figure 2.6. Section of 1meter strip of slab

The section of steel at each point of the beam is estimated using equation 2.17.

$$A_s = \frac{M_{Ed}}{0.9 d f_{yd}} \tag{2.17}$$

The section obtained has to verify the detailing of beams prescribed by the Eurocode2 which defines the maximum and the minimum reinforcement areas by the equation 2.18 and 2.19 respectively.

$$A_{s,max} = 0.004 A_c \tag{2.18}$$

$$A_{s,min} = max\left(0.26 \frac{f_{ctm}}{f_{yk}} b_t d \; ; 0.0013 b_t d\right) \tag{2.19}$$

Where:

b_t is the Mean width of the tension zone

d is the is the effective depth of the section

f_{ctm} Is the tensile strength of the concrete

A_c is the concrete section

EC2 prescribes the following limitations for the distance between the longitudinal bars:

$$s_{min} = \max \{\phi \text{ longitudinal bars} ; D_{aggregates} + 5 \text{ mm} ; 20 \text{ mm}\} \quad (2.20)$$

$$s_{max} = \min \{2.5h ; 400 \text{ mm}\} \quad (2.21)$$

An exception has to be done for regions of maximum moment and concentrated load where;

$$s_{max} = \min \{1.5h ; 250 \text{ mm}\} \quad (2.22)$$

With:

s_{min} is the minimum longitudinal bar spacing

s_{max} is the maximum longitudinal bar spacing

$D_{aggregates}$ is the diameter of the aggregates

h is the thickness of the slab section

The steel reinforcement section defined, the effective area of the steel reinforcement is obtained by computing the number of bars necessary and the corresponding area. The verification of the section is done by calculating the resisting bending moment of the section using the position of the neutral axis inside the section. This neutral axis is obtained using equation 2.23.

$$x = \frac{d}{2\beta_2} - \sqrt{\left(\frac{d}{2\beta_2}\right)^2 - \frac{M_{Ed}}{\beta_1 \beta_2 b f_{cd}}} \quad (2.23)$$

Where:

b is the width of the section

f_{cd} is the design compressive strength of the concrete

$\beta_1 \text{ and } \beta_2$ is a correction factor equal to 0.81 and 0.41 respectively

M_{Ed} is the moment acting on the section

The resisting moment is then given by equation 2.24

$$M_{Rd} = A_{s,eff} f_{yd} (d - \beta_2 x) \quad (2.24)$$

Where:

$A_{s,eff}$ is the effective area of the steel section

f_{yd} is the design yielding strength of steel

ii. Shear verification

From the envelope curve of the shear solicitation, it is verified that the acting shear V_{Ed} is less than the design shear resistance of our concrete section without shear reinforcement $V_{Rd,c}$ which is defined by equation 2.25.

$$V_{Rd,c} = max\left\{\left[C_{Rd,c}K(100\rho_1 f_{ck})^{\frac{1}{3}} + K_1\sigma_{cp}\right]b_w d\ ;(V_{min} + K_1\sigma_{cp})b_w d\right\} \quad (2.25)$$

Where:

$$C_{R,dc} = \frac{0.18}{\gamma_c}$$

$$K = min\left(1 + \sqrt{\frac{200}{d}}\ ;2\right)$$

$$\rho_1 = min\left(\frac{A_{sl}}{b_w d}\ ;0.02\right)$$

$$K_1 = 0.15$$

$$\sigma_{cp} = min\left(\frac{N_{Ed}}{A_C}\ ;0.2f_{cd}\right)$$

$$V_{min} = 0.035K^{\frac{3}{2}}f_{cd}$$

b_w is the smallest width of the section in the tensile area

N_{Ed} is the axial force in the cross-section due to loading or pre-stressing (in N)

If the design shear resistance of the concrete section is greater the acting shear, then no shear reinforcement is required and the minimum shear reinforcement is applied according to the detailing of that member. For sections where the design shear resistance is less than the acting shear, then shear reinforcement is required. The shear capacity is then given by the smallest of the terms $V_{Rd,s}$ and $V_{Rd,max}$ defined by equation 2.26 and equation 2.27.

$$V_{Rd.max} = \alpha_{cw}b_w z v_1 f_{cd}(cot\theta + cot\alpha)/(1 + cot^2\theta) \quad (2.26)$$

$$V_{Rd,s} = \frac{A_{sw}}{s}zf_{ywd}(cot\theta + cot\alpha)sin\alpha \quad (2.27)$$

For stirrups α=90° the equations become

$$V_{Rd.max} = \alpha_{cw} b_w z v_1 f_{cd} \frac{sin2\theta}{2} \quad (2.28)$$

$$V_{Rd,s} = \frac{A_{sw}}{s} z f_{ywd} \cot\theta \quad (2.29)$$

Where:

α_{cw} is a coefficient tacking into account of the state of stress in the compression ($\alpha_{cw} = 1$ for non-pre-stressed)

v_1 is a reduction factor for concrete cracked in shear ($v_1 = 0.6$ for $f_{ck} \leq 60$ N/mm²)

f_{ywd} is the design yield strength of the shear reinforcement

s is the spacing of the stirrup

A_{sw} is the cross sectional area of the shear reinforcement with a maximum value given by the relation;

$$\frac{A_{sw,max} f_{ywd}}{b_w s} \leq \frac{1}{2} \alpha_{cw} v_1 f_{cd}$$

d. Serviceability Limit State Verifications

The common serviceability limits states verifications are deflection, the cracking and the stress limitation. In this section only deflection is going to be verified.

i. Deflection

Deformations of structural elements have to be limited, in order not to compromise the functionality of the structure and its appearance. Limitations are not directly related to the deflections, but to the ratio deflection/span (f/l). The Eurocode 2 gives two methods to verify deflection, either by using the limiting value of the span to effective depth ratio (l/d), or by calculating the deflection with the help of formulas given in the EC2. The first method is going to be applied in this section. This verification is done at the characteristic (quasi-permanent) combination.

From Section 7.4.2 of the EC2, the limiting span to depth ratio is calculated using equation 2.30 or 2.31, depending on mechanical parameters and on reinforcement ratio in order to do the verification without calculating deflections.

$$\frac{l}{d} = K \left[11 + 1.5\sqrt{f_{ck}} \frac{\rho_0}{\rho} + 3.2\sqrt{f_{ck}} \left(\frac{\rho_0}{\rho} - 1 \right)^{\frac{3}{2}} \right] \qquad \text{If } \rho \leq \rho_0 \quad (2.30)$$

$$\frac{l}{d} = K\left[11 + 1.5\sqrt{f_{ck}}\frac{\rho_0}{\rho - \rho'} + 3.2\sqrt{f_{ck}}\sqrt{\frac{\rho'}{\rho_0}}\right] \qquad \text{If } \rho > \rho_0 \qquad (2.31)$$

With:

l/d is the limit span/depth ratio

K is the factor that takes into account the different structural systems. Its value is obtained from table A9 in annex A

$\rho_0 = 0.001\sqrt{f_{ck}}$ is the reference reinforcement ratio

$\rho = \frac{A_s}{A_c}$ is the required tension reinforcement ratio at mid-span to resist the moment due to the design loads (at support for cantilevers)

$\rho' = \frac{A'_s}{A_c}$ is the required compression reinforcement ratio at mid-span to resist the moment due to design loads (at support for cantilevers)

The computed value of l/d is introduced in equation 2.32.

$$K \times \frac{l}{d}\ computed \times F1 \times F2 \times F3 \qquad (2.32)$$

Where $F1, F2\ and\ F3$, are coefficients determined using in table 2.1

Table 2.1. Coefficients associated to the span to depth ratio

Coefficients	Conditions and value
$F1 = 1 - 0.1\left(\left(\frac{b_f}{b_w}\right) - 1\right) \geq 0.8$	For flanged sections where the ratio of the flange width (b_f) to the rib width (b_w) exceeds 3 $F1$=1 for all other cases
$F2 = \frac{7}{l_{eff}}$ l_{eff} = span length	For beams and slabs, other than flat slabs, with spans exceeding 7 m, which support partitions liable to be damaged by excessive deflections $F2$=1 for all other cases
$F3 = \frac{310}{\sigma_s} = \frac{500}{(f_{yk}A_{s,req}/A_{s,prov})}$	

Where:

σ_s is the tensile steel stress at mid-span (at support for cantilevers) under the design load at SLS

$A_{s,prov}$ is the area of steel provided at this section

$A_{s,req}$ is the area of steel required at this section for ultimate limit state

The value obtained from equation 2.30 or 2.31, is compared to the real value of the span to depth ratio calculated using the length of the longest span and the effective depth of our slab section deflection is verified if;

$$K \times \frac{l}{d}\,(computed) \times F1 \times F2 \times F3 > \frac{l}{d}\,(real)$$

2.5.2.2. Hollow block slab

The design if this type of this type of slab consist in designing the rib and the compression table.

a. Preliminary design of slab

For the hollow block slab the preliminary design is done according to the deflection condition as presented in section 2.4.2.2.a.

After calculation of the different loads applied on the slab, the rib is modelled in the software SAP 2000 and the different loads acting on the slab are converted to linear loads and applied on the rib. The results gotten from SAP 2000 are collected in terms bending moment and shear force. They are then exported to the software excel where there are used to plot the bending moment and the shear force solicitation curves. Using the same results, the envelope curves of shear and moment are also plotted and the results are gotten at SLS and ULS.

b. Ultimate Limit State Design

The ULS design of this element will be done for the bending moment and the shear force solicitations since there is not axial force on the element.

i. Bending moment design

Knowing the envelope solicitation curve, the quantity of steel reinforcement is evaluated for a T-beam section with height h_t, flange depth h_f, flange width b_f, web depth h_w, and web width b_w (see figure 2.7).

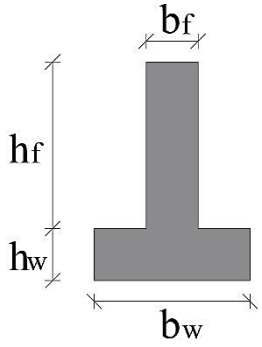

Figure 2.7. Section of rib

For the T-beam section, the position of the neutral axis is assumed to be in the flange. The resolution of equations 2.33 gives the value of the position of the neutral axis.

$$x = \frac{d}{2\beta_2} - \sqrt{\left(\frac{d}{2\beta_2}\right)^2 - \frac{M_{Ed}}{\beta_1\beta_2 b f_{cd}}} \tag{2.33}$$

The section of longitudinal reinforcement at each point of the rib is calculated using equation 2.17 in section 2.6.2.1.c.i. The section obtained has to verify the detailing of slabs prescribed by the Eurocode 2 which defines the maximum and the minimum reinforcement areas as shown in equations 2.18 and 2.19 in section 2.6.2.1.c.i.

With the longitudinal reinforcement section defined, the effective area of the steel reinforcement ($A_{s,eff}$) is obtained by computing the number of bars necessary and the corresponding area. The section is then verified by calculating the resisting moment (M_{Rd}) of the section using the real position of the neutral axis given by equation 2.34.

$$x = \frac{A_{s,eff} f_{yd}}{\beta_1 b f_{cd}} \tag{2.34}$$

The resisting moment is obtained using equation 2.24 in section 2.6.2.1.c.i.

ii. Shear verification

In order to take over the shear force acting on each section of our T-beam, transversal steel reinforcements have to be inserted inside the section as shown in figure 2.8.

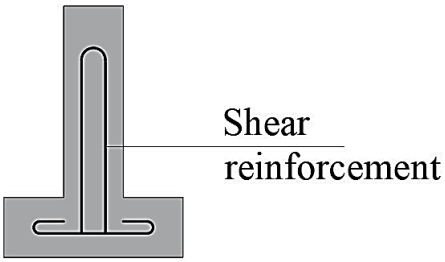

Figure 2.8. Shear reinforcement in rib

The design of shear reinforcement is done as in section 2.6.2.1.c.ii. The maximum spacing between the stirrups is given by the equation 2.35.

$$s_{max} = \min\{0.8d\ ; 333mm\} \tag{2.35}$$

c. Serviceability Limit State Verifications

The common serviceability limits states verifications are deflection, the cracking and

the stress limitation. Only deflection is going to be verified for the hollow block slab as presented in section 2.6.2.1.d.i.

2.5.3. Design of horizontal structural elements

The horizontal structural elements designed in this work will be the beam of the structure with a hollow core slab. The design will be done be performing an Ultimate Limit State (ULS) design and a Serviceability Limit State verification (SLS). The design of this element will be done through its modelling in the software SAP 2000. The definition of different loads arrangements will be done through the loads combination in the software to obtain different solicitations curves and extract the envelope curve for these solicitations.

2.5.3.1. Ultimate Limit State Design

The ULS design of this element will be done for the bending moment and the shear force solicitations only since there is no axial force acting on this element.

a. Bending moment design

Knowing the solicitation curve, the steel reinforcement is compute for a rectangular section with the height h, the width b and the effective depth d (see figure 2.9).

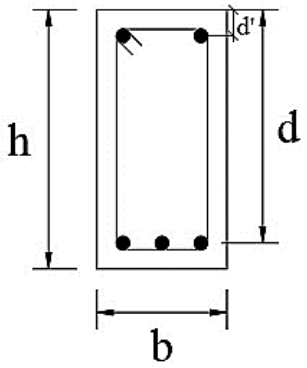

Figure 2.9. Beam section

The section of longitudinal reinforcement at each point of the rib is calculated using equation 2.17 in section 2.6.2.1.c.i. The section obtained has to verify the detailing of slabs prescribed by the Eurocode2 which defines the maximum and the minimum reinforcement areas as shown in equations 2.18 and 2.19 in section 2.6.2.1.c.i.

The steel reinforcement section defined, the effective area of the steel reinforcement is obtained by computing the number of bars necessary and the corresponding area. The verification of the section is done by calculating the resisting bending moment of the section using the position of the neutral axis inside the section (see figure 2.10) using equation 2.23 and 2.24 in section 2.4.2.1.c.i.

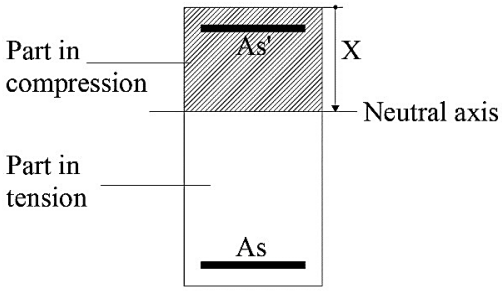

Figure 2.10. Position of neutral axis inside a section

b. Shear verification

In order to take over the shear force inside the beam, transversal steel reinforcement has to be inserted inside the section as illustrated in figure 2.11.

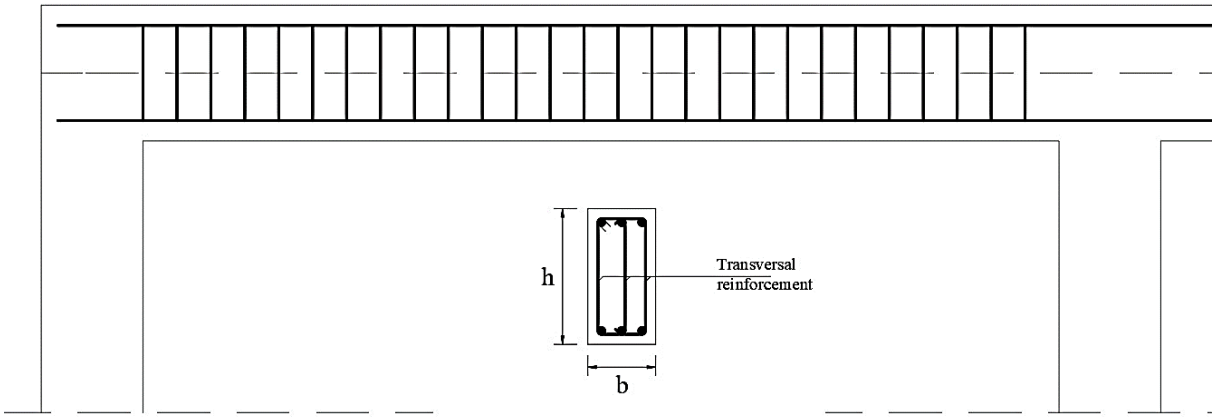

Figure 2.11. Longitudinal and transversal beam section with transversal reinforcement

From the envelope curve of the shear solicitation, the necessity of the shear reinforcement is verified by comparing the acting shear V_{Ed} to the design shear resistance of our concrete section without shear reinforcement $V_{Rd,c}$ which is defined by equation 2.25 in section 2.6.2.1.c.i.

If the design shear resistance of the concrete section is greater the acting shear, then no shear reinforcement is required and the minimum shear reinforcement is applied according to the detailing of that member. For sections where the design shear resistance is less than the acting shear, then shear reinforcement is required. The shear capacity is then given by the smallest of the terms $V_{Rd,max}$ and $V_{Rd,s}$ defined by equation 2.26 and equation 2.27 in section 2.6.2.1.c.i.

The design shear reinforcement obtained has to verify the detailing of members. In the case of the beam, it defines the maximum longitudinal spacing (s or s_l) of the shear assembly, the maximum transversal spacing (s_t) of the legs in a series of shear link and the minimum shear reinforcement ratio (ρ_w) as shown in figure 2.12. These limitations are given by equations

2.36, 2.37 and 2.38.

$$s_{l,max} = 0.75d(1 + cot\alpha) \tag{2.36}$$

$$s_{l,max} = 0.75d \leq 600\ mm \tag{2.37}$$

$$\rho_{w,min} = \frac{0.08\sqrt{f_{ck}}}{f_{yk}} \tag{2.38}$$

With the shear reinforcement ratio equal to:

$$\rho_{w,min} = \frac{A_{sw}}{s.b_w.sin\alpha} \tag{2.39}$$

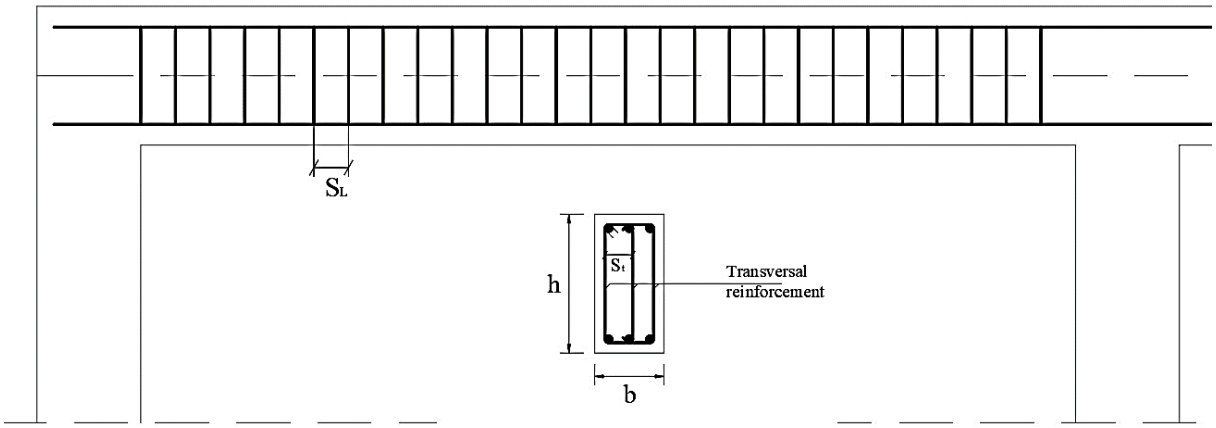

Figure 2.12. Maximum longitudinal and maximum transversal spacing of the stirrups

2.5.3.2. Serviceability Limit State Verification

The serviceability limit states (SLS) are the states beyond which requirements for the correct exercise and use of the structure are not satisfied. They model the behaviour of the structure under working loads instead of ultimate (collapse) loads (ULS). The common serviceability limit states are the stress limitation, the crack and the deflection control. In the following paragraphs, only the stress limitation is presented for the beam.

The verification of the allowable stress on the beam is done at the characteristic (rare) combination and permits to avoid inelastic deformation of the reinforcement and the formation of longitudinal cracks in concrete. The stress value is a function of the modular ratio for short term and long term loading expressed in equations 2.40 and 2.41 respectively.

$$n_0 = \frac{E_c}{E_s} \tag{2.40}$$

$$n_\infty = n_0(1 + \varphi_l \times \rho_\infty) \tag{2.41}$$

Where:

$\varphi_l = 0.55$ for shrinkage of concrete and the parameter $\rho_\infty = 2 \div 2.5$

The neutral axis position for an un-cracked concrete section is computed by equation 2.42.

$$x = \frac{-n(A'_s + A_s) + \sqrt{[n(A'_s + A_s)]^2 + 2bn(A'_s d' + A_s d)}}{b} \tag{2.42}$$

Where A'_s, A_s, are the upper and lower steel reinforcement inside the section respectively. b, d' and d are the geometrical characteristics of the section presented in the figure 2.13.

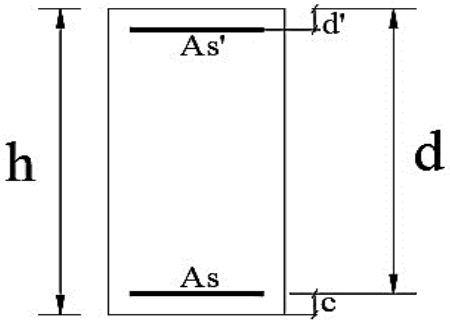

Figure 2.13. Transversal section of the beam with its different characteristics

The moment of inertia of the un-cracked section is given by equation 2.56.

$$J_{cr} = \frac{bx^3}{3} + nA_s(d - x)^2 + nA'_s(x - c)^2 \tag{2.43}$$

The stress in the concrete and in the steel reinforcement in tension are then obtained using equations 2.44 and 2.45.

$$\sigma_s = \frac{M_{ser}(d - x)}{J_{cr}} \times n_0 \tag{2.44}$$

$$\sigma'_s = \frac{M_{ser}(d' - x)}{J_{cr}} \times n_0$$

$$\sigma_c = \frac{M_{ser}.x}{J_{cr}} \tag{2.45}$$

With:

M_{ser} is the maximum bending moment at SLS

The Eurocode 2 limitation of these stresses as presented in the equations 2.60 and 2.61.

$$\sigma_c \leq 0.6 f_{ck} \tag{2.46}$$

$$\sigma_s \leq 0.8 f_{yk} \tag{2.47}$$

2.5.4. Design of vertical structural elements

The vertical structural element to be designed here is the column of the structure with the slab with embedded elements. For the column design, a 3D modelling of the whole structure is done on the software SAP 2000. The design is done at ULS for axial force, bending moment and shear verification. As for the verifications, slenderness is going to be verified. The verification of the shear force is the same for the beam but the procedure will not be detailed here but the detailing of members will be presented.

2.5.4.1. Preliminary design of column

The preliminary design of the column is done in two steps. The first step is based the axial loads resistance to determine the minimum area section and the second one on the modal analysis of the 3D model of the structure to verify the global dynamic behaviour.

a. Axial load resistance of the section

In a seismic area, the preliminary design of the column considers that 60% of the concrete resistance is used to take over the axial force. Then we can estimate the minimum area section of the column using equation 2.48.

$$N_{Rd} = 0.6 f_{cd} \times A_c \geq N_{sd} \tag{2.48}$$

Where:

N_{sd} is the axial load compute using the recovery area of the column

The axial loa acting on the section of the column is computed using equation 2.49.

$$N_{sd} = q \times S_r \times n \tag{2.49}$$

Where:

q is the uniform distributed loads on each floor compute at ULS combination

S_r is the recovery area of the column

n is the number of floor of the building

b. Modal analysis of the structure

The modal analysis of the structure permits an estimation of the section of the vertical element through the verification of the vibration modes of the structure and the period of the first vibration.

For this structure which is a 6-storey reinforced concrete building with the total height of 21m above the foundations, the fundamental period of the building is given equation 2.50.

$$T_1 = C_t H^{3/4} \tag{2.50}$$

Where:

C_t is equal to 0,075 for concrete frames

H is the total height of the building above the foundations

2.5.4.2. Bending moment and axial force verification

The envelope of the bending moment and the axial force solicitations obtained, the design is done through the M-N interaction diagram. For each level, we have to ensure that the maximum M-N solicitation belong to the M-N interaction diagram of the section considered.

The interaction diagram is a diagram that shows all the limit situation that can determine the failure of the section. The points which are lying onto the diagram represent the limit configuration and beyond them, failure occurs. This diagram is computed by determining some significant points. The procedure is presented below considering a rectangular section presented in figure 2.14.

a. First point

The section is completely subjected to tension, hence, the concrete is not reacting. We impose $\varepsilon_s = \varepsilon_{su}$, $\varepsilon_{s'} = \varepsilon_{syd}$ then the stress inside the element correspond to the design yielding strength of the steel reinforcement. The limit axial force and bending moment are obtained from the equations 2.51 and 2.52.

$$N_{Rd} = f_{yd}.A_s + f_{yd}.A'_s \tag{2.51}$$

$$M_{Rd} = f_{yd}.A_s\left(d - \frac{h}{2}\right) - f_{yd}.A'_s\left(\frac{h}{2} - d'\right) \tag{2.52}$$

b. Second point

The section is completely subjected to tension. We impose: $\varepsilon_s=\varepsilon_{su}$, $\varepsilon_c=0$. We should verify if the upper steel is yielded or not by determining the strain $\varepsilon_{s'}$. The limit axial force and bending moment are obtained from the equations 2.51 and 2.52.

c. Third point

We impose that the failure is due to concrete and the lower reinforcement is yielded. We assume $\varepsilon_s \geq \varepsilon_{syd}$, $\varepsilon_c = \varepsilon_{cu2}$ and we determine the neutral axis position using equation 2.53. Using the value obtained for the position of the neutral axis, we verify if the upper steel has yielded or not by determining the strain $\varepsilon s'$ (equation 2.54) in order to determine the corresponding stress. The limit axial force and bending moment are obtained from the equations 2.55 and 2.56.

$$\frac{X}{\varepsilon_{cu}} = \frac{d}{\varepsilon_{cu} + \varepsilon_s} \tag{2.53}$$

$$\frac{\varepsilon'_s}{X - d'} = \frac{\varepsilon_{cu}}{X} \tag{2.54}$$

$$N_{Rd} = \beta_1 . b . X f_{cd} + f_{yd} A'_s - f_{yd} A_s \tag{2.55}$$

$$M_{Rd} = \beta_1 . b . X f_{cd} \left(\frac{h}{2} - \beta_2 X\right) + f_{yd} . A'_s \left(\frac{h}{2} - d'\right) + f_{yd} . A_s \left(\frac{h}{2} - d\right) \tag{2.56}$$

d. Fourth point

We impose that the failure is due to concrete and the lower reinforcement reaches exactly $\varepsilon_s=\varepsilon_{syd}$. As for the previous point, we determine the neutral axis position and the strain $\varepsilon_{s'}$ using equations 2.53 and 2.54 respectively. The limit value of the axial force and the bending moment are determined using the equations 2.55 and 2.56 above.

e. Fifth point

We impose that the failure is due to concrete and the lower reinforcement reaches exactly $\varepsilon_s=0$ then the neutral axis position is equal to the effective depth of the section. $\varepsilon_{s'}$ is obtained using equation 2.54. The limit axial force and bending moment are obtained from the equations 2.57 and 2.58.

$$N_{Rd} = \beta_1 . b . X f_{cd} + f_{yd} A'_s \tag{2.57}$$

$$M_{Rd} = \beta_1 . b . X f_{cd} \left(\frac{h}{2} - \beta_2 X\right) + f_{yd} . A'_s \left(\frac{h}{2} - d'\right) \tag{2.58}$$

f. Sixth point

We impose that the section uniformly compressed. We assume $\varepsilon_s = \varepsilon_c \geq \varepsilon_{c2}$. The limit axial force and bending moment are obtained from the equations 2.59 and 2.60.

$$N_{Rd} = b . h . f_{cd} + f_{yd} A'_s + f_{yd} A_s \tag{2.59}$$

$$M_{Rd} = f_{yd} . A'_s \left(\frac{h}{2} - d'\right) + f_{yd} . A_s \left(d - \frac{h}{2}\right) \tag{2.60}$$

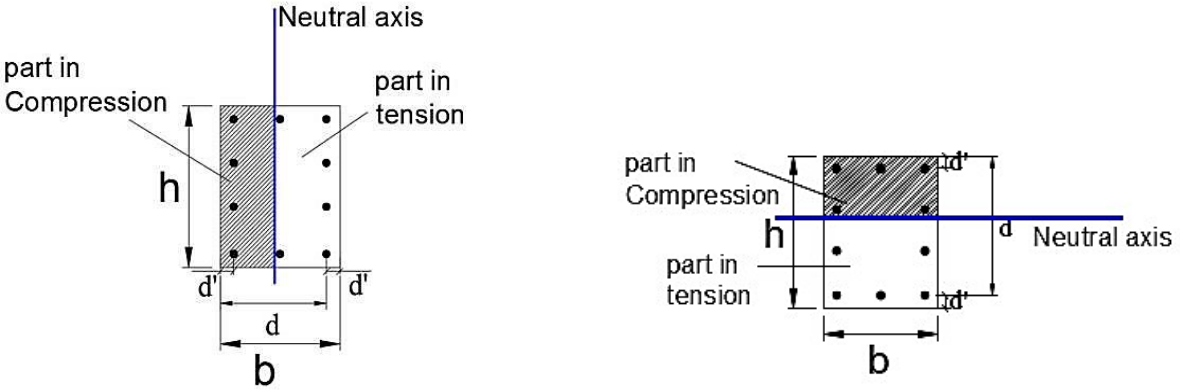

Figure 2.14. Rectangular section to illustrate the computation of the M-N diagram for different direction of the neutral axis (Djeukoua,2018).

The section of steel reinforcement in the column has to verify the limitations of the Eurocode 2 presented in equations 2.61 and 2.62:

$$A_{s,min} = \max\left(\frac{0.10 N_{Ed}}{f_{yd}} ; 0.002 A_c\right) \tag{2.61}$$

$$A_{s,max} = 0.04 A_c \tag{2.62}$$

Where:

N_{Ed} is the design axial compressive force

2.5.4.3. Shear verification

The verification procedure is the same for the beam. The detailing of members prescribed by the Eurocode 2 imposed a minimum diameter of 6mm or one quarter the maximum diameter of the longitudinal bars.

The maximum spacing of the transverse reinforcement is given by the equation 2.63.

$$S_{cl,max} = min(20\phi_{l,min}\ ;b\ ;400\ mm) \tag{2.63}$$

Where:

$\phi_{l,min}$ is the minimum diameter of the longitudinal bars

b is the lesser dimension of the column

This maximum spacing has to be reduced by a factor 0.6 in sections within a distance equal to the larger dimension of the column cross-section above or below the beam.

2.5.4.4. Slenderness verification

The slenderness verification permits to know if we have to consider the second order effect or not. It consists in verifying if the slenderness of the element is below a limit value defined by the Eurocode 2 by equation 2.64

$$\lambda_{lim} = \frac{20ABC}{\sqrt{n}} \tag{2.64}$$

Where:

$A = \frac{1}{1+0.2\varphi_{ef}}$ (φ_{ef} is the effective creep ratio; A=0.7 if φ_{ef} is not known)

$B = \sqrt{1+2\omega}$ ($\omega = \frac{A_s f_{yd}}{A_c f_{cd}}$ is the mechanical reinforcement)

$C = 1.7 - r_m$ ($r_m = \frac{M_{01}}{M_{02}}$ is the moment ratio; equal to 1 for unbraced systems)

$n = \frac{N_{Ed}}{A_c f_{cd}}$ is the relative normal force

The slenderness of an elements is evaluated using equation 2.65.

$$\lambda_{lim} = \frac{l_0}{i} \tag{2.65}$$

Where:

l_0 is the effective length of the element (l_0=0.7l)

i is the gyration radius of the un-cracked concrete section

The gyration radius of the un-cracked concrete section is given equation 2.66.

$$i = \sqrt{\frac{I}{A}} \tag{2.66}$$

Where I is the moment of inertia and A is the area of the un-cracked section

2.6. Soil structure interaction

Soil-structure interaction is defined as the process in which the response from the soil influences the motion of the structure and the response of the given structure affects the response from the soil. Thus, it is particularly important to consider this parameter in the analysis of the structure. The adopted method to represent the soil-foundation-structure interaction is the sub-structure approach. The footing sections first need to be evaluated and then the stiffness of the soil springs will also be determined according to the soil characteristics.

2.6.1. Evaluation of the footing section

The area of the section of footing can be evaluated using the axial load and the soil bearing capacity as shown in equation 2.67.

$$A = \frac{N_{Ed}}{\sigma_{adm}} \tag{2.67}$$

With:

A is the area of the footing

N_{Ed} is the axial load acting on the footing

σ_{adm} is the soil bearing capacity

With the area of the section of footing, the dimensions ($L \times$ B) are determined with respect to the dimensions of the column ($l \times$ b) according to equations 2.68 and 2.69.

$$A = \text{L} \times \text{B} \tag{2.68}$$

$$\frac{l}{b} = \frac{L}{B} \tag{2.69}$$

With:

L is the length of the footing

B is the width of the footing

l is the length of the column section

b is the width of the column

The thickness of the footing H is then obtained using the flexible footing condition shown in equation 2.70. An illustration of the footing is shown in figure 2.15.

$$H = \max\left(\frac{L-l}{4}; \frac{B-b}{4}\right) \tag{2.70}$$

The section of footing defined, we verify the pressure exerted by the structure on the soil (σ_{soll}) is less than the soil bearing capacity (σ_{adm})

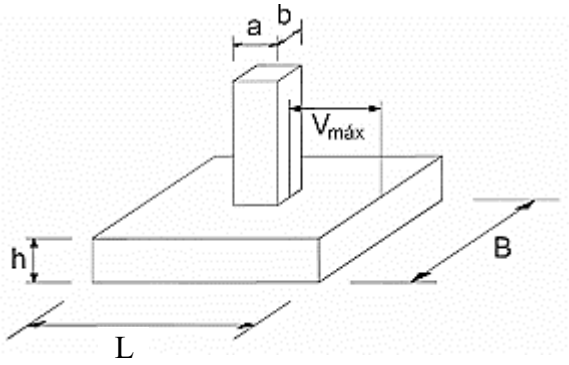

Figure 2.15. Isolated footing (www. http://www.tocasa.es/ingeniero)

2.6.2. Soil springs

The adopted method to represent the soil-foundation-structure interaction is the sub-structure approach. This approach required to use linear springs associated to the structure as shown in figure 2.16.

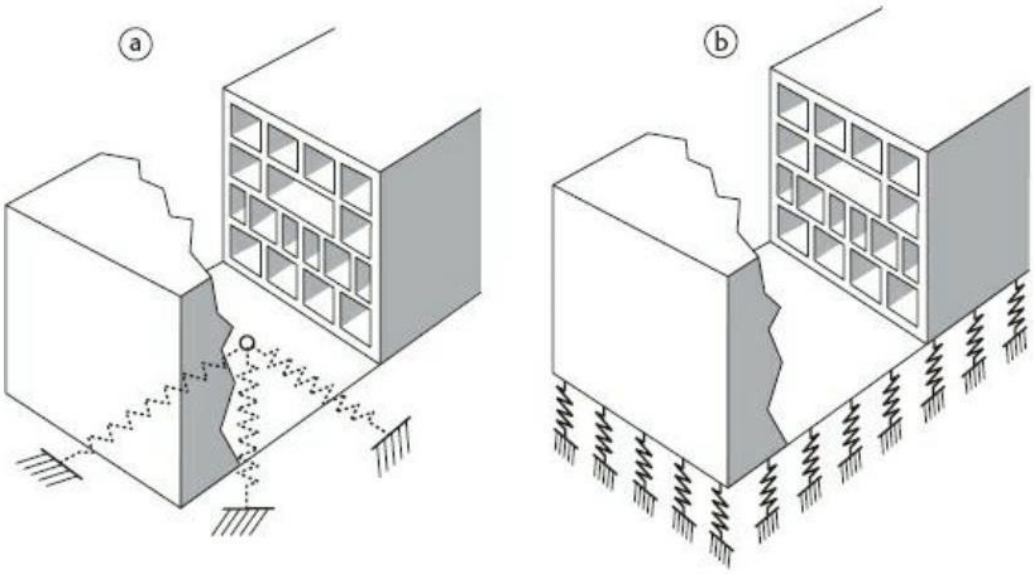

Figure 2.16. Soil modeling by a linear springs system: (a) concentrated spring (b) distributed springs (Djeukoua 2017)

In the case of this study the distributed spring system will be used. The characteristics of these springs being function the soil properties and the interaction surface between the soil

and the building.

In the case of a rectangular foundations located on the surface or embedded within a uniform soil the computing of the vertical stiffness k_Z (assigned as area stifness) and the two translational stiffness is done using equations 2.71 and 2.72 respectively.

$$K_z = C \quad \text{(in KN/m²)} \tag{2.71}$$

$$K_y = K_x = C \times H \times L_f \tag{2.72}$$

Where:

- C is the subgrade modulus of the soil obtained in table A10 of annex
- H is the thickness of the footing
- L_f is the influence width of the spring

For a rectangular section $K_y and\ K_x$ may not be equal since the influence width can be different for each side.

With the values of the spring stiffness obtained, they are assigned to the footings of the model. After analysis the new solicitations at the footings and the soil bearing are obtained.

2.7. Ground motion selection

The structural model will be subjected to the 1995 Kobe earthquake acceleration record. This earthquake has been chosen by the International Association for Structural Control and Monitoring for benchmark seismic studies. This record is downloaded from the website of the Pacific Earthquake Engineering Research center (PEER). The time history of the Kobe is shown in the figure 2.17.

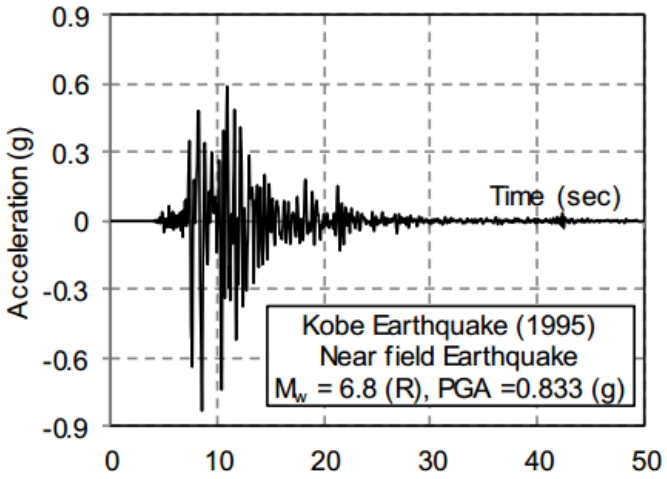

Figure 2.17. Horizontal component of the 1995 Kobe earthquake (Van Nguyen et al, 2017).

2.8. Analysis criteria

The results of the study will be analysed on five parameters which are the period of vibration modes of the structure, the story displacements, the inter-story drift ratio, the story shears and the torsional moments.

2.8.1. Modelling of the structure

Using the software SAP2000 version 22 and ETABS version 18, the structure was modelled in other to perform the static and dynamic analyses.

2.8.1.1. In SAP2000 22

The first part of the structural analysis is performed with the software SAP2000 which is a structural design software through the finite element method specially dedicated to the analysis of the stability and the resistance of structures. Only the static analyses under the effect of vertical loads were done with this software, in order to perform the static design of the structure. The load induced by the slabs are distributed and directly applied on the beams as well as the linear loads provided by the external wall as distributed frame loads. The beams and the columns of the structure are modelled as frame elements. The connection between these elements is done through the insertion of joints between the elements.

2.8.1.2. In ETABS 18

The second part of the analysis is performed in ETABS 18 which is a structural design software through the finite element method specially dedicated to the analysis of the stability and the resistance of buildings. The dynamic analysis done with this software are the modal analysis and the response spectrum analysis for seismic action. Load induces by the seismic actions induce a seismic response of the building which can be observed through different parameters. The load induced by the slabs are distributed and directly applied on the beams as well as the linear loads provided by the external wall as distributed frame loads. The beams and the columns of the structure are modelled as frame elements. The connection between these elements is done through the insertion of joints between the two elements. In the case of rigid slabs, they are modelled by affecting a rigid diaphragm to all the joints belonging to the x-y plane of the slab and for flexible diaphragms, they are modelled by affecting no diaphragm to the joints.

A total of three analyses were performed, one static analysis and two dynamic analyses. The static analysis was done on the software SAAP 2000 to perform the static design of the structure. The dynamic analyses were done on ETABS to extract the dynamic characteristics of the structure and the results of the response of the building under seismic actions.

2.8.2. Period of vibration modes

The fundamental period of a building is an inherent property which depends on the properties of the structure. In seismic zone, the spectral acceleration of a building is function of this period of the structure then these properties of the structure can increase or reduce this spectral acceleration and then become an important parameter in the response of a structure.

Some empirical formulas permit to estimate this period. It's the case of the one defined by the Eurocode 8 for buildings with heights up to 40m expressed in equation 2.73

$$T_1 = C_t H^{3/4} \tag{2.73}$$

Where:

C_t is a coefficient that depends on the type of lateral load resisting system

H is the total height of the building above the foundations

The real values of this properties of the building are obtained through a dynamic analysis of the structure and this parameter is associated to a mode shape (vibration mode) and a mass participating ratio. The mode shape of the structure describes the configurations into which a structure will deform naturally while the mass participation ratio indicated the contribution of this mode shapes to the structural response. The vibration mode hence indicates the deformations modes of the structure.

2.8.3. Story displacement

The storey displacement is the absolute value of displacement of the storey with respect to the base of the structure, under action of the lateral forces. It permits also a proper estimation of the separation distance between buildings. Figure 2.15 shows the displacement of the last storey of the top of the building.

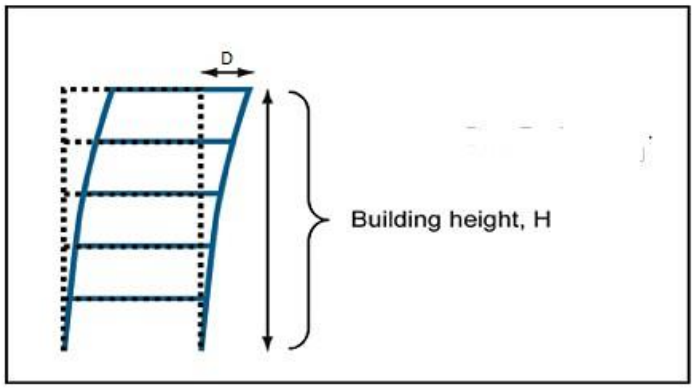

Figure 2.18. Storey displacement of the top of the building (Zahura et al, 2016)

The total displacements must be controlled to mitigate the effects of secondary P-Δ effects and overall stability of the building. In seismic design, this displacement can affect both

the structural elements that are part of the lateral force resisting system and structural elements that are not part of the lateral force resisting system.

2.8.4. Inter story drift ratio

Inter-story drift represents one the most important parameter to be analysed as they are strictly connected to the damage suffered by both structural and non-structural elements. The inter-story drift has been employed as an index to evaluate the deformation capacity of a building and to further determine its performance. This parameter is evaluated as the difference of the average lateral displacements at the top and the bottom of a storey.

The limitation of the inter-storey drift by the Eurocode 8 for buildings having non-structural elements of brittle material attached to the structure is given by the equation 2.74.

$$d_r v \leq 0.005h \tag{2.74}$$

Where:

d_r is the design inter-storey drift as defined by equation 2.75.

$$d_r = d_{i+1} - d_i \tag{2.75}$$

d_{i+1} is the story displacement at the (i+1) level

d_i is the story displacement at the (i) level

v is a reduction factor that depends on the importance class of the building

h is the storey height

2.8.5. Base shear and storey forces

The total design lateral force at the base of a structure is the base shear. The base shear is the total inertial force acting at the base of the building under the effect of a lateral load. The seismic response of the structure in terms of the base shear as well as internal forces over the height of the structural elements is selected as response parameters of interest as they are generally considered the most important response parameters in seismic design practice.

The EC8 prescribes a formula (equation 2.76) to calculate the base shear generated at the base of a structure. The calculated base shear is then distributed to each storey relative to its mass and displacement under seismic action. This distributed base shear at each level are the story forces given by equation 2.77.

. The aim is to see if the variation in the slab rigidity can lead to reduction in base shear and therefore story forces due to the way the slab transfers lateral loads to the VLLRS. A representation of the base shear and the story forces is shown in figure 2.19 with V being the

base shear and F_i the story force at the i-th storey.

$$F_{bk} \leq S_d(T_K) \times m_k \tag{2.76}$$

Where:

F_{bk} is the base shear generated for the corresponding mode k

S_d is the ordinate of the elastic spectrum at period T_k

T_K is the fundamental period of vibration of the mode k

m_k is the effective modal mas corresponding to the mode the mode k

The sum of the effective modal masses for the modes taken into account should amount to at least 90% of the total mass of the structure. From the base shear, the seismic force acting at each storey F_i is obtained using the expression from Eurocode 8 shown in equation 2.77.

$$F_i = F_{bk} \frac{s_i m_i}{\sum s_j m_j} \tag{2.77}$$

Where:

s_i, s_j are the displacements of masses m_i, m_j in the fundamental mode shape

m_i, m_j are the storey masses

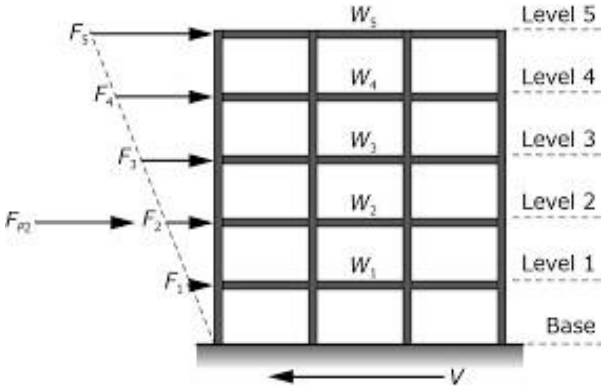

Figure 2.19. Base shear and story forces acting on structure (ASCE seismic design criteria)

2.8.6. Torsional moment

Due the plan irregularity, seismic actions generate torsional effect which causes a torsional response of the building which has some effects that can cause structural damage as described in section 1.4.1.2. The torsional moment acting at each storey i expressed in equation 2.78

$$M_{ai} = e_i \times F_i \tag{2.78}$$

Where:

M_{ai} is the torsional moment acting at story i

e_i is the total eccentricity of storey mass i

F_i is the story force acting at story i

Conclusion

This chapter had as objective to present the different codes, the different procedures that will be used in this work and the seismic performance on which will be based the analysis. The analysis will be performed using a structural analysis software SAP 2000 version 22 for the static analysis and ETABS 18 for the dynamic analysis. The different designs will be done manually through the software Excel applying the European standards. After all the different procedures have been well described, the case study will be presented, analysed statically in the software SAP 2000 following the process presented in this section and finally using the software ETABS, the rigid slab model and flexible slab model for different types of soil conditions will be compared using the previous analysis criteria.

CHAPTER 3: PRESENTATION AND INTERPRETATION OF RESULTS

Introduction

The methodology presented previously is applied on the case study and the results are highlighted here. This chapter will consist in a preliminary part in presentation of the site, presentation of the case study and the different loads and material properties considered for its analysis. This will be followed by a static and dynamic analysis in order to determine the different sections of the structural elements of the superstructure and the substructure. Finally, the results of the comparison of the seismic demands in terms of vibration periods, lateral displacement, inter-storey drift, storey shear and torsional moment for the rigid and flexible slab condition will then be presented and interpreted. Furthermore, the effect of SSI on the seismic demand in terms of vibration period, lateral displacement and story shear will also be presented for rigid and flexible slab conditions.

3.1. General presentation of the site

Here, the area of study is presented through its location, geology, relief and soil, climate, hydrology, population and socio-economic activities.

3.1.1. Geographic location

Yaoundé is the political capital of Cameroon and chief town of the Centre region; situated at latitude 3.87° (3°50') North and longitude 11.52° (11°31') East at an elevation of 760 metres above sea level. Located 300km from the Atlantic Ocean and surrounded by 7 hills, Yaoundé belongs to the Mfoundi division of the Centre region and measures a total surface area of 183km2 (18300ha).

3.1.2. Climate

Yaoundé features a tropical wet and dry climate, with record high temperatures of 36°C, an average of 23.8°C and a record low temperature of 14°C. Primarily due to the altitude, temperatures are not as high as would have been expected for a city located near the equator.
The town of Yaoundé features a lengthy rainy season covering a nine-month span between March and November. However, there is a noticeable decrease in precipitation within the rainy season, observed during the months of July and August, giving the city the appearance of having two rainy and two dry seasons. The average precipitation is 1650 mm of rain per year.

3.1.3. Relief

Concerning the relief, the land rises gently in escarpments from the southwestern coastal plain before joining the Adamawa Plateau via depressions and granite massifs. The field is characterised by rolling, forested hills, the tallest of which have bare rocky tops.

3.1.4. Geology

The bedrock in Yaoundé is mainly composed of gneiss. This rock is neither porous nor soluble, but it is its discontinuities that give fissure permeability to the formation. The hydrogeology is characterized by continuous aquifers, approximately exploitable overlying water bearing fissures or fracture aquifers in the bedrock; these types of aquifers are superimposed or isolated.

3.1.5. Socio-economic parameters

Yaoundé has a total population estimated at 3.8 million in 2019. The city of Yaoundé being a cosmopolitan city, there is a considerable portion of population coming from several other region of the country (west, far north etc.). Most of Yaoundé's economy is centred on the administrative structure of the civil services and the diplomatic services. Due to these, Yaoundé has a higher standard of living and security than the rest of Cameroon. However, Yaoundé is a tertiary city and there are a few industries: breweries, sawmills, carpentry, tobacco, paper mills, machinery and building materials.

3.2. Presentation of case study

In this section, the case-study will be described, the properties of the materials used will be presented and finally the different actions on the building will be outlined.

3.2.1. Description of case study

The case study is a six-storey reinforced concrete residential building for hotel use. A distribution plan of the building to be use as a hotel is presented in figure 3.1 followed by the plan views of the form work plan of the structure for the two different types of slabs, are presented in figure 3.2 and 3.3. The structure is a C-shaped building symmetric along the y-axis. The building is irregular in plan and regular in elevation. A vertical section of the building is presented in figure 3.4.

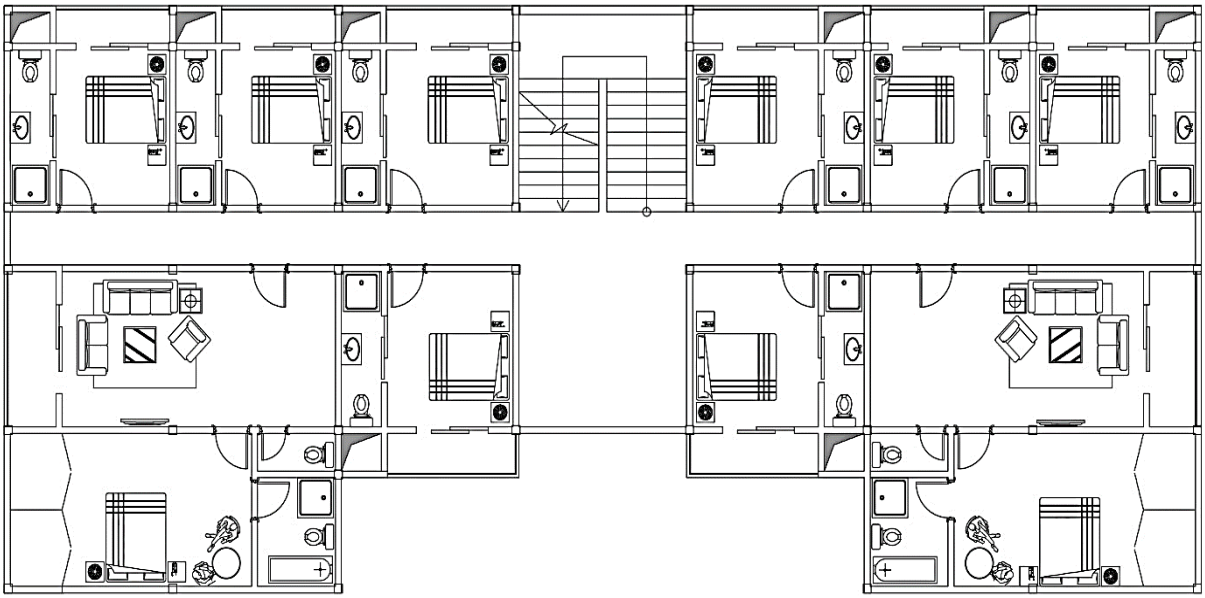

Figure 3.1. Distribution plan of building to be used as a hotel

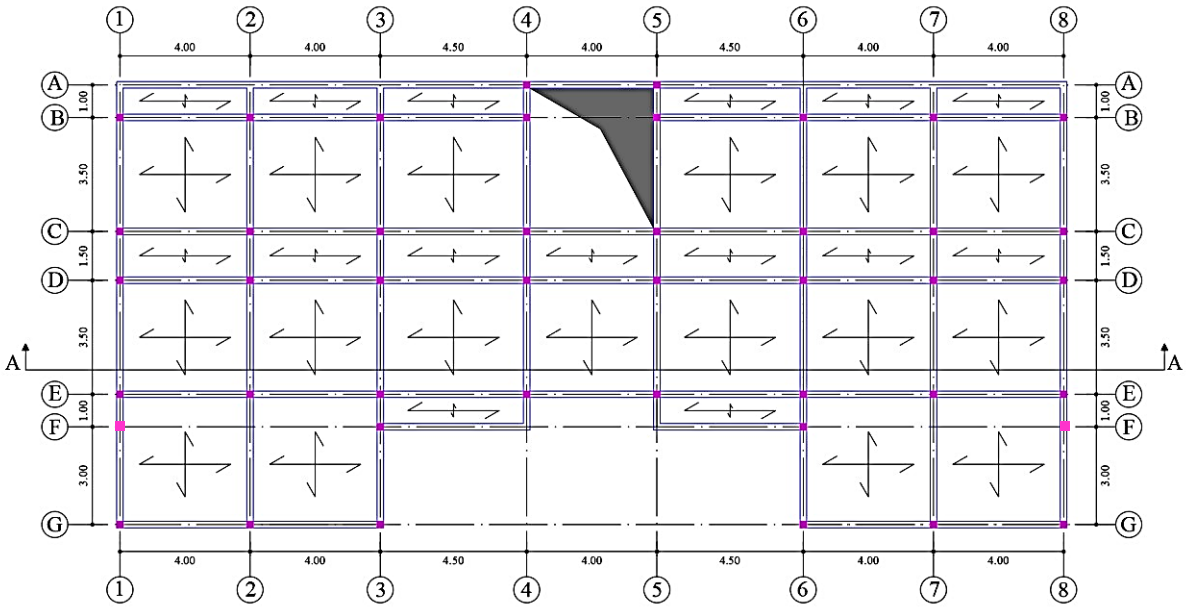

Figure 3.2. Formwork plan of case study with Two-way RC slab

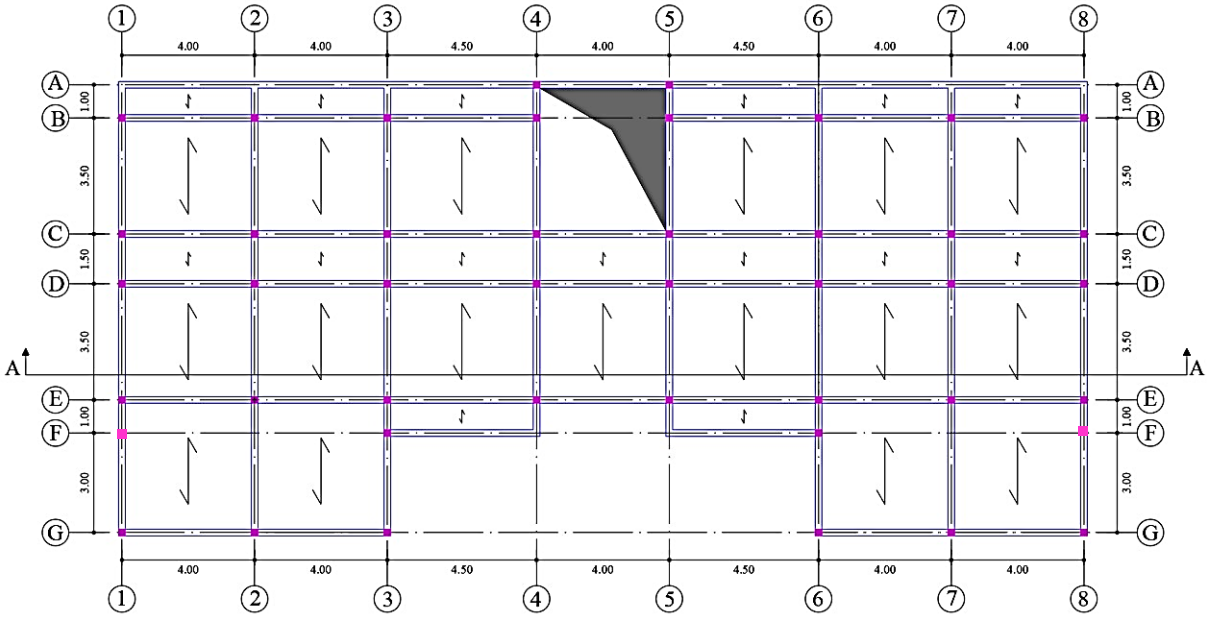

Figure 3.3. slab Formwork plan of case study with RC Slab with embedded elements

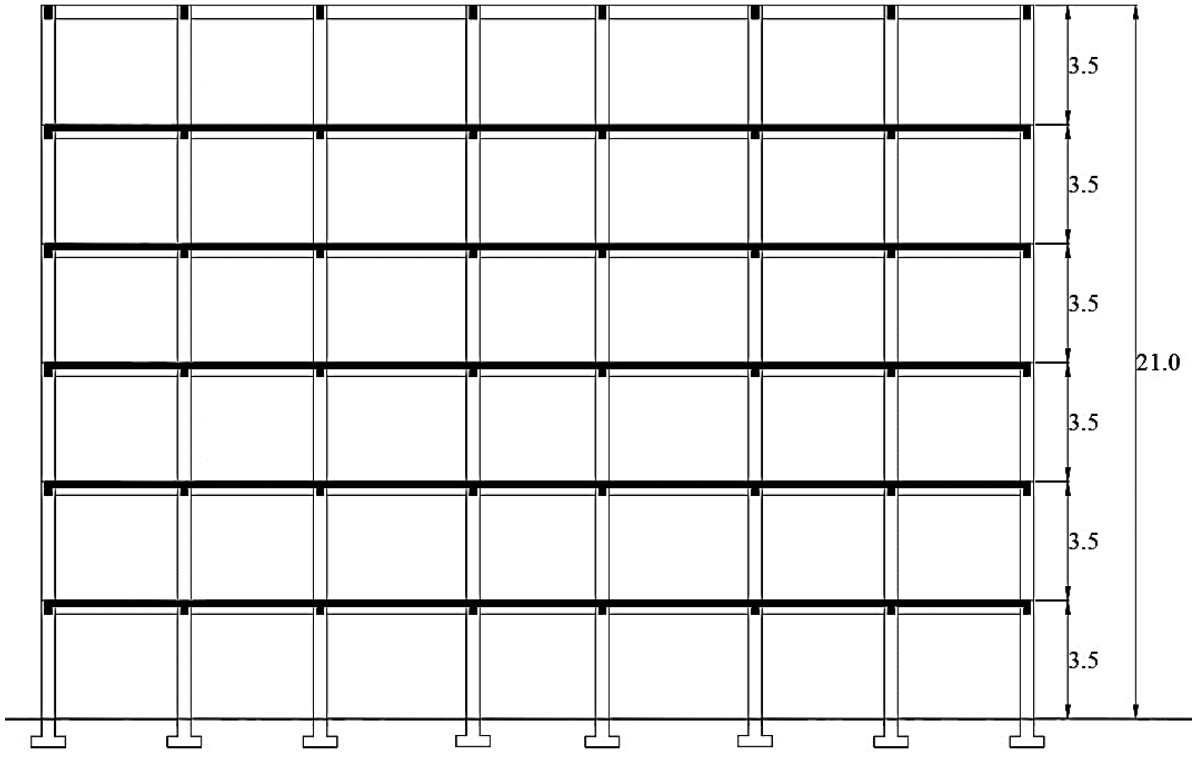

Figure 3.4. Vertical section of the formwork (section A-A)

3.2.2. Material properties

For the analysis of our building the class of concrete adopted is C25/30 and the longitudinal steel reinforcement is B400C. For the transversal reinforcement, we consider a characteristic yield strength of 235 N/mm. The main characteristics of these materials for linear analysis and design of the structure are given in table 3.1 for the concrete and table 3.2 for the steel reinforcement.

Table 3.1. Concrete characteristics

Property	Value	Unit	Definition
Class	C25/30		Concrete class
f_{ck}	25	N/mm²	Characteristic compressive strength at 28 days
$f_{cm} = f_{ck} + 8$	33	N/mm²	Mean value of concrete cylinder compressive strength
γ_c	1.5	-	Partial safety factor for concrete
$f_{cd} = \alpha_{cc} f_{ck} / \gamma_c$	14.17	N/mm²	Design value of compressive strength
$f_{ctm} = 0.3 \times (f_{ck})^{2/3}$	2.56	N/mm²	Mean value of axial tensile strength of concrete
$f_{ctd} = 0.7 \times f_{ctm} / \gamma_c$	1.2	N/mm²	Design resistance in traction
$E_{cm} = 22000 \times (f_{cm}/10)^{0.3}$	31 476	N/mm²	Secant modulus of elasticity
v	0.2	-	Poisson ratio
G	13115	N/mm2	Shear modulus
γ	25	KN/m^3	Specific weight of concrete

Table 3.2. Longitudinal bars and shear reinforcement characteristics

Property	Value	Unit	Definition
Class	B400C	-	Steel class
f_{yk}	400	N/mm²	Characteristic yield strength of steel
γ_s	1.15	-	Partial safety factor
$f_{yd} = f_{yk} / \gamma_s$	347.83	N/mm²	Design yielding strength
E_s	210 000	N/mm²	Secant modulus of elasticity
γ	78.5	kN/m3	Specific weight of steel
v	0.3	-	Poission's ratio

3.3. Actions on the building and load combinations

Based on the European standards, the actions and the load combinations used for the design of our structure are presented below.

3.3.1. Actions

The different loads acting on the building are the permanent loads, the imposed loads and the loads due to seismic action.

3.3.1.1. Permanent actions

The permanent loads acting on the building are of two categories; structural loads (table 3.3) and non-structural loads (table 3.4).

Table 3.3. Structural loads on the building

Nature	Description	Value	Unit
G_{1k}	Two-way slab of thickness 18cm	4.5	kN/m²
G_{1k}	Slab with embedded elements of thickness 20cm	2.85	kN/m²

Table 3.4. Non-structural loads acting on the building

Nature	Description	Value	Unit
G_{2k}	Tiles (2cm) 0.2 KN/m² per cm	0.4	kN/m²
G_{2k}	Cement mortar (2cm) 0.2 KN/m² per cm	0.4	kN/m²
G_{2k}	Partition walls	1	kN/m²
G_{2k}	Coated under slab (2.5cm) 0.18 KN/m² per cm	0.45	kN/m²
Total G_{2k}		2.25	kN/m²

3.3.1.2. Imposed actions

The use of the building is a residential building for which the imposed loads ranges between 1.5 to 2 kN/m². We are going to consider an imposed load of 2 kN/m².

3.3.1.3. Seismic action

For the application of the seismic action, ground type D will be considered. This ground type corresponds to a deposit of loose to medium cohesion less (with or without some soft cohesive layers) or of predominantly soft to firm cohesive soil. With the choice of the ground type, the values of the soil factor, T_B, T_C and T_D are obtained from table A2 in the annex. The building is classified as importance class II and the corresponding importance factor amounts to $\gamma I = 1.0$. The peak ground acceleration $a_g R$ is considered to be equal to 0.29g. The design ground acceleration on type D ground a_g is defined as;

$$a_g = \gamma I \times a_g R = 1.0 \times 0.29g = 0.29g$$

Table 3.5. Input data for the elastic spectrum

Ground type	Damping	Soil factor S	a_g	T_B	T_C	T_D	Behaviour factor q
-	%	-	g	s	s	s	-
D	5	1.35	0.3	0.2	0.8	2	1

Using these parameters, the equations 2.1 to 2.4 are applied to obtain the elastic response spectrum function of the project. This function is generated using the software ETABS as presented in figure 3.5 and the data obtained is represented on the software Excel for a better use as shown in figure 3.6.

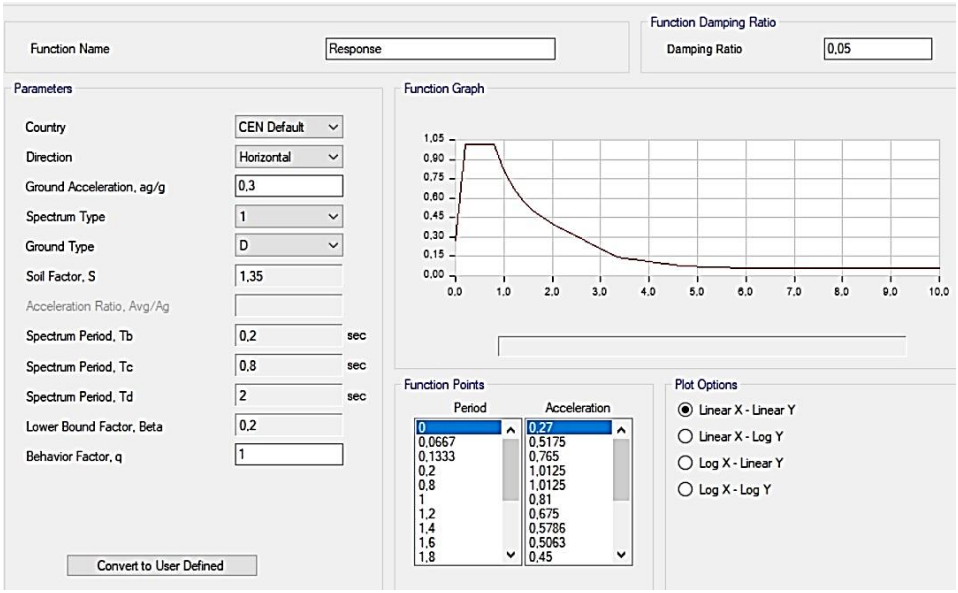

Figure 3.5. Horizontal elastic response spectrum from the software ETABS 18

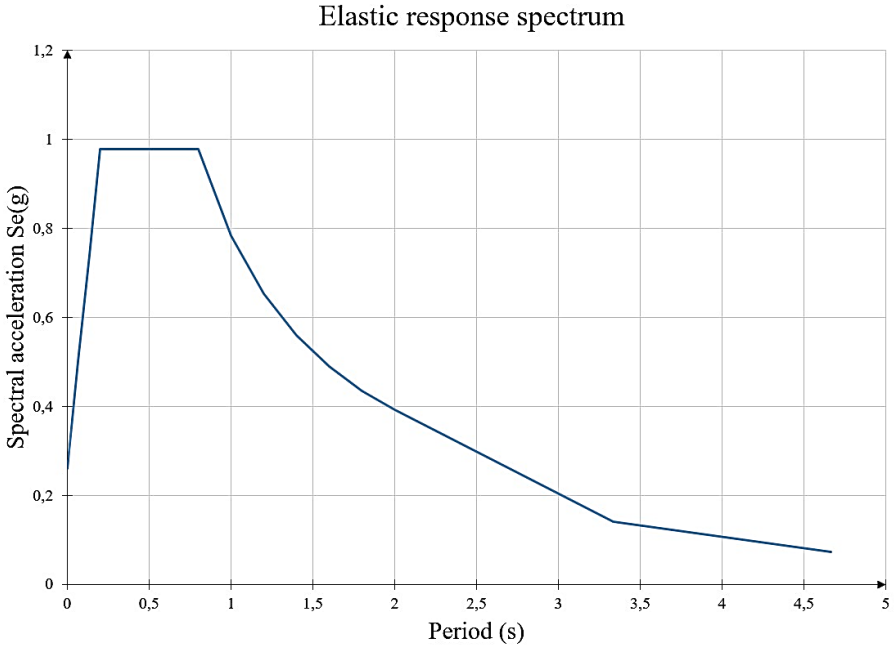

Figure 3.6. Representation of horizontal elastic response spectrum on EXCEL

3.3.2. Load combinations

For the verification of the structure at ultimate limit state (ULS) the load combination is given by the equation 3.1.

$$1.35G_{1k} + 1.35G_{2k} + 1.5Q_k \quad (3.1)$$

For the verification of the structure for non-reversible serviceability limit states (SLS), the load combination used is the characteristic rare combination expressed in equation 3.2.

$$G_{1k} + G_{2k} + Q_k \quad (3.2)$$

Concerning the seismic load combinations, it is defined by equation 3.3 and expressed in this case as follows;

$$G_{1k} + G_{2k} + 0.3Q_k + E \quad (3.3)$$

Where E is action effect due to the combination of the effects of the horizontal components of the seismic action. Expressing into its horizontal components we have eight seismic load combinations expressed in the following equations.

$$G_{1k} + G_{2k} + 0.3Q_k + E_x + 0.3E_y \quad (3.4)$$

$$G_{1k} + G_{2k} + 0.3Q_k + E_x - 0.3E_y \quad (3.5)$$

$$G_{1k} + G_{2k} + 0.3Q_k - E_x + 0.3E_y \quad (3.6)$$

$$G_{1k} + G_{2k} + 0.3Q_k - E_x - 0.3E_y \quad (3.7)$$

$$G_{1k} + G_{2k} + 0.3Q_k + 0.3E_x + E_y \quad (3.8)$$

$$G_{1k} + G_{2k} + 0.3Q_k + 0.3E_x - E_y \quad (3.9)$$

$$G_{1k} + G_{2k} + 0.3Q_k - 0.3E_x + E_y \quad (3.10)$$

$$G_{1k} + G_{2k} + 0.3Q_k - 0.3E_x - E_y \quad (3.11)$$

Where:

E_x horizontal component of the seismic action along the x-axis

E_y horizontal component of the seismic action along the y-axis

3.4. Static design of the case study

The static design of the building is done under the vertical static action meaning considering only the permanent and the imposed loads. We will start by designing a portion of each of our two types of slabs followed by the design of one horizontal element and one vertical element considered as representative of the other elements of the structure. Before the design phase of these structural elements, we need to define the concrete cover in order to fulfil the durability requirements of the structure.

3.4.1. Durability and concrete cover

Applying the procedure presented on the section 2.6.1 and considering a structural class S4 and the exposure class XC1, a minimum concrete cover obtained is equal to

$$C_{min} = \max(16; 15; 10) = 16\ mm,$$

Applying equation 2.12 for a nominal cover $C_{nom} = 26\ mm$. So, we will consider a concrete cover of C = 30 mm

3.4.2. Design of slabs

For the purpose of this study, the two most used slabs in Cameroon are going to be designed. These slabs are, the two-way slab supported by beams and a hollow block slab.

3.4.2.1. Two-way slab

The slabs of the considered building are two-way slabs supported by beams that is the slab carries and transfers loads in two directions.

a. Preliminary design of slab

The portion of slab chosen to be designed is highlighted in figure 3.7.

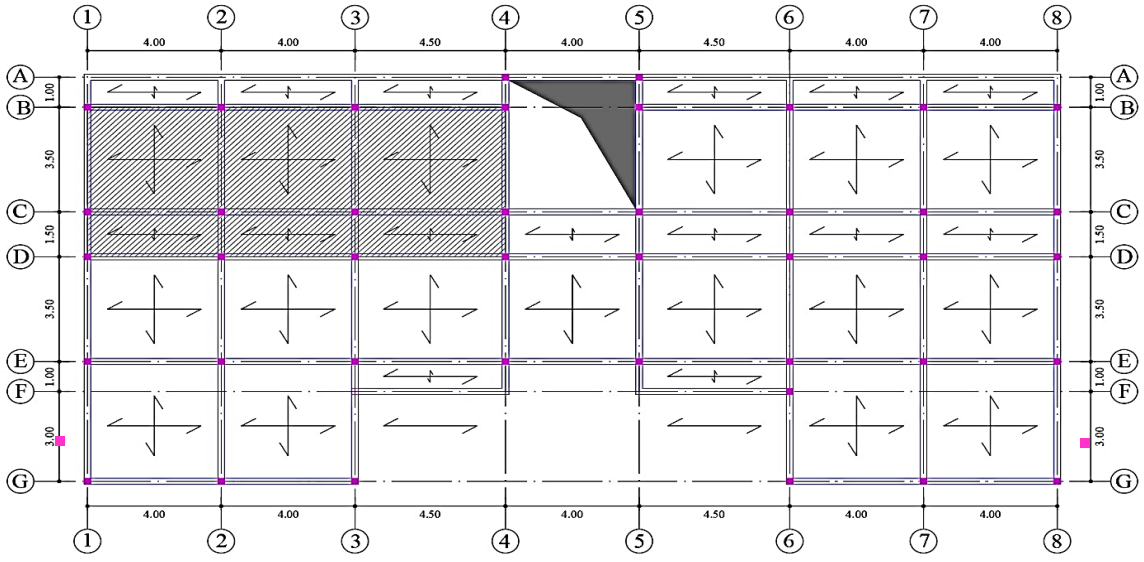

Figure 3.7. Portion of slab to be designed

For two-way slabs we have that; $\frac{Shorter\ span}{Longer\ span} \geq 0.4$

From the case study we have; $L_y = 3.5\ m$ and $L_x = \max(4\ , 4.5) = 4.5\ m$

$$\frac{L_y}{L_x} = 0.8 \quad OK$$

Applying equation 2.13 we have; $h \geq 0.18\ m$. So, a slab of thickness $h = 18\ cm$ is going to be designed

b. Grashoff method

The different loads acting on the slab are;

- Permanent structural loads $G_{1,k}$ = 4.5 kN/m²
- Permanent non-structural loads $G_{2,k}$ = 2.25 kN/m²
- Imposed loads Q_k = 2 kN/m²

Since we have a two-way slab, we have to evaluate the proportion of charges carried in each direction (x and y). For this we are going to use the method of Grashoff which is illustrated in figure 3.8.

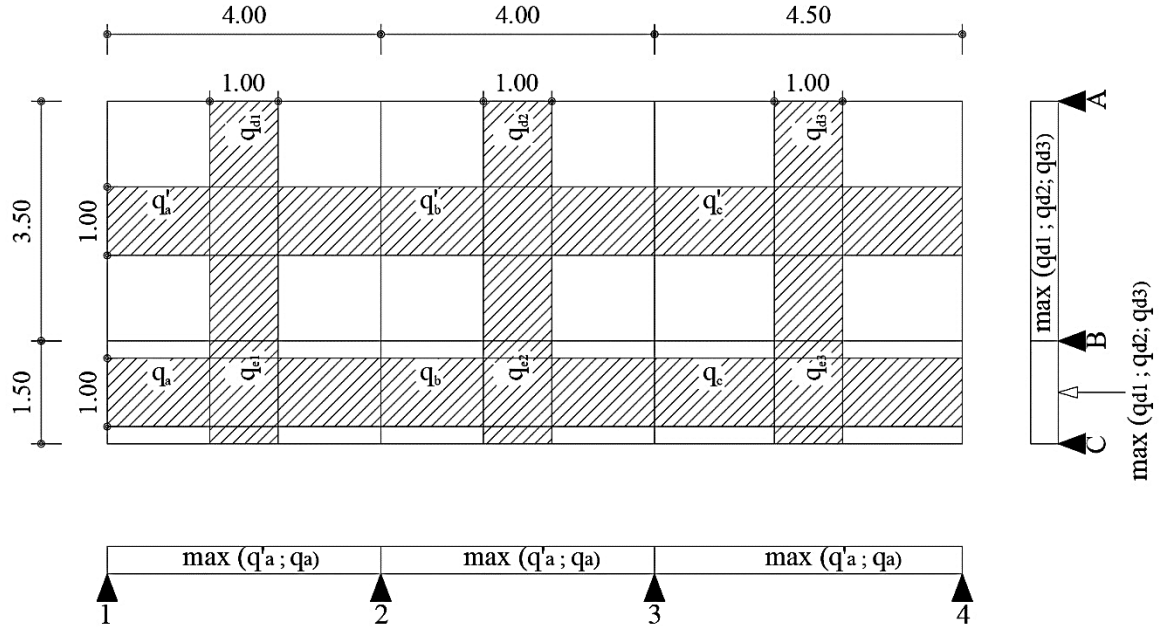

Figure 3.8. Illustration of the method of Grashoff

With an influence width of L_f = 1 m, the loads acting on the shaded portions of the slab in figure 3.8 are evaluated and presented below.

- $G_{1,k}$ = 4.5 kN/m²
- $G_{2,k}$ = 2.25 kN/m²
- Q_k = 2 kN/m²

Applying the method of Grashoff described in section 2.6.2.1.b we have; the proportion

of loads carried by the slab along the x-axis presented in table 3.6 and the proportion of loads carried by the slab along the y-axis presented in table 3.7.

Table 3.6. Proportion loads carried by the slab along the x-axis

	l_x	l_x	$q_x = \frac{l_y^4}{l_y^4 + l_x^4} q$	$G_{1,x}$	$G_{2,x}$	$Q_{k,x}$
	m	m	-	kN	kN	kN
q'_a	4	3.5	0.37	1.67	0.83	0.74
q'_b	4	3.5	0.37	1.67	0.83	0.74
q'_c	4.5	3.5	0.37	1.22	0.61	0.54
q_a	4	1.5	0.02	0.09	0.05	0.04
q_b	4	1.5	0.02	0.09	0.05	0.04
q_c	4.5	1.5	0.01	0.05	0.02	0.02

Table 3.7. Proportion loads carried by the slab along the y-axis

	l_x	l_x	$q_y = \frac{l_x^4}{l_y^4 + l_x^4} q$	$G_{1,x}$	$G_{2,x}$	$Q_{k,x}$
	m	m	-	kN	kN	kN
q_{d1}	4	3.5	0.63	2.84	1.42	1.26
q_{d2}	4	3.5	0.63	2.84	1.42	1.26
q_{d2}	4.5	3.5	0.73	3.3	1.64	1.46
q_{e1}	4	1.5	0.98	4.41	2.21	1.96
q_{e2}	4	1.5	0.98	4.41	2.21	1.96
q_{e2}	4.5	1.5	0.99	4.46	2.23	1.98

c. Load combinations

i. Along the x-axis

There are seven different load combinations for the slab at ULS and at SLS. Figures 3.9 (a) and (b) illustrate the static models used for the load combinations and studies on the software SAP 2000.

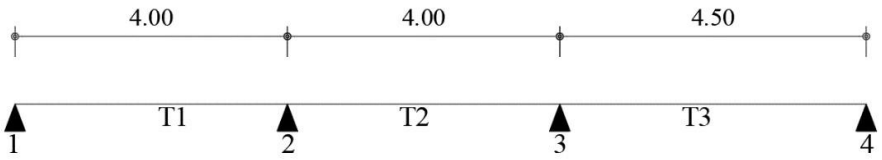

(a)

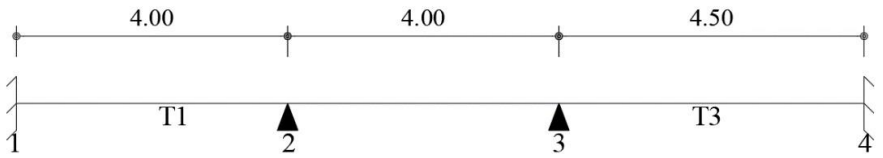

(b)

Figure 3.9. Static models along the x-axis

Assuming a rigid connection between the slab and the horizontal structural elements, the design of the region at the supports 1 and 4 is done using the static scheme with fixed supports (figure 3.9(b)) and the region at mid-span is done using the static scheme with simple supports (figure 3.9(a)). The following load combinations are used for the design.

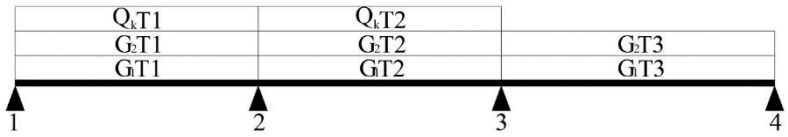

Load combination ULS T1T2

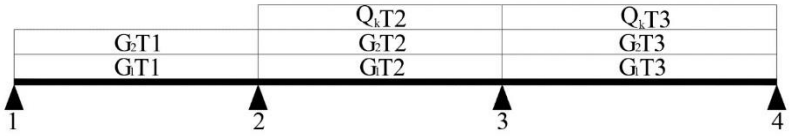

Load combination ULS T2T3

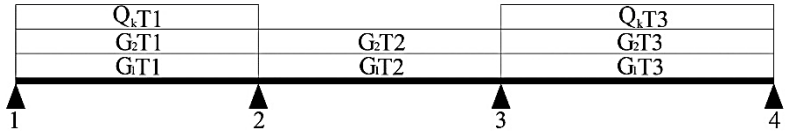

Load combination ULS T1T3

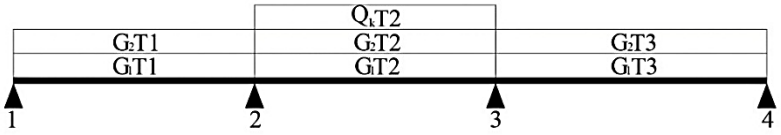

Load combination ULS T2

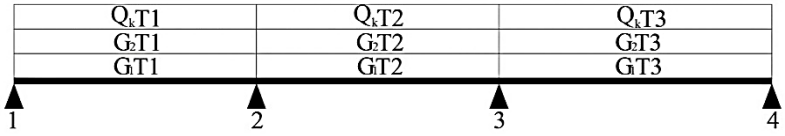

Load combination ULS T1T2T3

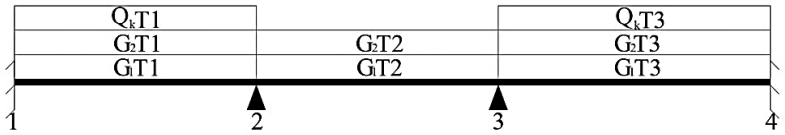

Load combination ULS T1T2 Encaster

Figure 3.10. Load combinations on slab along the x-axis

ii. In the y-direction

Here there are two load combinations at ULS and SLS. The static models used for the load combinations and studies on SAP 2000 are shown in figure 3.11.

(a) (b)

Figure 3.11. Static models in the Y-direction

Assuming a rigid connection between the slab and the horizontal structural elements, the design of the region at the supports is done using the static scheme with fixed supports (figure 3.11(a)) and the region at mid-span is done using the static scheme with simple supports (figure 3.11(b)). The following load combinations are used for the design.

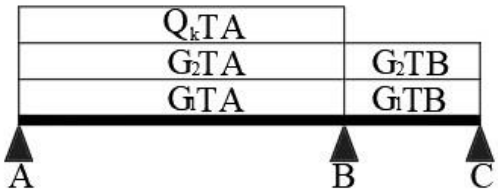

Load combination ULS T_A

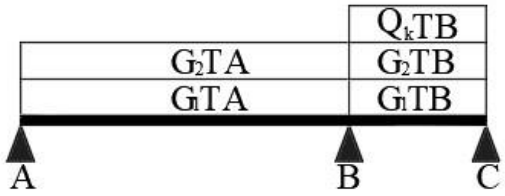

Load combination ULS T_B

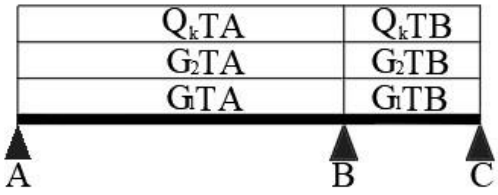

Load combination ULS $T_A T_B$

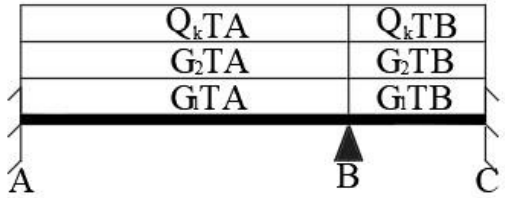

Load combination ULS $T_A T_B$ Encaster

Figure 3.12. Load combinations on slab in the Y-direction

d. Ultimate Limit State design

The slab is designed along the x and y axes

i. Along the x-axis

The eight load arrangements inserted in the software SAP 2000 permitted us to obtain eight solicitation curves for bending moment and for shear force represented in figure 3.13 and 3.14.

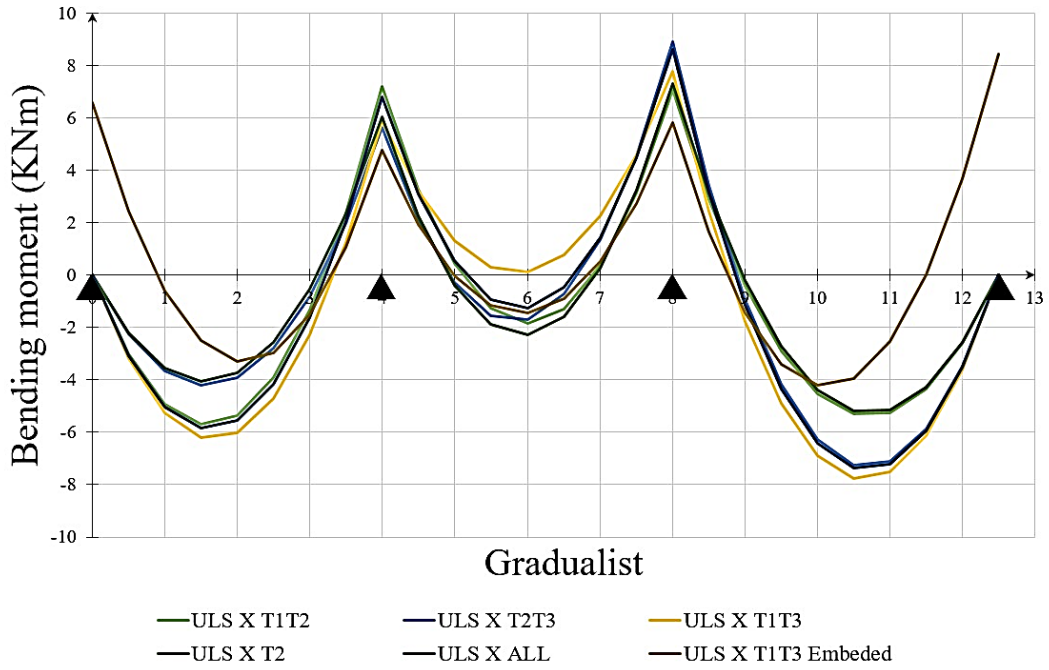

Figure 3.13. Bending moment solicitations curves on the slab along the x-axis

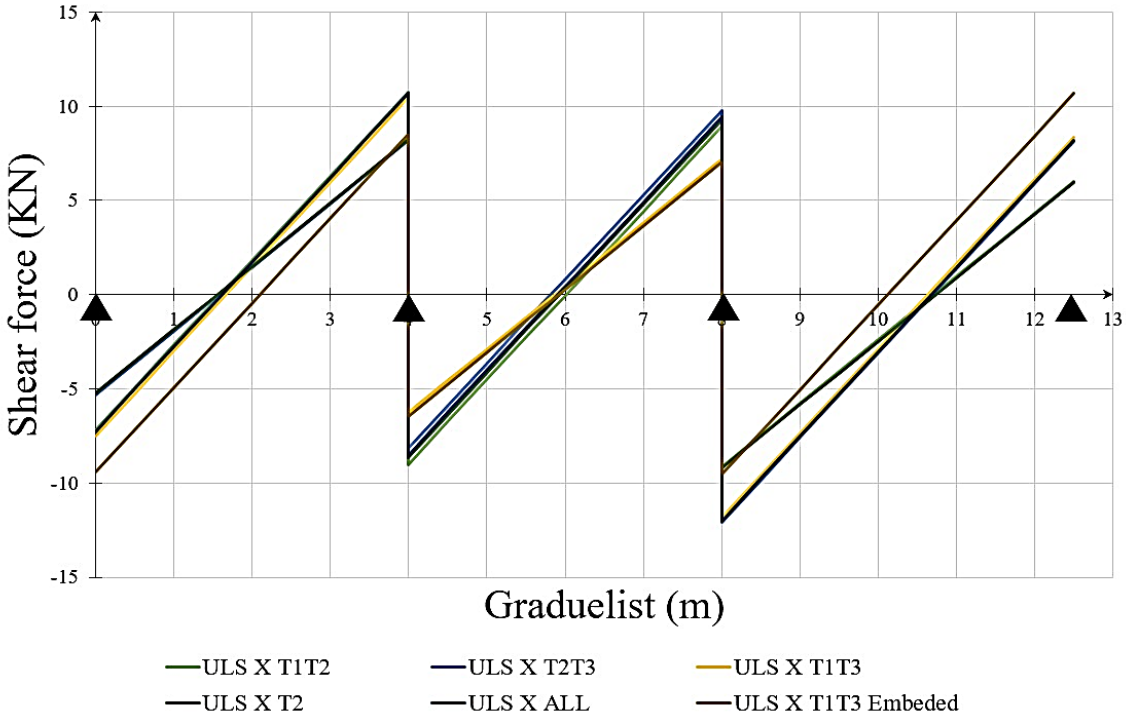

Figure 3.14. Shear solicitation curves on the slab along the x-axis

These solicitation curves permit to permit to obtain the envelope curves of moment and shear represented in figure 3.15 and figure 3.16.

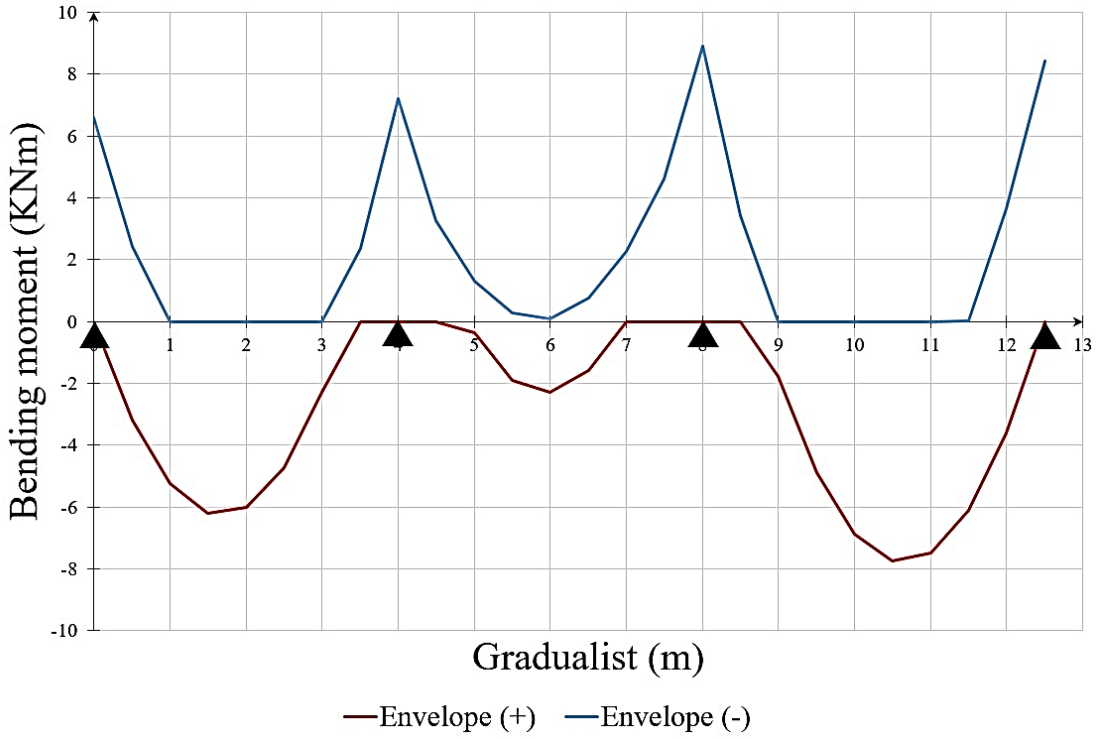

Figure 3.15. Envelope curve of bending moment along the x-axis of slab

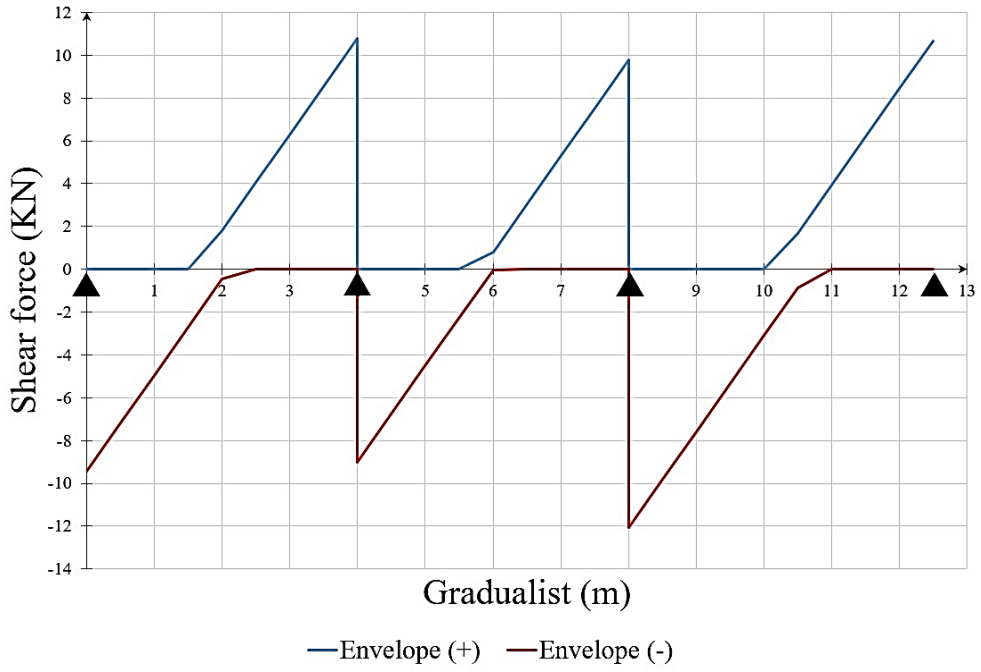

Figure 3.16. Envelope curve of Shear along the x-axis of slab

ii. Along the Y-axis

The two load arrangements inserted in the software SAP 2000 permitted us to obtain two solicitation curves for bending moment and for shear force represented in figure 3.17 and 3.18

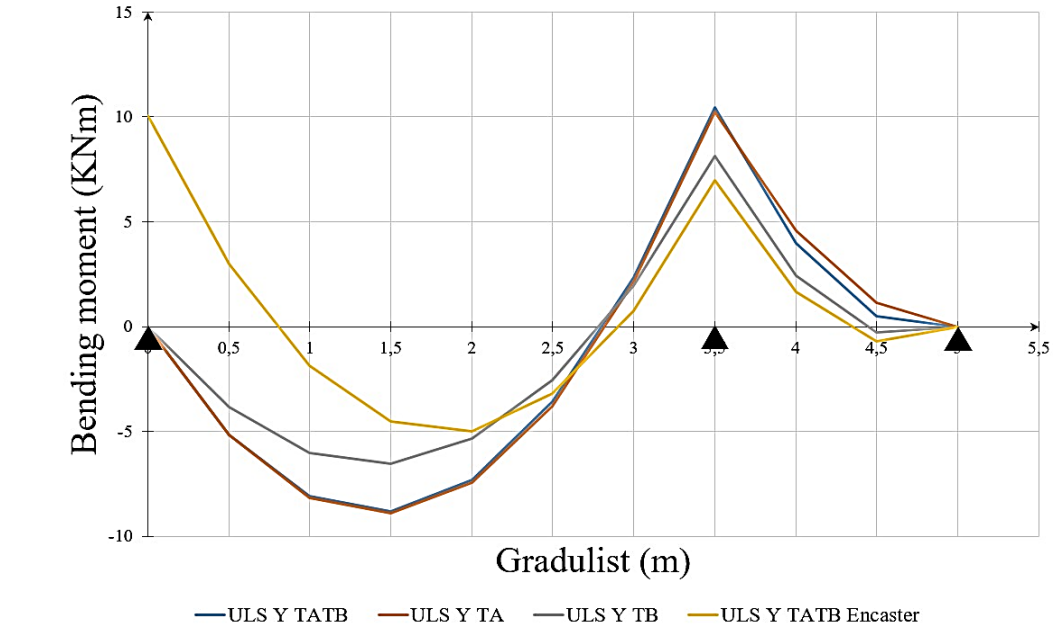

Figure 3.17. Bending moment solicitations curves on the slab along the y-axis

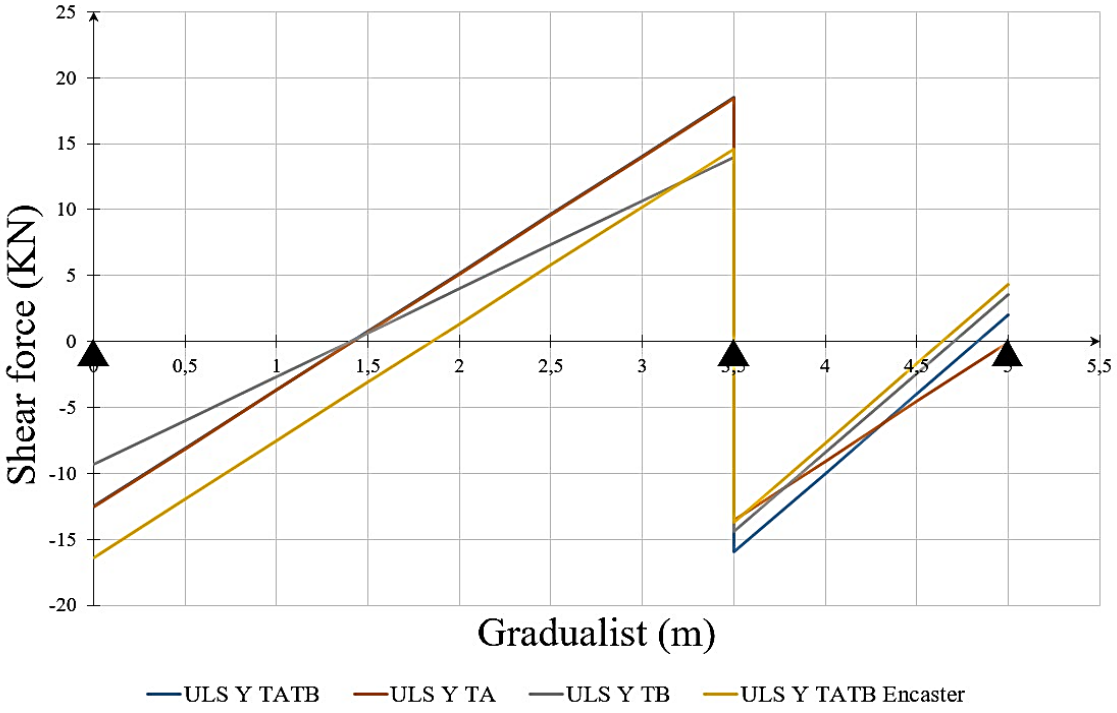

Figure 3.18. Shear solicitation curves on the slab along the y-axis

These solicitation curves permit to permit to obtain the envelope curves of moment and shear represented in figure 3.19 and figure 3.20

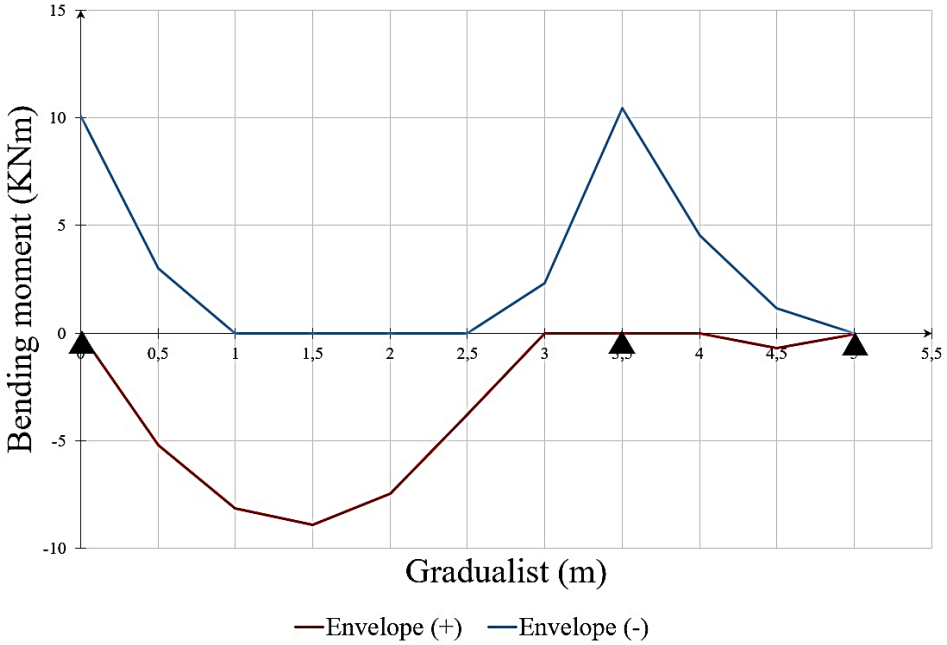

Figure 3.19. Envelope curve of bending moment along the y-axis of slab

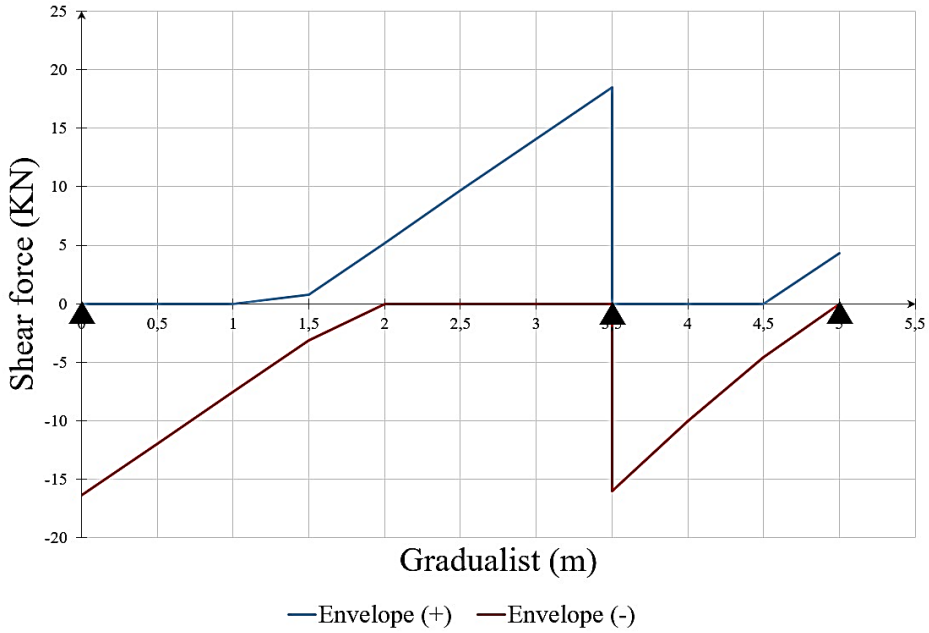

Figure 3.20. Envelope curve of Shear along the y-axis of slab

e. Section of longitudinal bars in slab

The section of longitudinal bars in the slab is evaluated along the x and y axes.

i. Along the x-axis

From the envelope curve of bending moment, the maximum moments acting at mid spans and at the support are obtained. From the procedure presented in section 2.6.2.1.c.i the section of steel reinforcement in the slab along the x-axis is evaluated and the results presented in table 3.8.

Table 3.8. Design and verification of section of longitudinal bars in slab along x-axis

	Mid-span	**Support**
M_{Ed} max	7.79 kNm	8.89 kNm
As calculated	165.7 mm²	17 mm²
As_{eff}	3ϕ10	3ϕ10
Verification of spacing $s_{min} = 30mm$ $s_{max} = 250mm$	S = 500mm Not verified	S = 500mm Not verified
Adopted spacing, s	250 mm	250 mm
New As_{eff}	5ϕ10	5ϕ10
Position of neutral axis, x	9.67 mm	12.1 mm
Moment verification ($M_{Rd} > M_{Ed}$)	19.94 kNm Verified	19.86 kNm Verified

ii. Along the y-axis

From the envelope curve of bending moment, the maximum moments acting at mid spans and at the support are obtained. From the procedure presented in section 2.6.2.1.c.i the section of steel reinforcement in the slab along the y-axis is evaluated and the results presented in table 3.9.

Table 3.9. Design and verification of section of longitudinal bars in slab along y-axis

	Mid-span	**Support**
M_{Ed} max	8.92 kNm	10.87 kNm
As calculated	190.2 mm²	231.5 mm²
As_{eff}	3ϕ10	3ϕ10
Verification of spacing $s_{min} = 30mm$ $s_{max} = 250mm$	S = 500mm Not verified	S = 500mm Not verified
Adopted spacing, s	250 mm	250 mm
New As_{eff}	5ϕ10	5ϕ10
Position of neutral axis, x	11.16 mm	13.80 mm
Moment verification ($M_{Rd} > M_{Ed}$)	19.85 kNm Verified	19.71 kNm Verified

f. Shear verification of slab

For the shear verification, the equation 2.25 permits us to obtain the maximum shear capacity of the concrete section and compare it to the maximum shear gotten from the envelope curve of shear solicitations.

i. Along the x-axis

$V_{edmax} = 10.80$ kN

$V_{Rdc} = 74.25$ kN

$V_{Rdc} \geq V_{Ed}$ then there is no need for shear reinforcement.

ii. In the Y-direction

$V_{edmax} = 16.12$ kN

$V_{Rdc} = 74.25$ kN

$V_{Rdc} \geq V_{Ed}$ then there is no need for shear reinforcement.

g. Plan view of distribution of steel reinforcement in slab

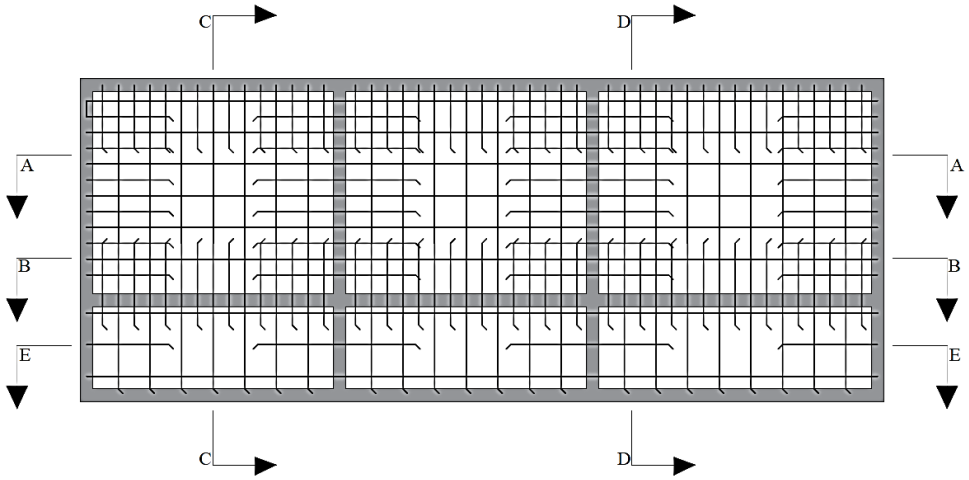

Figure 3.21. Plan view showing the distribution of longitudinal bars at the top layer of slab

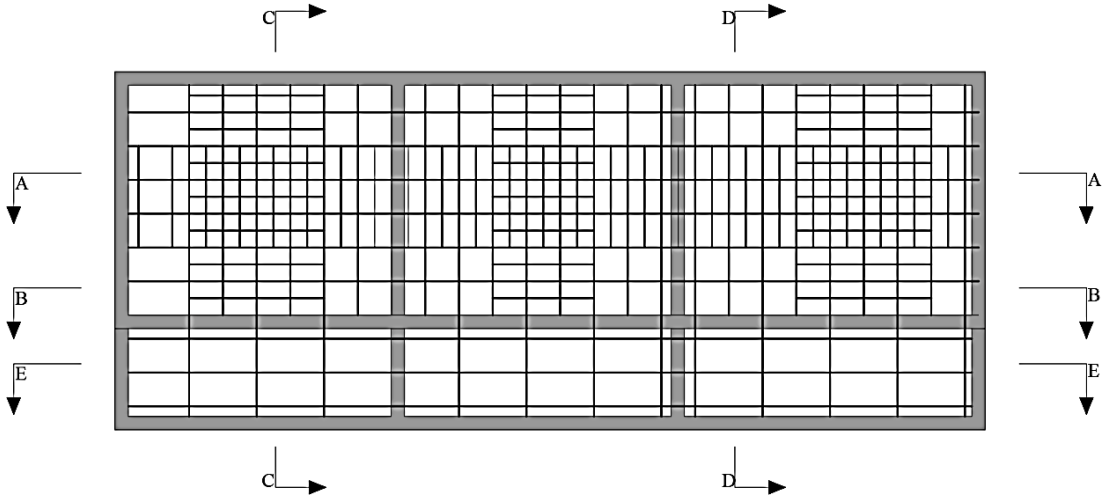

Figure 3.22. Plan view showing the distribution of longitudinal bars at bottom layer of slab

h. Cross-section of slab along the x-axis

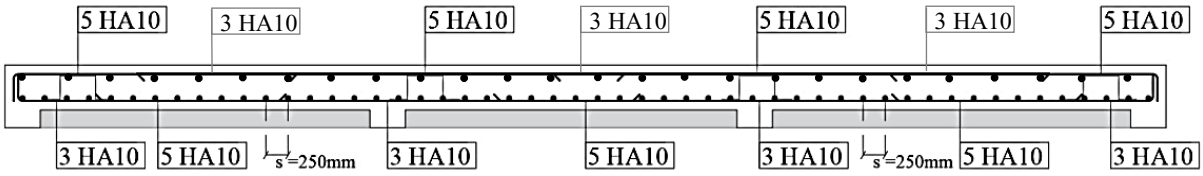

Figure 3.23. Section A-A of slab

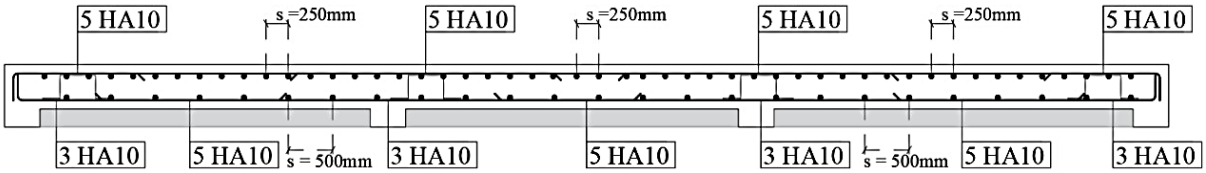

Figure 3.24. Section B-B of slab

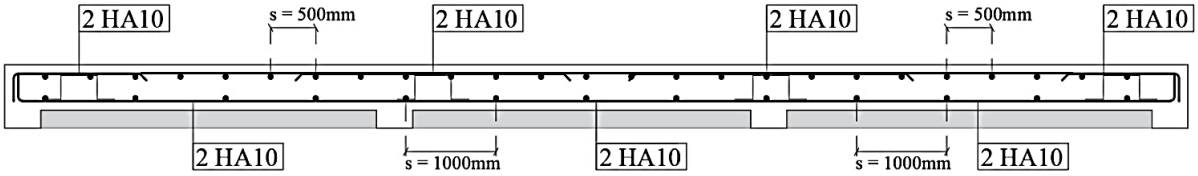

Figure 3.25. Section E-E of slab

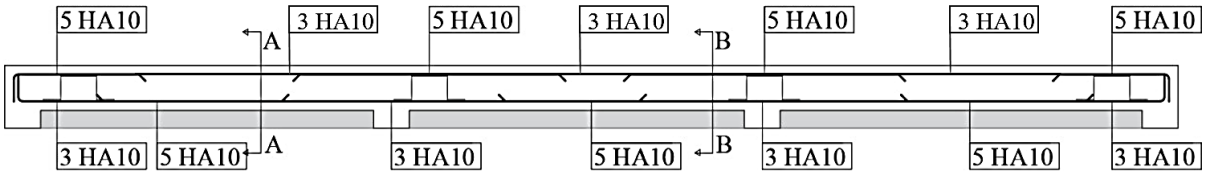

Figure 3.26. Distribution of longitudinal bars in slab in the X-direction

Figure 3.27. Section A-A and Section B-B

i. Cross-section of slab along the y-axis

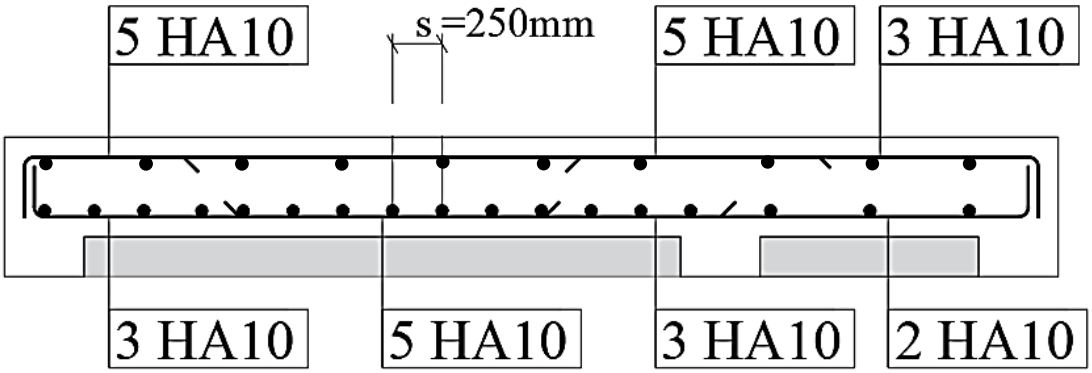

Figure 3.28. Section C-C of slab

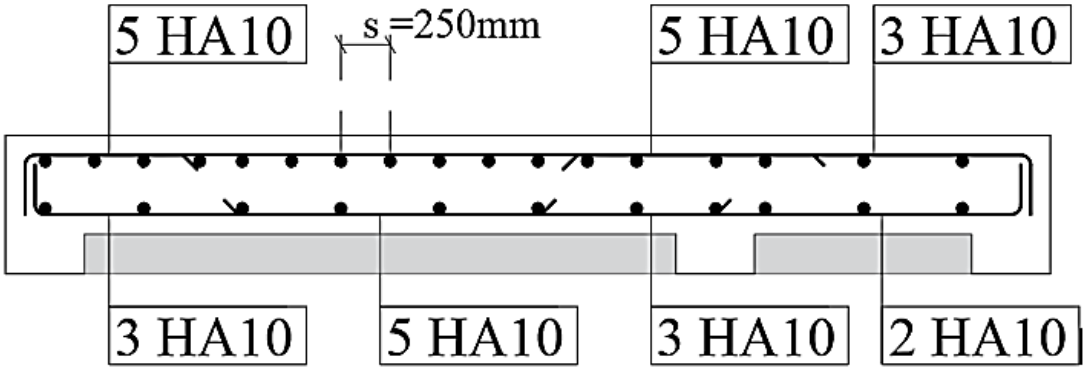

Figure 3.29. Section D-D of slab

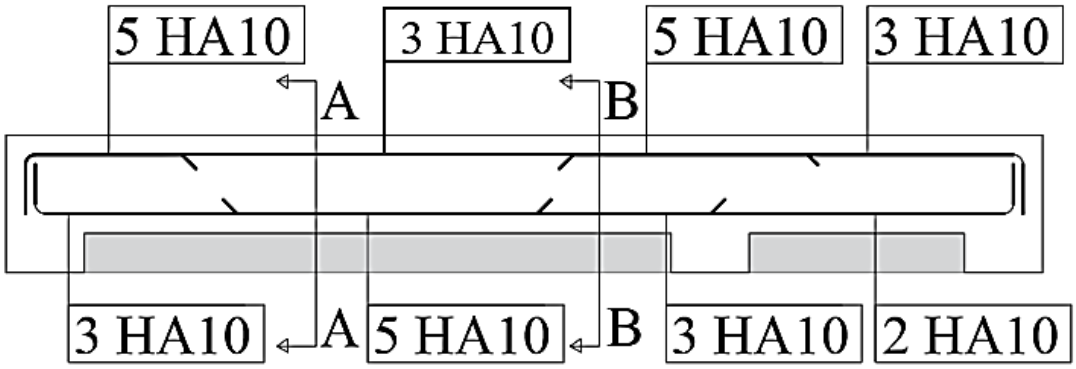

Figure 3.30. Distribution of longitudinal bars in slab along the Y-axis

Figure 3.31. Section A-A and Section B-B

j. Serviceability limit state verifications

The serviceability limit state verification done for this slab is deflection

Along the x-axis, applying the procedure in section 2.6.2.1.d on the longest span of the slab we have;

$$l/_d\,(real) = \frac{4500\ mm}{130\ mm} = 34.62$$

$A_s = 392.5\ mm^2$ and $A'_s = 392.5\ mm^2$

$$l/_d\,(calculated) = 66.32\ mm$$

$l/_d\,(real) < l/_d\,(calculated)$ So, deflection is verified along the x-axis

Along the y-axis, applying the procedure in section 2.6.2.1.d on the longest span of the slab we have;

$$l/_d\,(real) = \frac{3500\ mm}{130\ mm} = 26.9$$

$A_s = 392.5\ mm^2$ and $A'_s = 392.5\ mm^2$

$$l/_d\,(calculated) = 66.32\ mm$$

$l/_d\,(real) < l/_d\,(calculated)$ So, deflection is verified along the y-axis

3.4.2.2. Hollow block slab

The slab of the considered building is a hollow core slab made of concrete ribs and embedded masonry blocks. This type of slab carries loads in one direction.

a. Preliminary design of slab

The portion of slab and consequently the rib chosen for the designed is highlighted in figure 3.32.

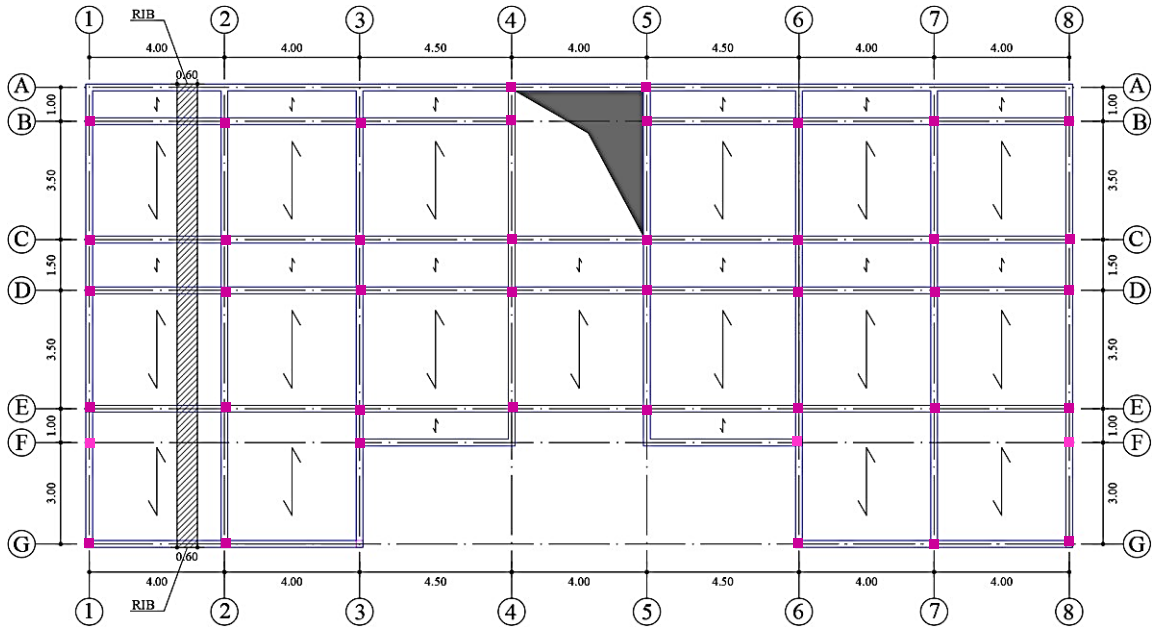

Figure 3.32. Choice of slab to design

From the case study, the longest is given by;

$$L_{max} = \min(L_{max,x} ; L_{max,y}) = \min(3.5m ; 4.5m)$$

$$L_{max} = 3.5\ m$$

With $L_{span} = L_{max}$, applying equation 2.13 we obtain $h \geq 0.18\,m$. So, a slab of thickness 20 cm whose section illustrated in figure 3.33 is going to be designed.

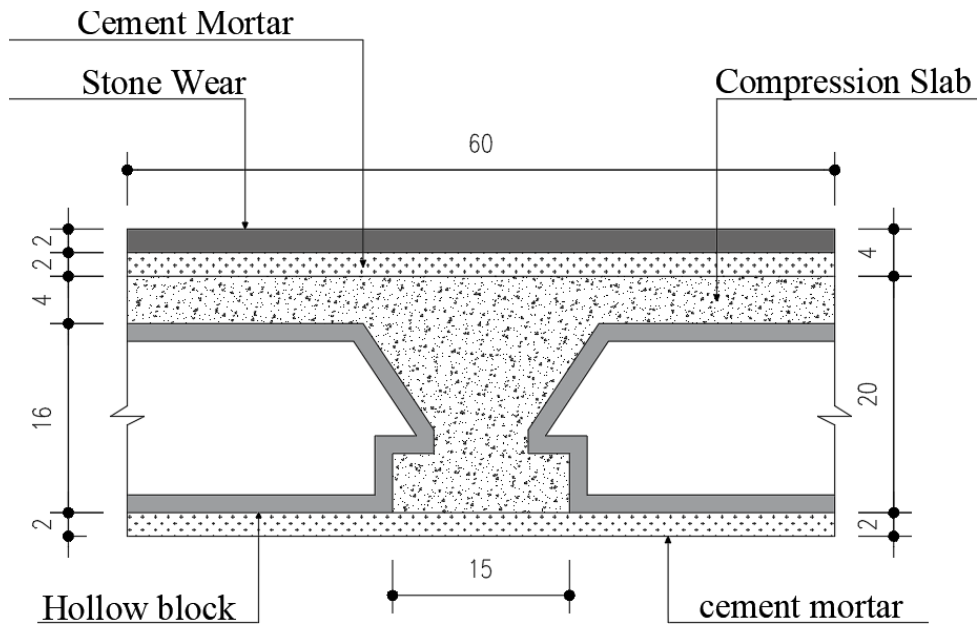

Figure 3.33. Section of hollow block slab

b. Loads on slab

The different loads acting on the slab are;

- Permanent structural loads $G_{1,k}$ = 2.85 kN/m²
- Permanent non-structural loads $G_{2,k}$ = 2.25 kN/m²
- Imposed loads Q_k = 2 kN/m²

With an influence width L_f = 0.6m the loads carried by each rib are;

- Permanent structural loads $G_{1,k}$ = 1.71 kN/m
- Permanent non-structural loads $G_{2,k}$ = 1.35 kN/m
- Imposed loads Q_k = 1.2 kN/m

c. Load combinations

There are nine different load combinations for the slab at ULS and at SLS. The static models used for the load combinations and studies on the software SAP 2000 are illustrated in figure 3.34.

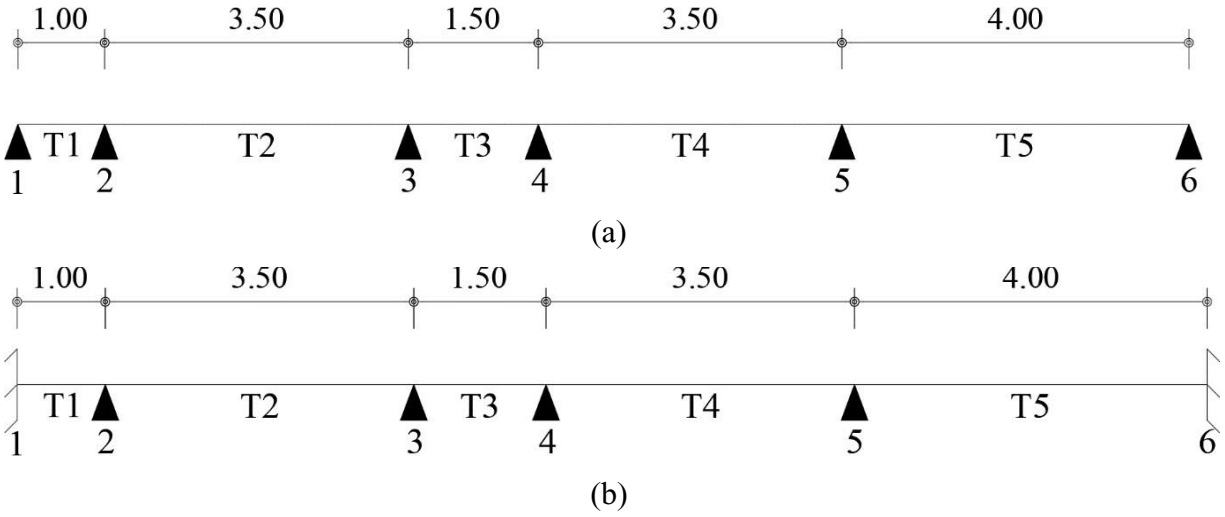

Figure 3.34. Static models of rib

Assuming a rigid connection between the slab and the horizontal structural elements, the design of the region at the supports 1 and 4 is done using the static scheme with fixed supports (figure 3.34(b)) and the region at mid-span is done using the static scheme with simple supports (figure 3.34(a)). The load combinations used for the design are shown in figure 3.35.

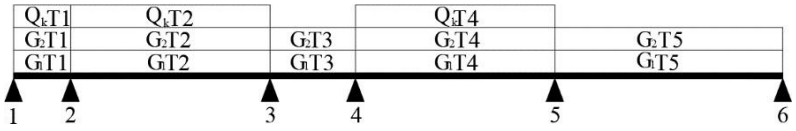

Load combination ULS T1T2T4

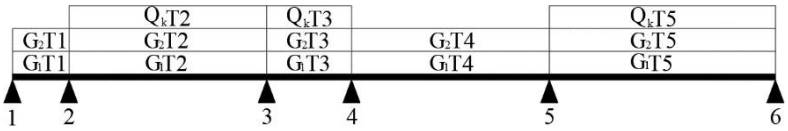

Load combination ULS T2T3T5

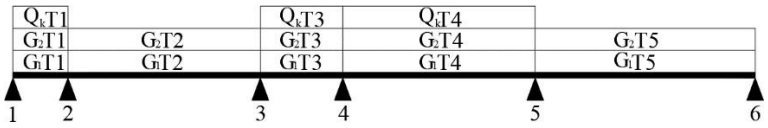

Load combination ULS T1T3T4

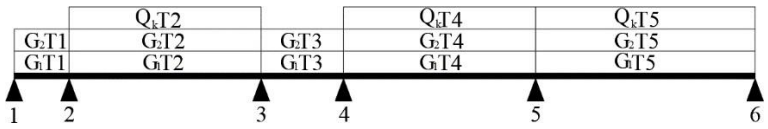

Load combination ULS T2T4T5

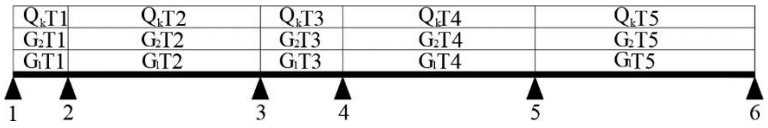

Load combination ULS T1T2T3T4T5

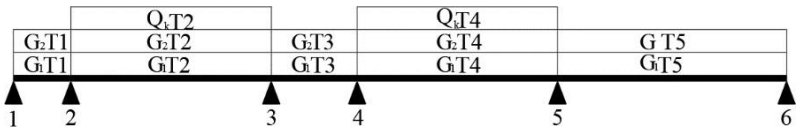

Load combination ULS T2T4

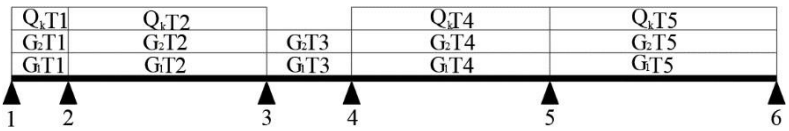

Load combination ULS T1T2T4T5

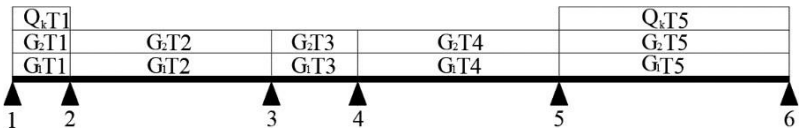

Load combination ULS T1T5

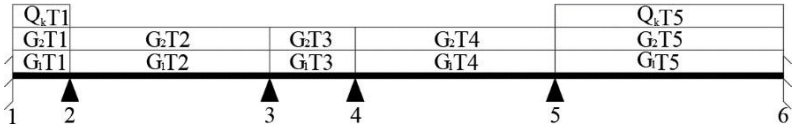

Load combination ULS T1T5 encaster

Figure 3.35. load combinations on the rib

d. Ultimate limit state design

The ten load arrangements inserted in the software SAP 2000 permitted us to obtain ten solicitation curves for bending moment and for shear force represented in figure 3.36 and 3.37.

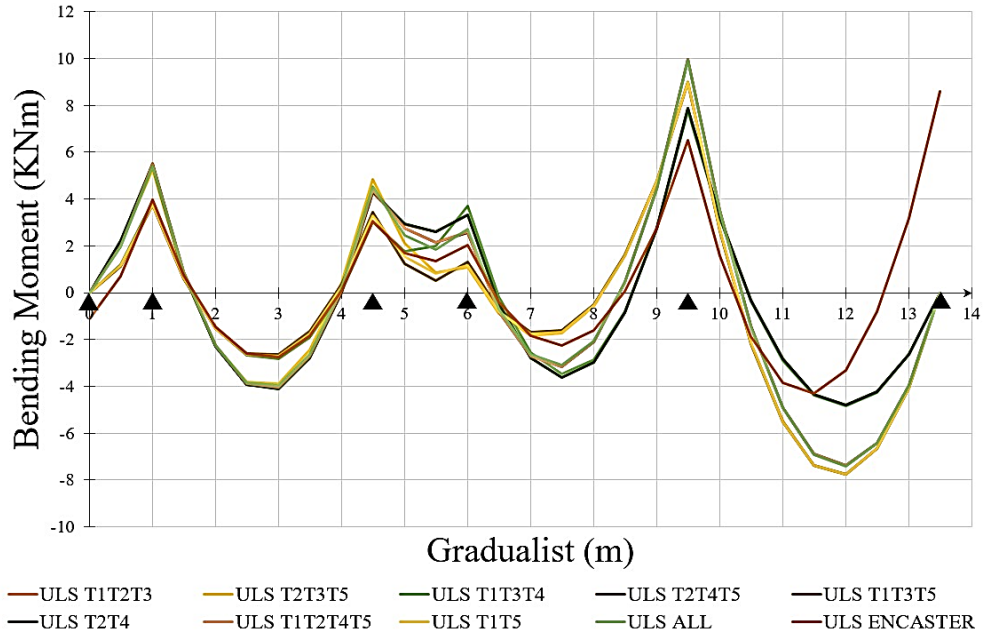

Figure 3.36. Bending moment solicitations curves for the rib

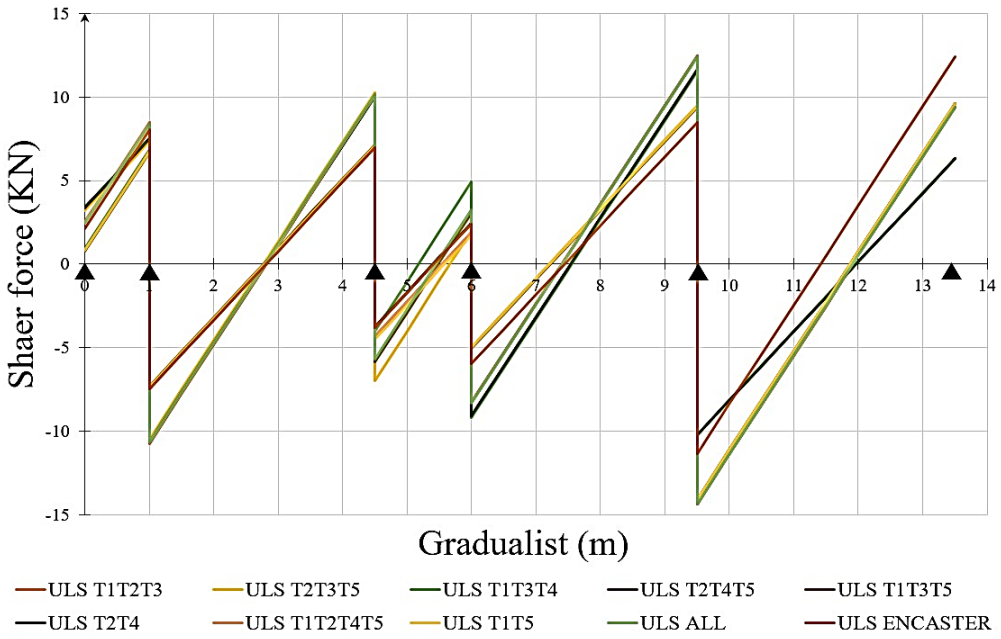

Figure 3.37. Shear force solicitations curves for the rib

These solicitation curves permit to obtain the envelope curves of moment andshear represented in figure 3.38 and figure 3.39

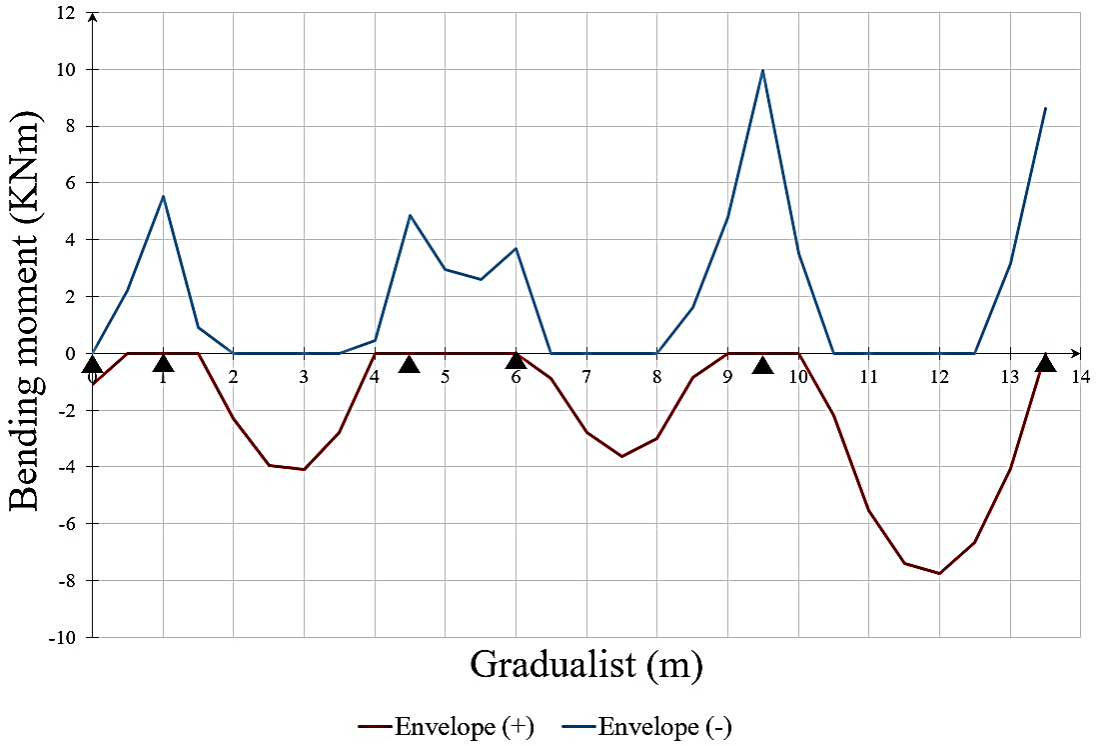

Figure 3.38. Envelope curve of bending moment for the rib

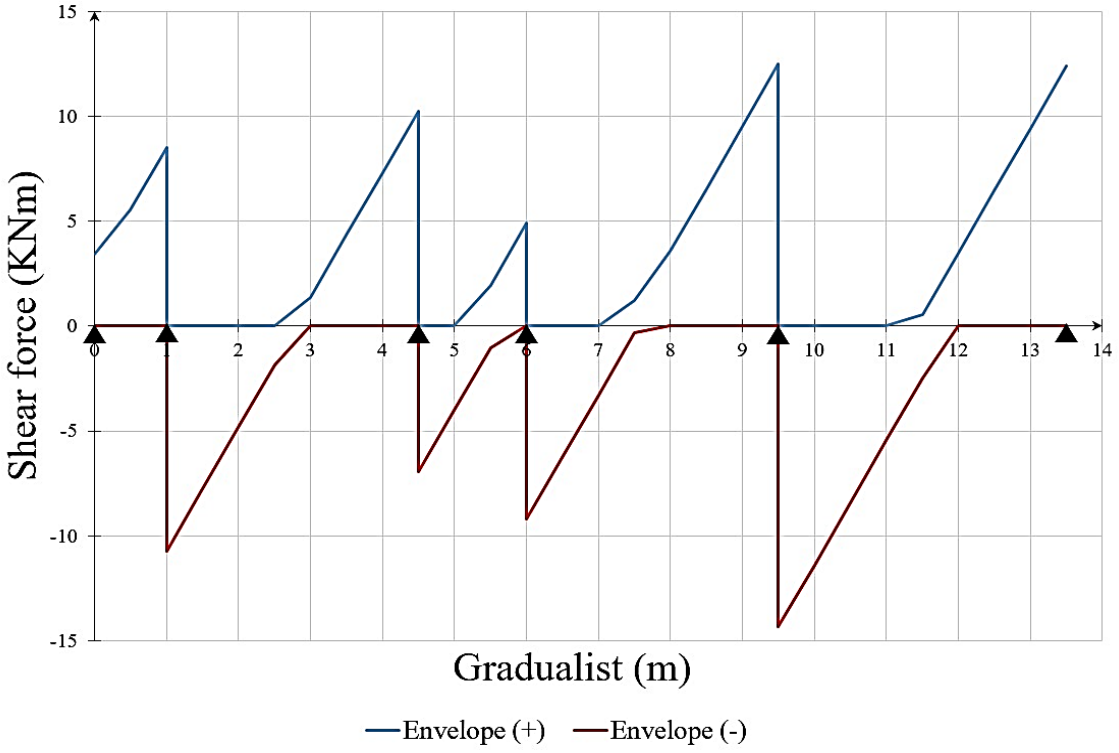

Figure 3.39. Envelope curve of shear force for rib

e. Section of longitudinal bars in rib

From the envelop curve of moment the maximum moments at the supports ant at mid-span are obtained. The procedure presented in section 2.6.2.2.b.i permits to evaluate the section of steel reinforcement needed to resist the maximum moment solicitations and hence do the verifications. Table 3.10 presents the results obtained from this procedure.

Table 3.10. Design and verification of section of longitudinal bars in rib

	At mid span	**At support 1/2/3 and 4**	**At support 5 and 6**
M_{ed} max	7.76 kNm	5.53 kNm	9.95 kNm
A_s calculated	133.40 mm²	122.48 mm²	159.77 mm²
As_{eff}	2ϕ10	1ϕ12	1ϕ12 and 1ϕ10
Verification of steel section $A_{s,min} = 41.43mm$ $A_{s,max} = 580mm$	Verified	Verified	Verified
Position of neutral axis X	7.93 mm	22.84 mm	38.71 mm
Moment verification ($M_{Rd} > M_{ed}$)	9.11kNm Verified	6.32 kNm Verified	10.27 kNm Verified

f. Shear verification

From the envelope curve of shear, we have; Max $V_{Ed} = 14.35$ kN

The maximum shear capacity of the rib section is calculated using equation 2.25

$$V_{Rdc} = 8.21 \text{ kN} < V_{Ed}$$

Considering a stirrup of diameter 6mm, the design procedure presented in section 2.6.2.2.b.i permits to obtain the spacing between the stirrups necessary to resist the maximum shear

For supports 1, 2, 3 and 4:

$$V_{Ed} = 10.76 \text{ KN} \qquad V_{Rdc} = 8.21 \text{ kN} < V_{Ed}$$

$$s = 237.56 \text{ mm}$$

For supports 5 and 6:

$$V_{Ed} = 14.35 \text{ KN} \qquad V_{Rdc} = 8.21 \text{ kN} < V_{Ed}$$

$$s = 178.95 \text{ mm}$$

The following figures show the distribution of the longitudinal bars and the shear reinforcements in the rib.

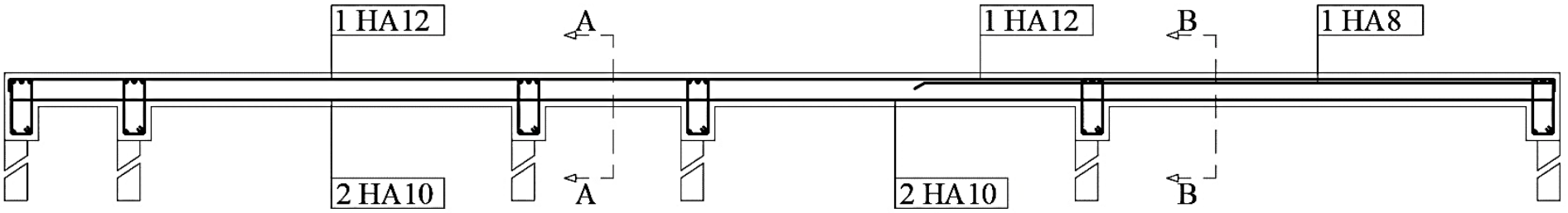

Figure 3.40. Longitudinal section of slab

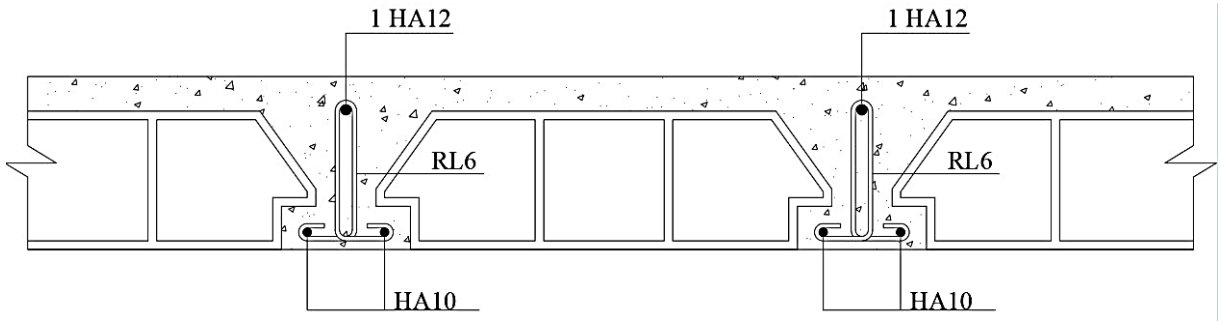

Figure 3.41. Transversal section A-A of slab

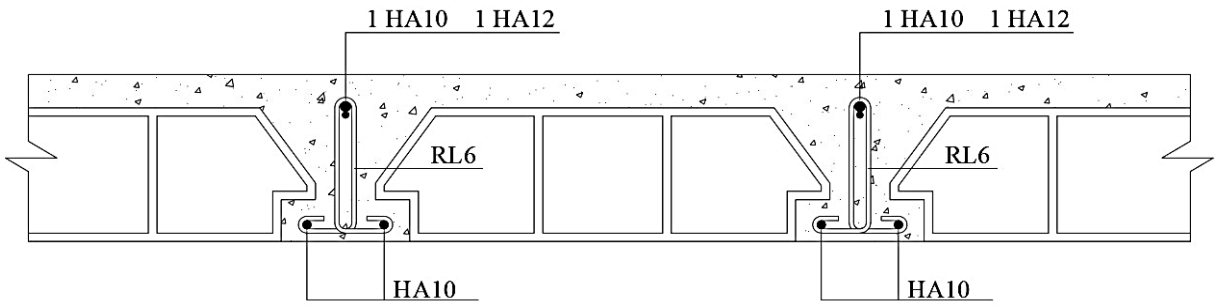

Figure 3.42. Transversal section B-B of slab

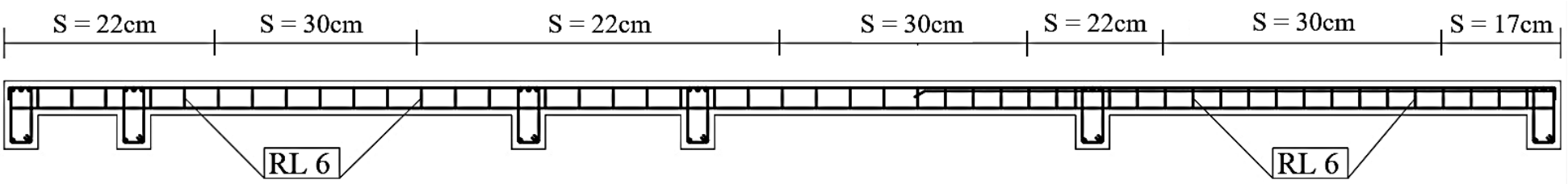

Figure 3.43. Distribution of stirrups in slab

g. Serviceability limit state verifications

The serviceability limit state verification done for this slab is deflection

Applying the procedure in section 2.6.2.1.d on the longest span of the slab we have;

$$l/_d\,(real) = \frac{3500\ mm}{170\ mm} = 20.52$$

$$A_s = 157\ mm^2 \text{ and } A'_s = 191.54\ mm^2$$

$$l/_d\,(calculated) = 36.45\ mm$$

$l/_d\,(real) < l/_d\,(calculated)$; So, deflection is verified for the hollow-block slab

3.4.3. Design of horizontal structural elements

Considering the building with the hollow block slab, the horizontal structural elements to be designed are composed of the beams which support the slabs. The principal beam chosen for the design is highlighted in figure 3.44 and has the same influence area for all the spans.

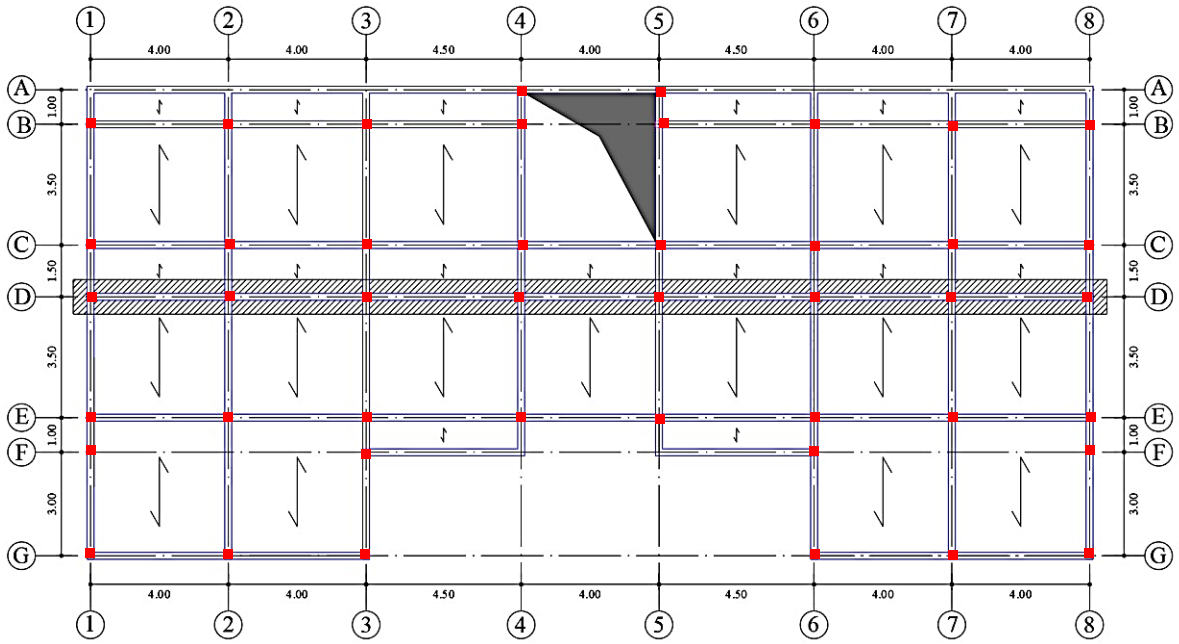

Figure 3.44. Principal beam to be designed

Since our building is perfectly symmetric along y axis, we are going to simplify design of our beam by considering the first four span our beam (between grid line 1 and 4) for the design.

3.4.3.1. Loads on beam

With an influence width L_f = 2.5m, the different loads acting on the beam are as follows;

- Self-weight of slab $G_{1,slab}$ = 9.13 kN/m
- Self-weight of beam $G_{1,beam}$ = 2 kN/m
- Self-weight of non-structural elements G_2 = 3.13 kN/m
- Imposed load Q_k = 5 kN/m

3.4.3.2. Load combinations

There are ten different load combinations for the slab at ULS and at SLS. The static models used for the load combinations and studies on the software SAP 2000 are illustrated in figure 3.45.

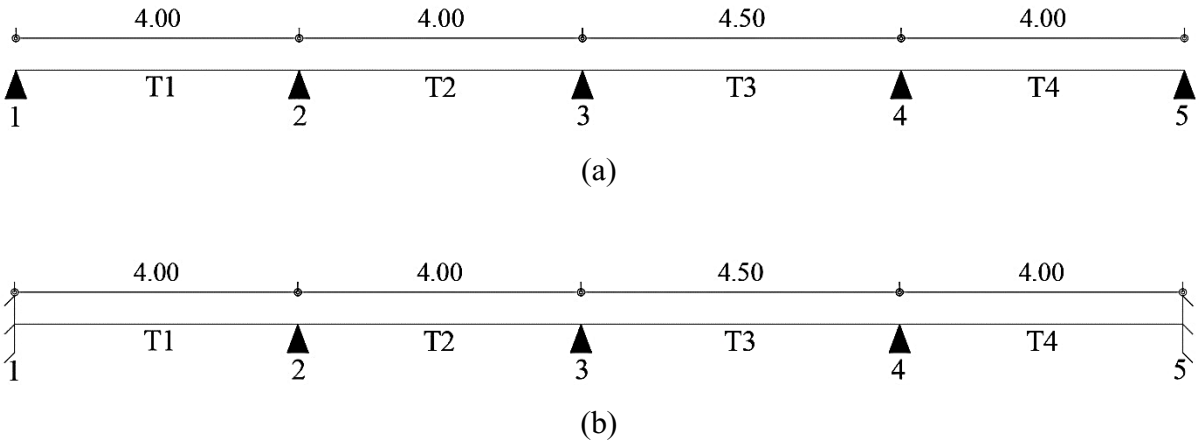

Figure 3.45. Static models of beam

Assuming a rigid connection between the slab and the horizontal structural elements, the design of the region at the supports 1 and 4 is done using the static scheme with fixed supports (figure 3.45(b)) and the region at mid-span is done using the static scheme with simple supports (figure 3.45(a)). The load combinations used for the design are shown in figure 3.46.

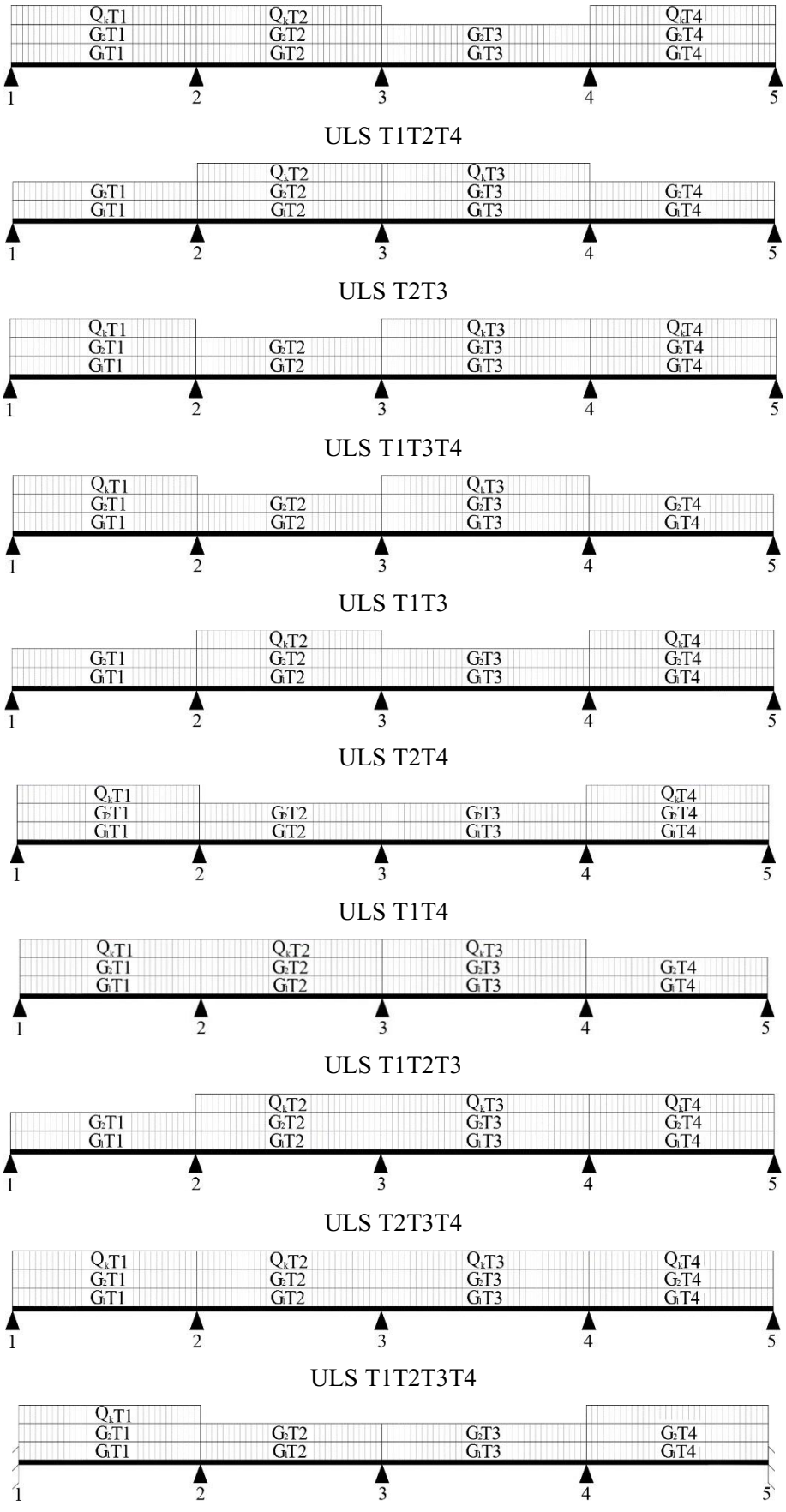

Figure 3.46. Load combinations on the beam

3.4.3.3. Ultimate limit state design

The ten load arrangements inserted in the software SAP 2000 permitted us to obtain ten solicitation curves along the beam for bending moment and for shear force represented in figures 3.47 and 3.48.

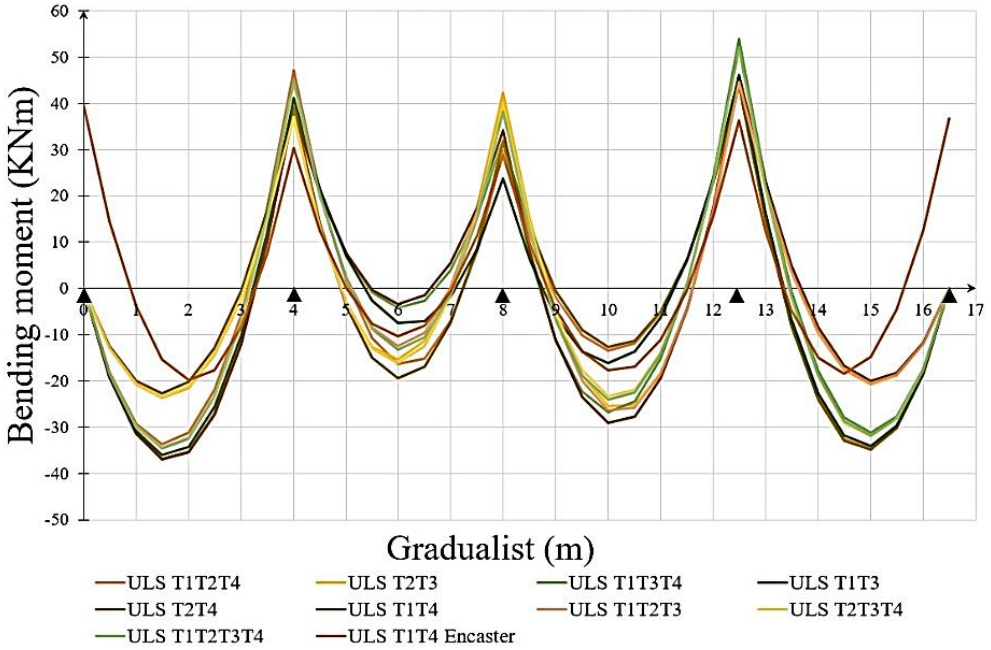

Figure 3.47. Bending moment solicitations curves for the beam

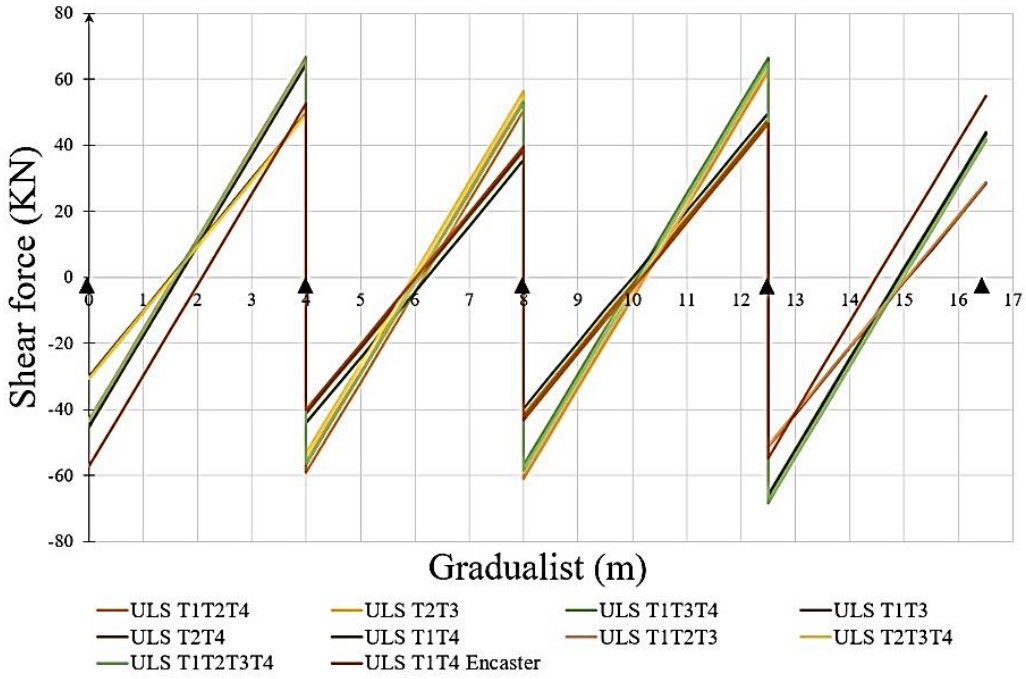

Figure 3.48. Shear force solicitations curves for the beam

These solicitation curves permit to permit to obtain the envelope curves of moment and shear represented in figure 3.49 and figure 3.50.

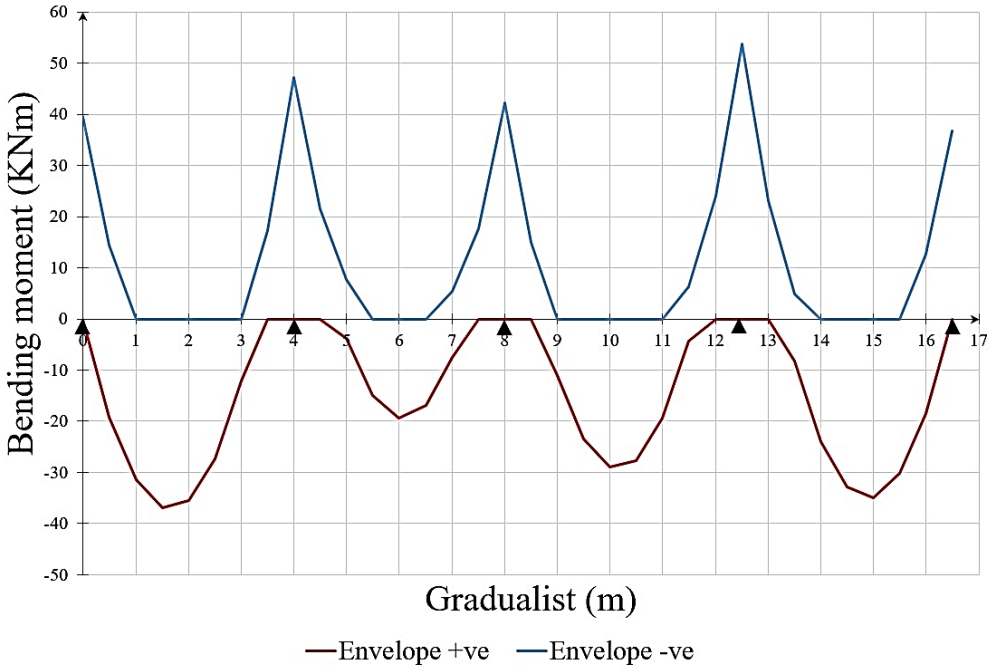

Figure 3.49. Envelope curve of bending moment for the beam

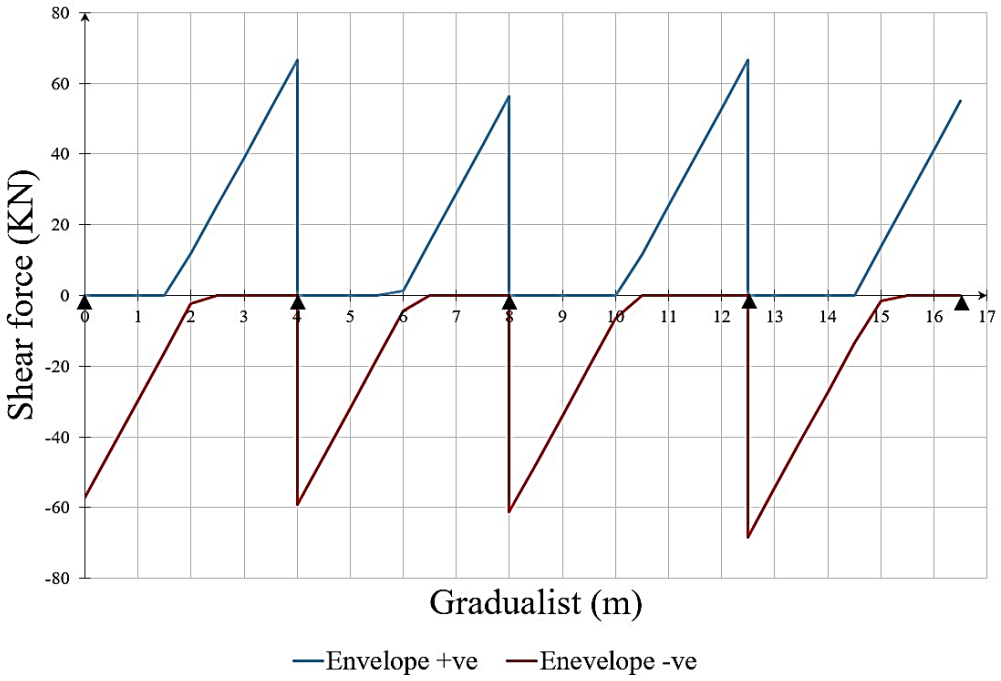

Figure 3.50. Envelope curve of bending moment for the beam

3.4.3.4. Section of longitudinal bars in beam

From the envelop curve of moment we have the maximum moments at the supports ant at mid-span. The procedure presented in section 2.6.3.1.a permits us to evaluate the section of steel reinforcement to resist the maximum moment solicitations and hence do the verifications. Table 3.11 presents the results obtained from this procedure.

Table 3.11. Design and verification of steel reinforcement in beam

	At mid span	At supports
M_{ed} max	36.92 kNm	53.78 kNm
A_s calculated	302.91 mm²	463.43 mm²
A_{Seff}	3ϕ12	3ϕ14
Verification of steel section $A_{s,min} = 120.25\ mm^2$ $A_{s,max} = 3200\ mm^2$	Verified	Verified
Position of neutral axis X	51.4 mm	69.96 mm
Moment verification($M_{Rd} > M_{ed}$)	41.16 kNm Verified	54.80 kNm Verified

A recapitulative curve of bending moment verification on beam is presented in figure 3.51.

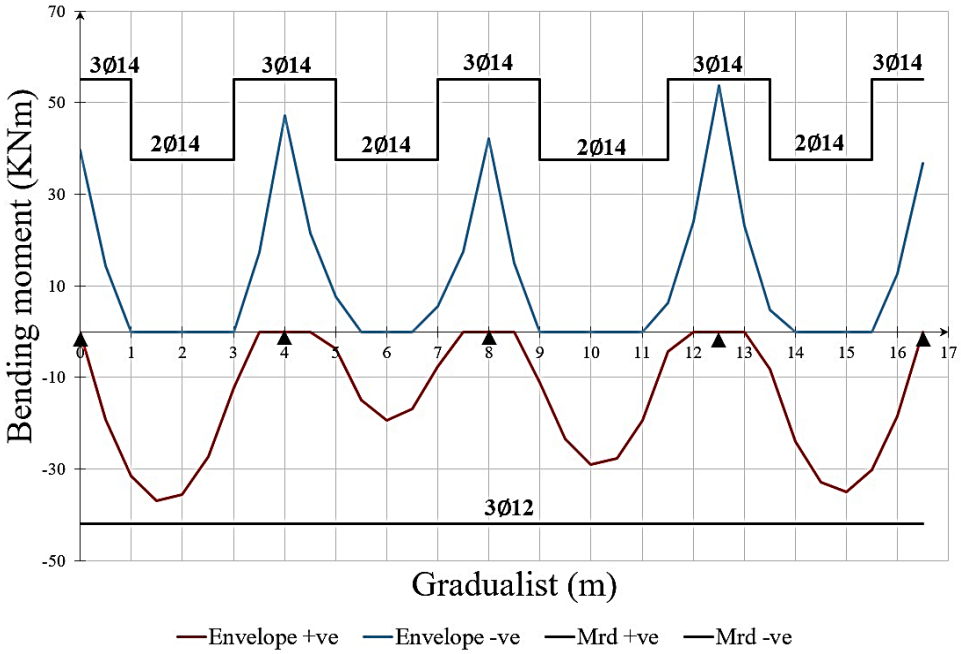

Figure 3.51. Recapitulative curve of bending moment verification on beam

3.4.3.5. Shear verification

From the envelope curve of shear we have; Max $V_{Ed} = 68.2$ KN. The maximum shear capacity of the rib section is calculated using equation 2.25

$$V_{Rdc} = 50.74 \text{ KN} < V_{Ed}$$

Considering a stirrup of diameter 6mm, the design procedure presented in section 2.6.2.2.b.i permits to obtain the spacing between the stirrups necessary to resist the maximum shear.

For supports 1,2,3,4 and 5:

V_{Ed} = 68.2 KN

V_{Rdc} = 50.74 KN < V_{Ed}

s = 111.48 mm

A recapitulative curve of shear verification on beam is presented in figure 3.52.

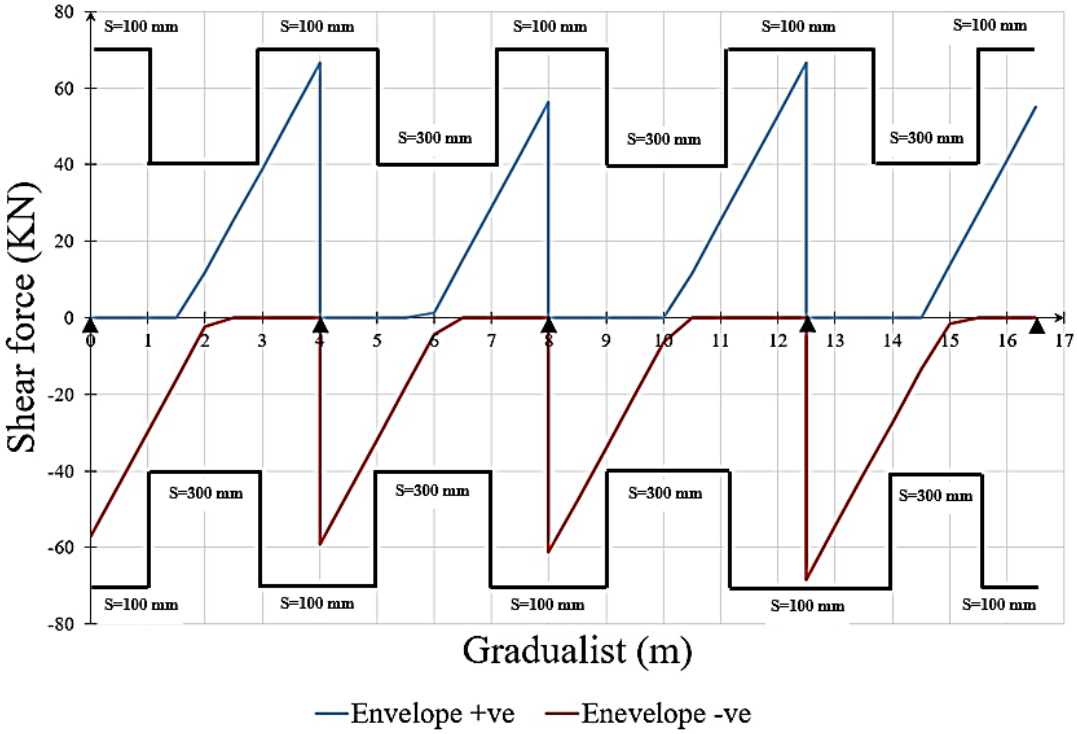

Figure 3.52. Recapitulative curve of shear verification on the beam

3.4.3.6. Serviceability limit state verifications

a. Stress limitations

The ten load arrangements inserted in the software SAP 2000 at the characteristic rare combination permit to obtain ten solicitation curves along the beam for bending moment represented in figure 3.53.

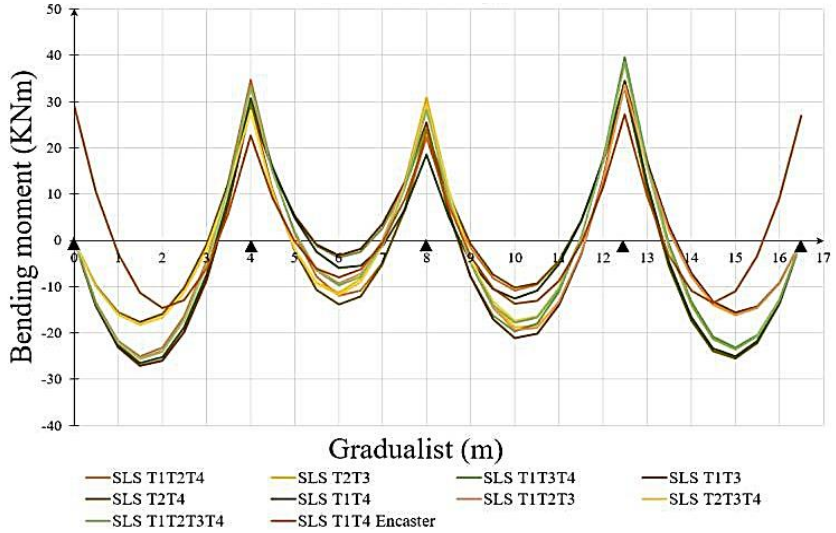

Figure 3.53. Solicitation curves of bending moment at SLS for the beam

These solicitation curves permit us to obtain the envelop curve presented in figure 3.54

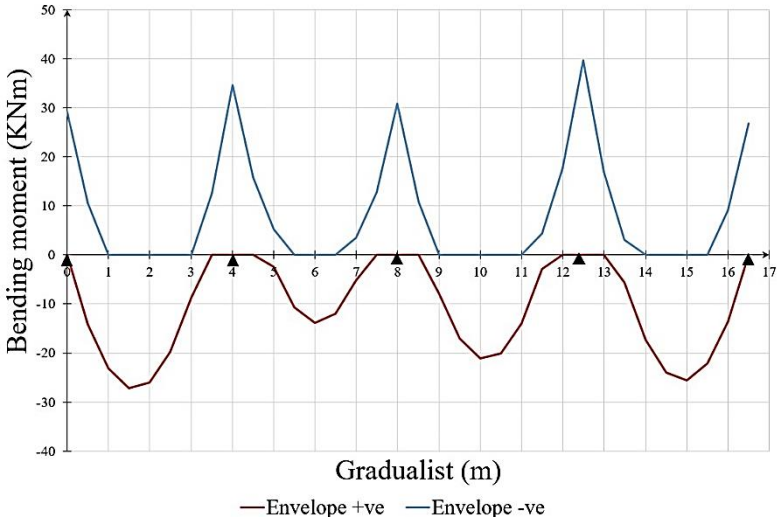

Figure 3.54. Envelope curve of bending moment at SLS

With this envelope curve of bending moment at serviceability limit state the stress in the concrete and in the reinforcement are obtained using the equations 2.44 and 2.45. The limit value of the stress is evaluated from the equations 2.46 and 2.47 using the recommended values of the Eurocode 2, means taken $k1$= 0.6 and $k3$ = 0.8. Figure 3.55 and figure 3.56 shows the stress inside the concrete and the steel reinforcement compared to the admissible stress.

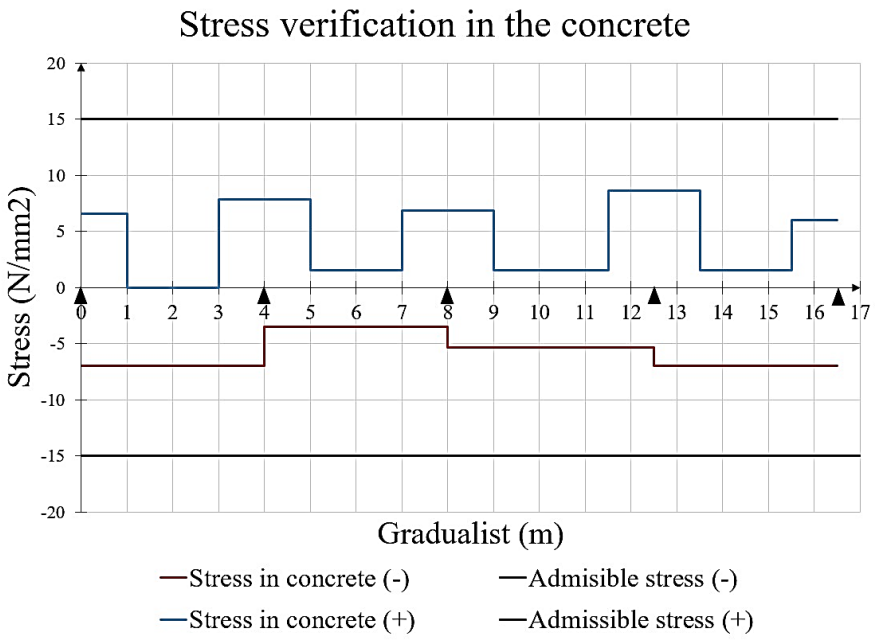

Figure 3.55. Recapitulative curve of stress verification on the beam in the concrete

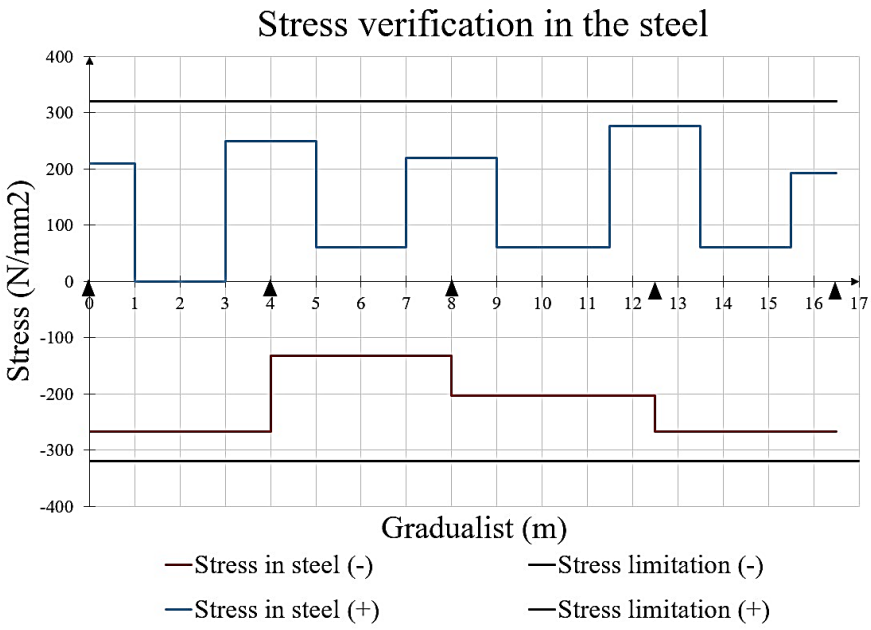

Figure 3.56. Recapitulative curve of stress verification on the beam in the steel reinforcement

The structural detailing of the beam is presented in the following figures:

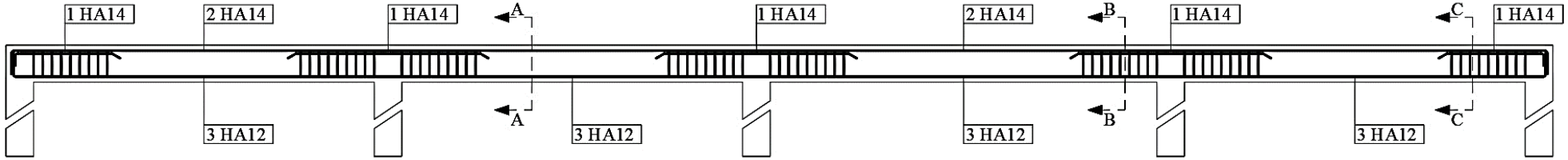

Figure 3.57. Distribution of longitudinal reinforcement in beam

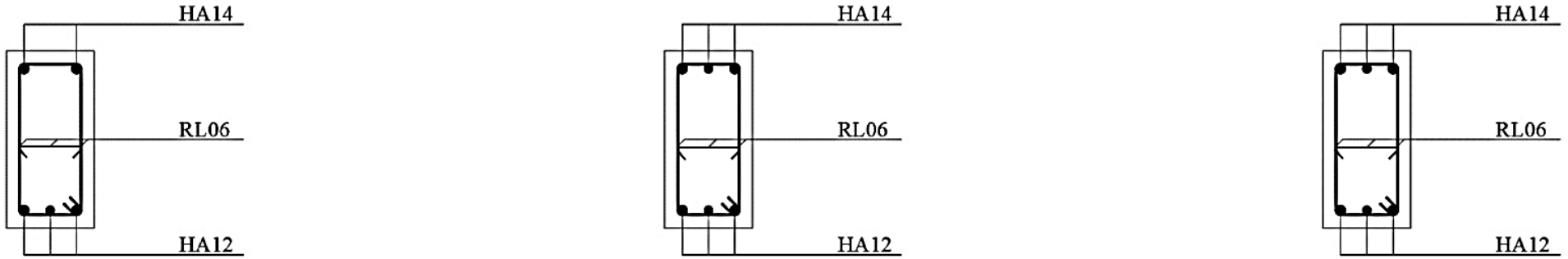

(a) Section A-A **(b)** Section B-B **(c)** Section C-C

Figure 3.58. Cross sections of beam

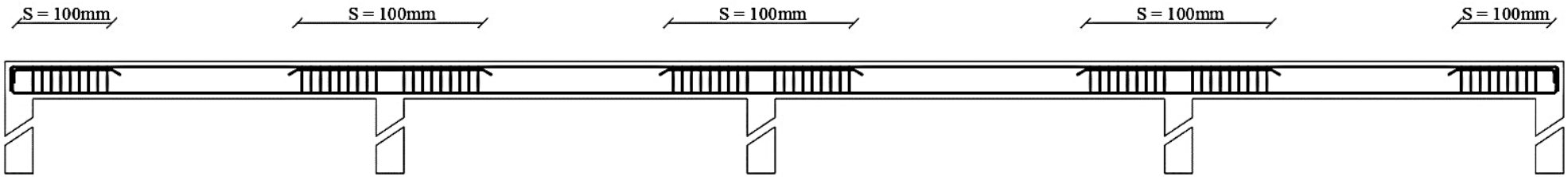

Figure 3.59. Distribution of transversal reinforcements in beam

3.4.4. Design of vertical structural elements

Considering the building with the hollow block slab, the vertical structural elements of the building are composed only of the columns. The design of the column is done by the 3D modelling of the structure with a fixed base. The vertical elements as well as the horizontal elements are modelled as frame elements.

3.4.4.1. Preliminary design

The column chosen for the design is the column D3 highlighted in figure 3.60.

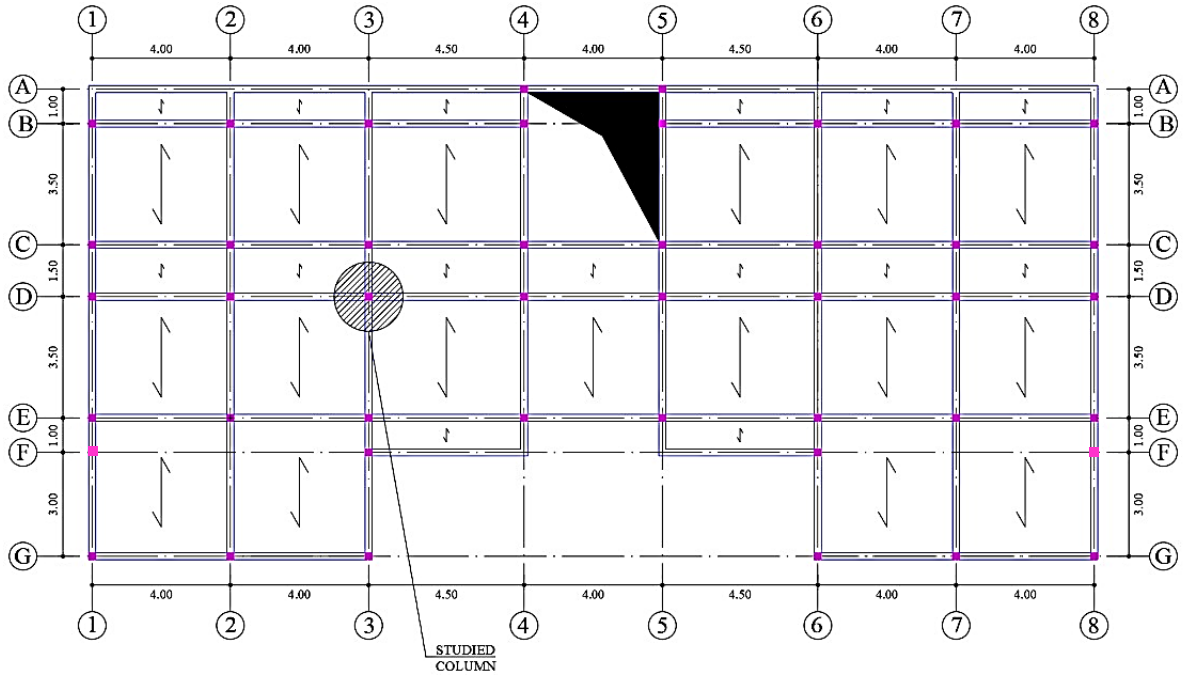

Figure 3.60. Column to be designed

a. Axial load resistance of the section

Applying the procedure in section 2.6.4.1.a, equations 2.49 gives;

$N_{sd} = 591.3\text{KN}$ and we have; $A_c \geq 69760.45$

Considering a square section, we have $a \geq 264.3mm$

The 3D modelling of the building in SAP 2000 is done with the beams section of 20 cm widthand 40 cm height and a column section of 30 cm width and 40 cm height.

b. Modal analysis of the structure

Applying equation 2.50 we have;

$$T_1 = 0.075 \times 21^{3/4} = 0.73s$$

The 3D modelling of the building in ETABS 18 with a fixed base and a percentage of participation of the imposed loads of 30% permitted to observe that, the first mode is translational along the y-axis, the second mode is translational along the x-axis with a small

torsion and the third mode is torsional. The period the first vibration mode is T = 0.913s. The vibration modes are shown in the following figures.

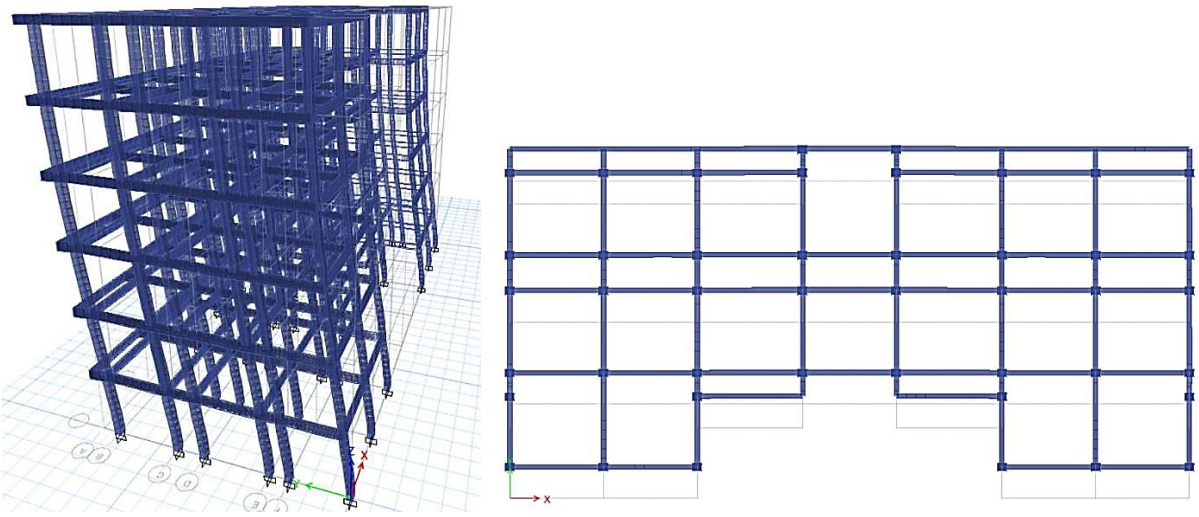

Figure 3.61. First mode of vibration of the structure: translation along the y-axis

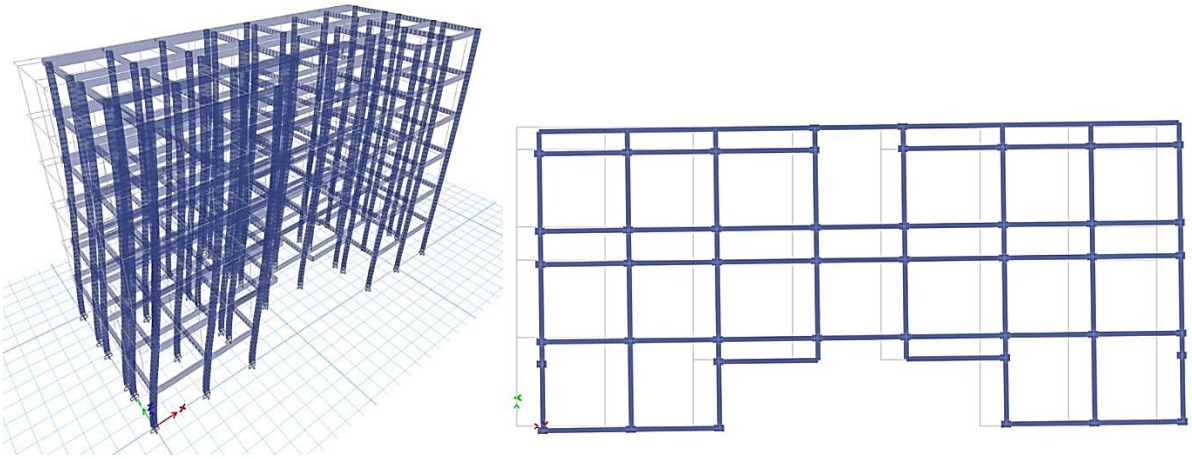

Figure 3.62. Second mode of vibration of the structure: translation along the x-axis with a small torsion

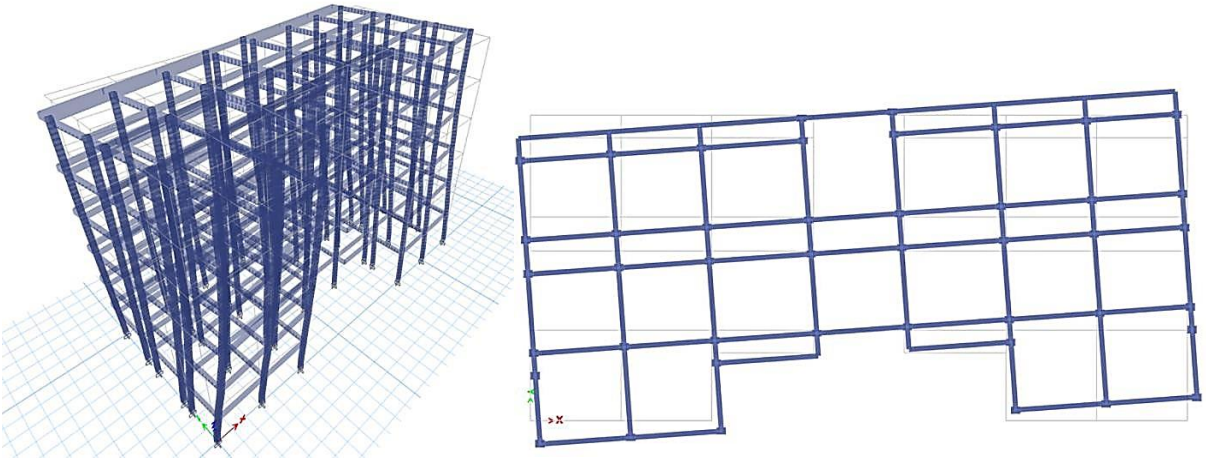

Figure 3.63. Third mode of vibration of the structure: torsion around the z-axis

3.4.4.2. Verification of bending moment and axial force

The seven load combinations considered for the principal beam permit to obtain the solicitation curves of the bending moment and the axial force for the column presented in figure 3.64 and 3.65.

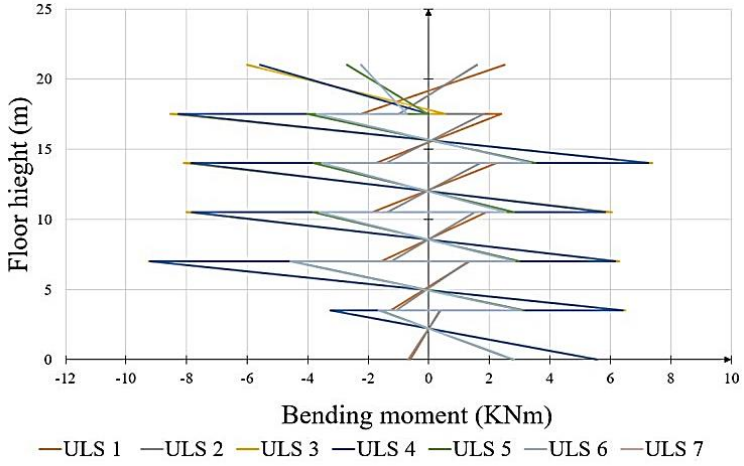

(a)

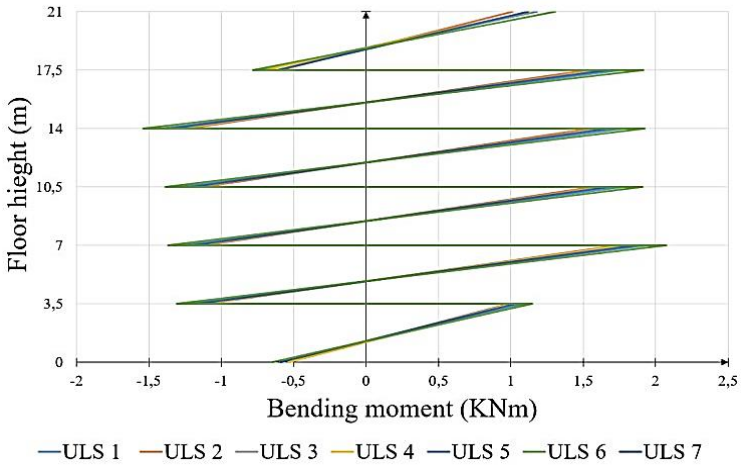

(b)

Figure 3.64. Bending moment solicitation curves for the column along (a) x-axis (b) y-axis

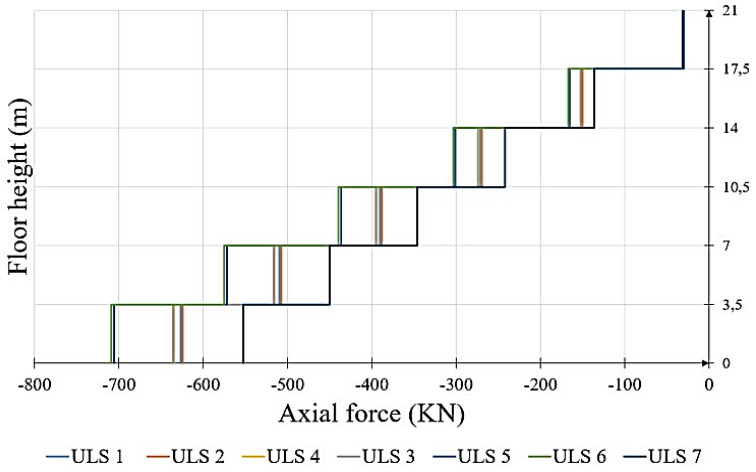

Figure 3.65. Axial load solicitation curves on column

These solicitation curves enable the obtainment of the envelop curves of the bending moment and axial loads solicitation presented in figure 3.66 and 3.67.

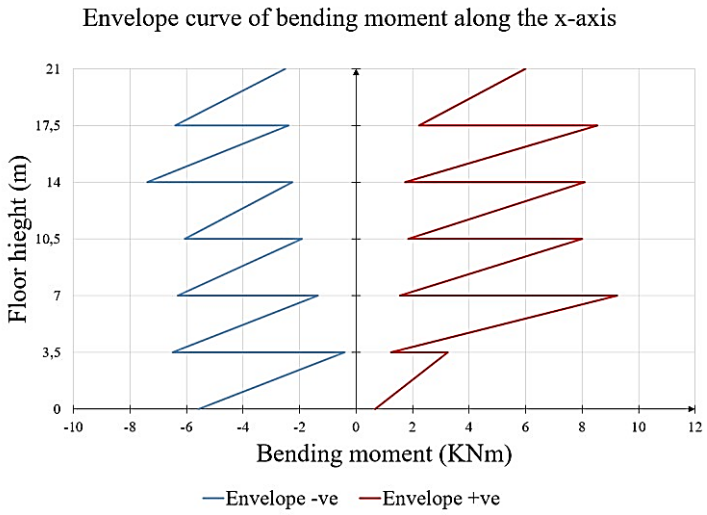

(a)

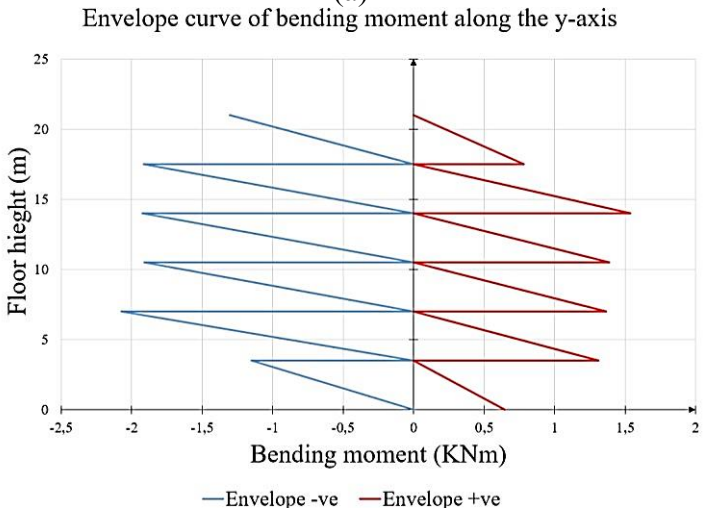

(b)

Figure 3.66. Envelop curve of bending moment on the column along the (a) x-axis (b) y-axis

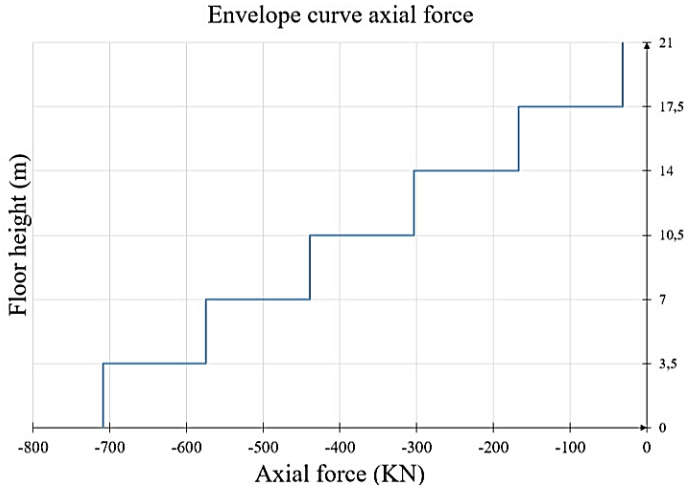

Figure 3.67. Envelop curve of the axial force on the column

The verification of the axial loads and the bending moment is done through the M-N interaction diagram as presented in the section 2.6.4.2.

In this case study, considering a concrete section 30×40 cm, the limitations prescribed in equations 2.18 and 2.19 result in the expression

$$240\ mm^2 \leq As \leq 4800\ mm^2$$

This corresponds to a minimum number of 6 bars of 10 mm diameter (6Ø10). The interaction diagram of the column in the two directions, considering a concrete section of 30 cm width and 40 cm height and a steel reinforcement of 6Ø10 are presented in figures 3.68 and 3.69 for the two directions.

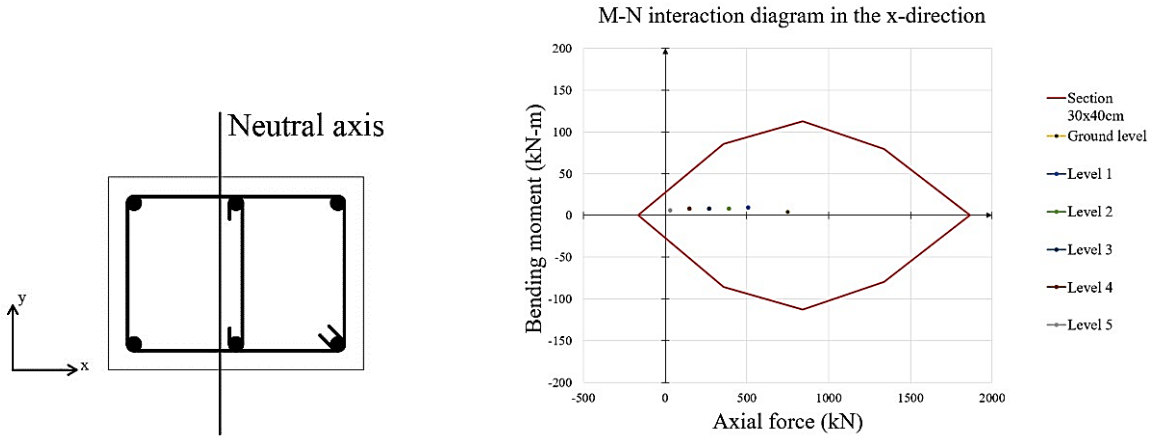

Figure 3.68. Interaction diagram of the column D3 along the x-axis

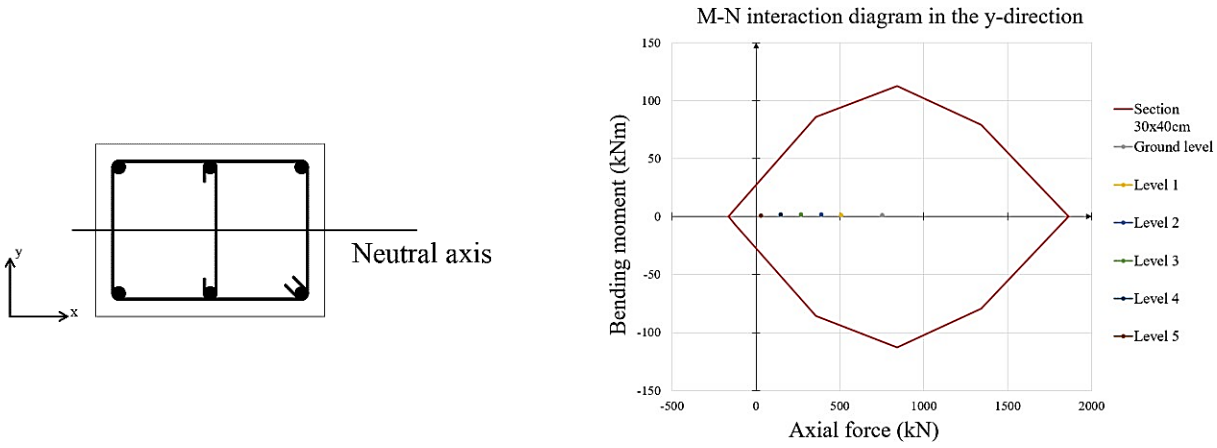

Figure 3.69. Interaction diagram of the column D3 along the y-axis

3.4.4.3. Shear verification

The different loads arrangements permit to obtain the shear solicitation curves along the x and y axes as presented in figure 3.70.

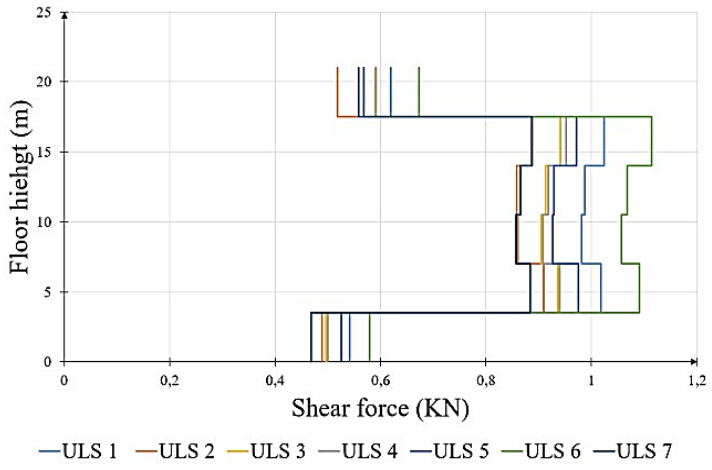

(a)

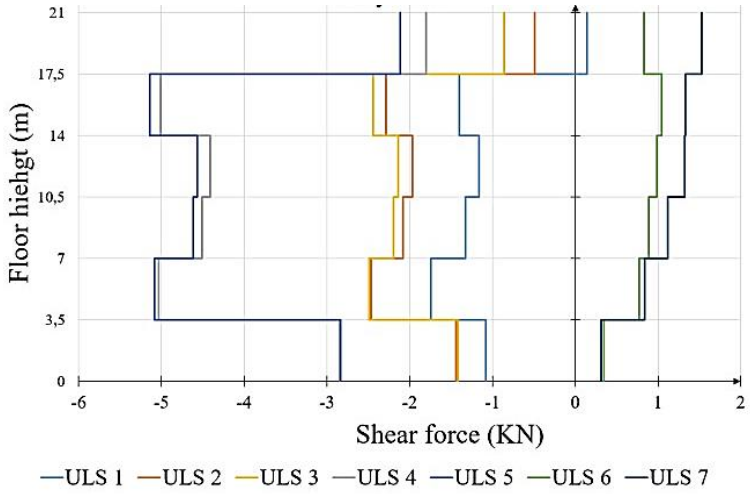

(b)

Figure 3.70. Shear force solicitation curves on the column along the (a) x-axis; (b) y-axis

These solicitation curves enable the obtainment of the envelop curves of the shear solicitations along the x and y axes presented in figure 3.71

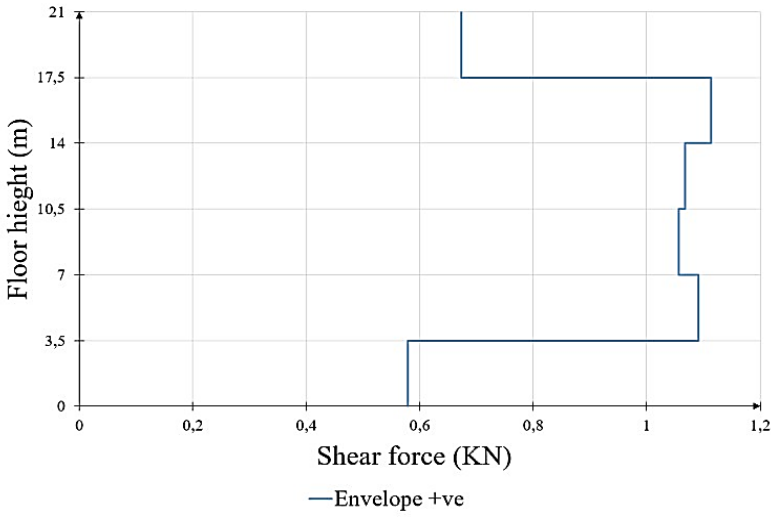

(a)

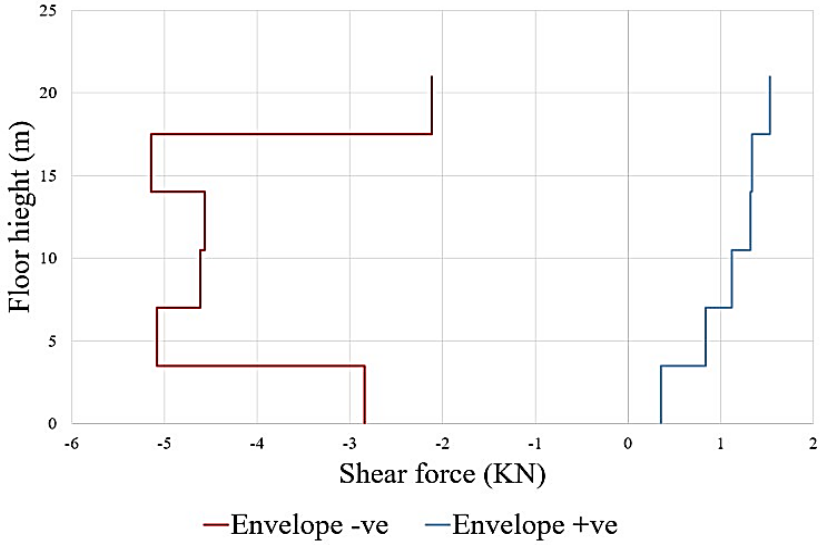

(b)

Figure 3.71. Shear force envelope curve on the column along the (a) x-axis; (b) y-axis

Applying the procedure presented in the section 2.6.2.1.b, it is observed that the shear resistance of the section without shear reinforcement is greater than the maximum shear solicitation on the column so the detailing of members has to be applied to have the spacing.

In our case, we consider a diameter of 6 mm and the maximum spacing of the transverse reinforcement is given by equation 2.63

$$s_{cl,} = \min(200, 300, 400)$$

So applying the prescriptions of the section 2.6.2.1.b, we obtain a spacing of the shear reinforcement of 15 cm within 0.4 m above and below the beam, and 25 cm along the rest of the column section

3.4.4.4. Slenderness verification

Following the procedure presented on the section 2.4.4.4, the different parameters are evaluated and presented below:

A	ω	B	C	n
0.7	0.098	1.09	1.7	0.446

The limit value of the slenderness obtained is;

$$\lambda_{lim} = 38.7$$

The slenderness of an element is evaluate using equations 2.65 and 2.66. For a height of 3.5m, the slenderness of the slenderness of the column is obtained.

$$\lambda = 21.22 < \lambda_{lim}$$

The slenderness is the verified for the column

3.5. Soil structure interaction

The loads arrangements used for the column are the same used to obtain the loads acting on the footings. The sections of footings are evaluated using the model with fixed base and then modelled on our structure. The stiffness of the soil springs are then evaluated and assigned to the footings to represent the soil structure interaction.

3.5.1. Classification of footing

The axial loads that arrive at the base of the structure with fixed base permit to classify the footing into two classes presented in table 3.12.

Table 3.12. Classification of footing in function of loads

Footing class	Class 1	Class 2
Load interval (kN)	300 – 600	600 - 900

Applying the procedure in section 2.7.1 and assuming a soil bearing capacity of 0.25 MPa, the sections and thickness of footing are evaluated and presented in table 3.13.

Table 3.13. Footing sections

Footing class	**Maximum load**	**Footing section**	**Footing thickness**
-	kN	m²	m
Class 1	587.35	1.5 x 2.0	0.4
Class 2	885.5	1.8 x 2.4	0.5

3.5.2. Evaluation of the spring stiffness for each footing class

Considering a dry clay soil, the soil spring stiffness are calculated for vertical and horizontal directions using the equations in section 2.7.2. The calculated soil springs values are applied to the footings of the model by defining soil spring in SAP 2000 software. Table 3.14 presents the soil spring stiffness obtained.

Table 3.14. Spring constant for the soil structure interaction

Footing class	**Vertical springs (Z-direction) (kN/m)**	**Translation springs along x-direction (kN/m)**	**Translation springs along y directions (kN/m)**
Class 1	100000	100000	60000
Class 2	100000	120000	90000

Applying the vertical springs as area springs and the translation springs as joint springs, the new model obtained considering soil-structure interaction is shown in figure 3.72.

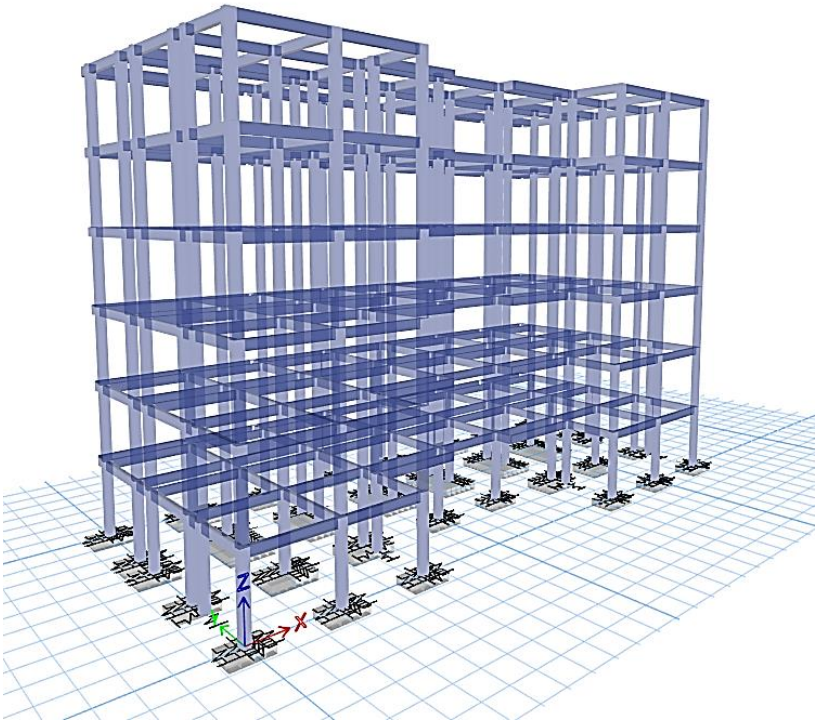

Figure 3.72. Model with soil-structure interaction

From the analysis of the model in figure 3.71, it is observed that the maximum axial loads acting at the footing are less than those of the structure with fixed base. We also observe from the software that, the maximum solicitation pressure is of 0.19 MPa as illustrated in figure 3.73 which is less than the bearing capacity of the soil of $\sigma_{adm} = 0.25\ Mpa$

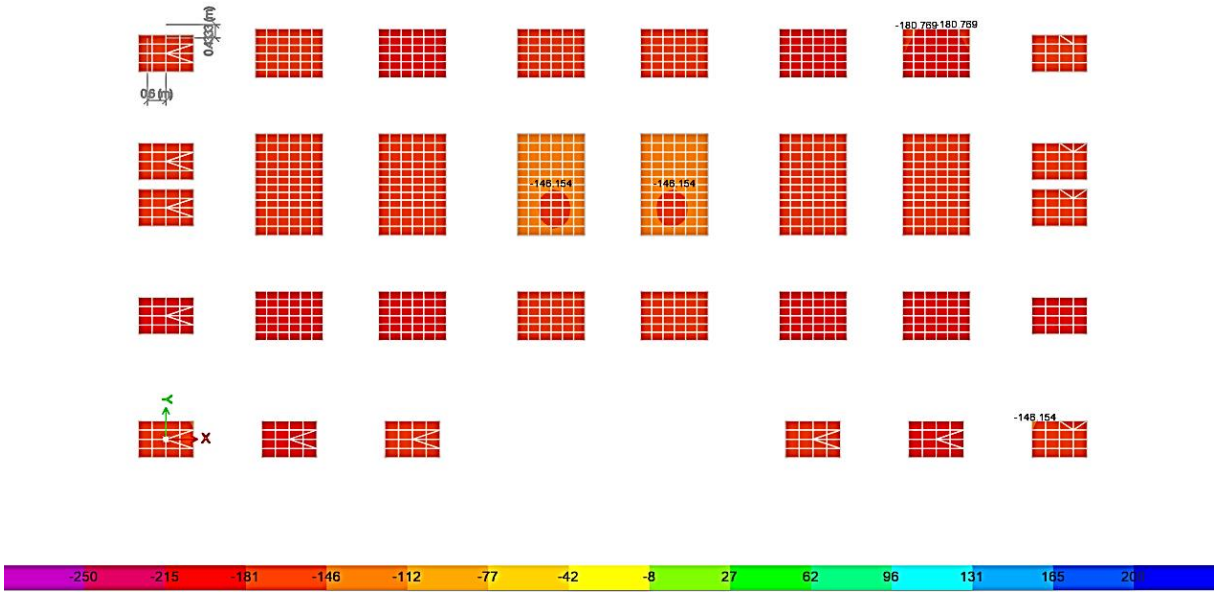

Figure 3.73. Soil pressure on footing in KN/m²

Table 3.15. Verification of settlement on the footings

Footing	Settlement (mm)
B1	-1.634
C7	-1.66
D3	-2.042
D6	-3.293
E8	-1.592
G6	-1.956

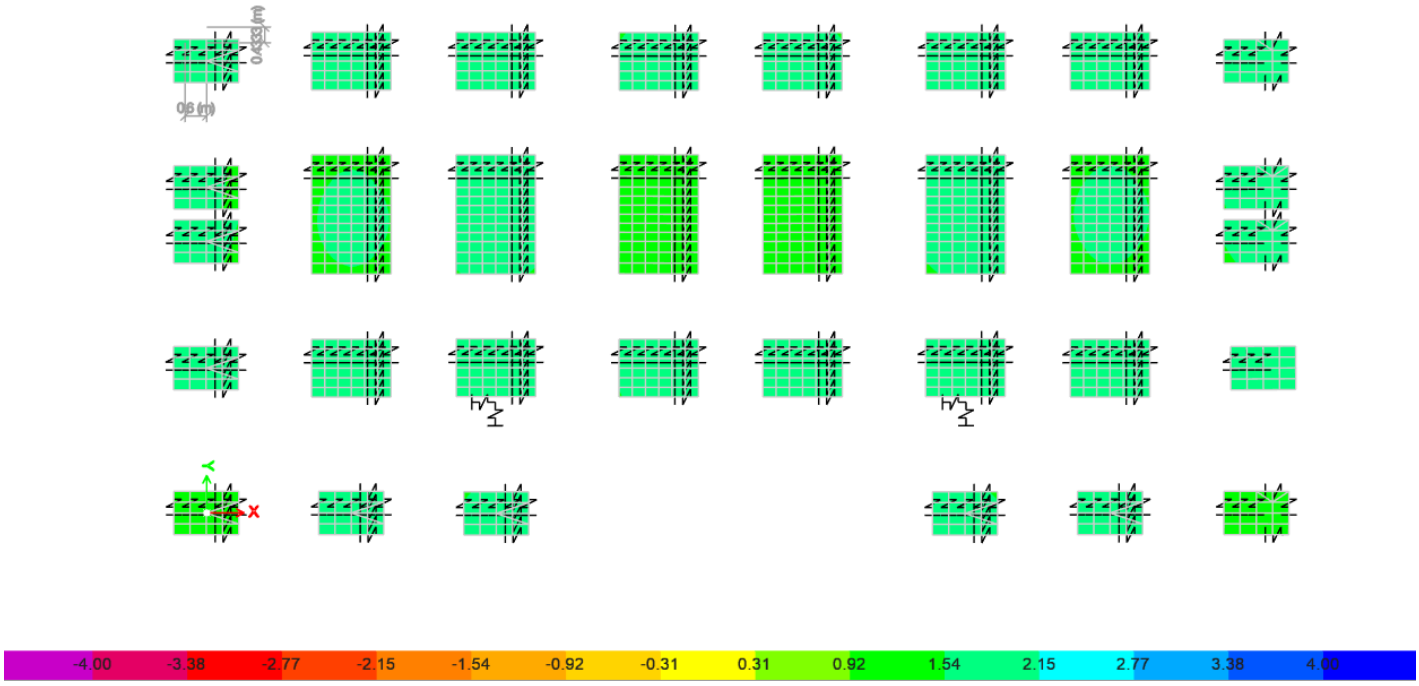

Figure 3.74. Foundation settlement

3.6. Analysis response

For this study, the two models that differ by the slab rigidity are compared. In the first model the slabs are modelled as rigid diaphragms and in the second model the slabs are modelled as flexible diaphragms.

3.6.1. Presentation of models

A 3D and a plane view of the two models are presented in figure 3.75 and 3.76 The analysis of the building under the effect of seismic loads permitted us to obtain the dynamic response of these two models in terms of the time period, maximum story displacements, inter story drift ratio, story shear and torsional moment of the building.

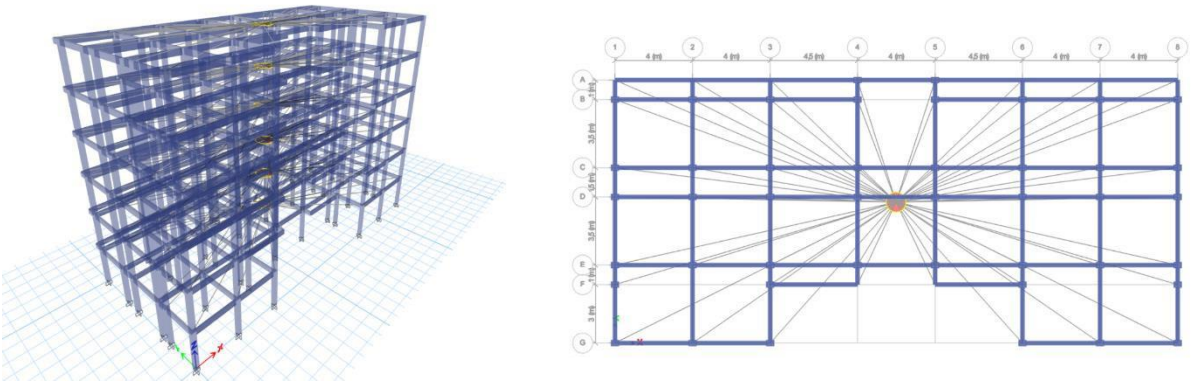

Figure 3.75. Structure with rigid slab

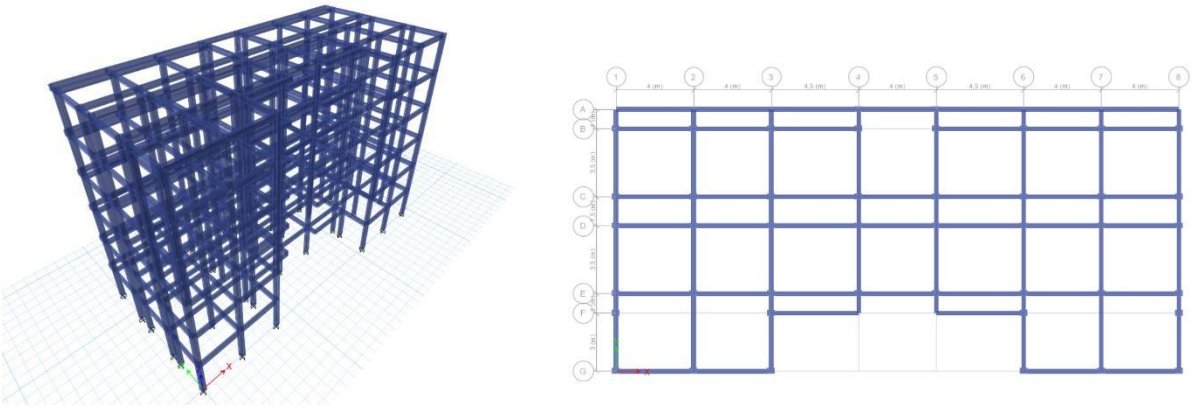

Figure 3.76. Structure with flexible slabs

The deformed shape (3d view and plane view) of the structures with the rigid and flexible slab under the action of seismic loads are presented in figures 3.77 and 3.78

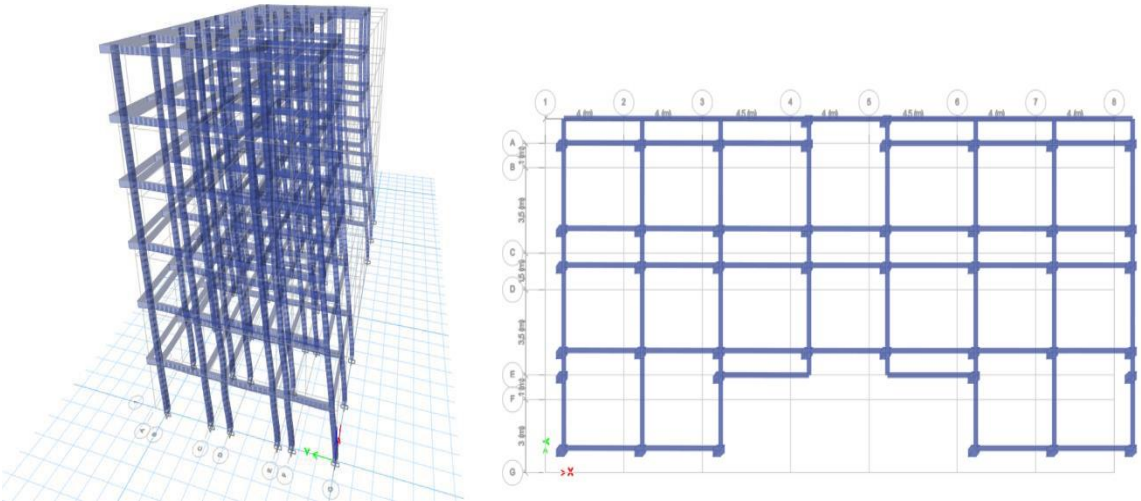

Figure 3.77. Deformed shape of structure with rigid slab under seismic action

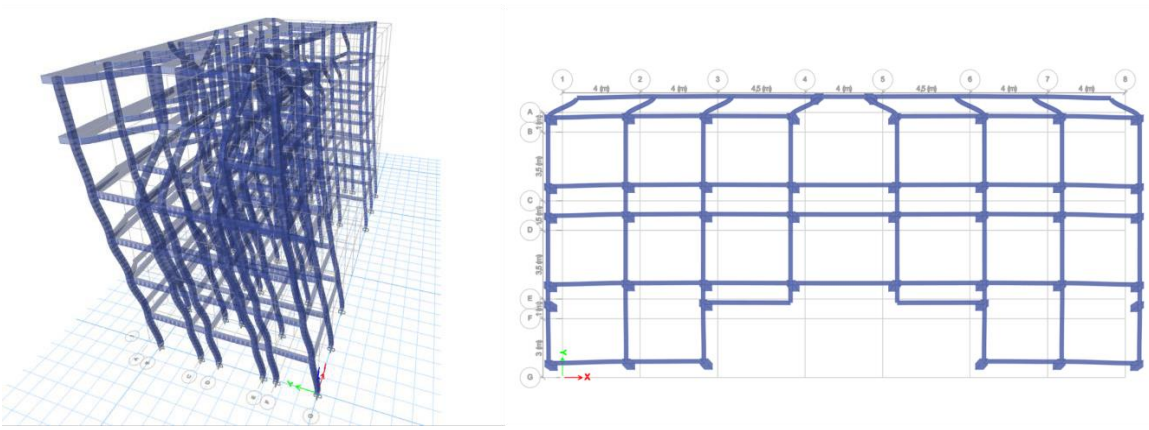

Figure 3.78. Deformed shape of structure with flexible slab under seismic action

3.6.2. Time period

The vibration period is an important parameter of a structure to estimate its seismic demand. Table 3.16 provides the vibration periods and the mass participation ratios of the building models with the different slab conditions.

Table 3.16. Periods of vibration and mass participation ratios for rigid and flexible slab model

	Rigid slab				Flexible slab			
Mode	**Period**	**Mass participation ratio**			**Period**	**Mass participation ratio**		
-	sec	X	Y	Z	sec	X	Y	Z
1	0,913	0	0,8395	0	0,917	0	0,8383	0
2	0,864	0,8141	0,8395	0	0,865	0,7031	0,8384	0
3	0,85	0,8277	0,8396	0	0,858	0,8279	0,8384	0
4	0,298	0,8277	0,9454	0	0,536	0,8279	0,8395	0
5	0,277	0,8294	0,9454	0	0,512	0,8279	0,8395	0
6	0,274	0,9313	0,9454	0	0,366	0,8279	0,8395	0
7	0,173	0,9313	0,9803	0	0,333	0,8279	0,8397	0
8	0,161	0,932	0,9803	0	0,321	0,8281	0,8397	0
9	0,153	0,9715	0,9803	0	0,308	0,8281	0,9067	0
10	0,124	0,9715	0,9951	0	0,298	0,8283	0,9087	0
11	0,114	0,9718	0,9951	0	0,297	0,8283	0,942	0
12	0,104	0,991	0,9951	0	0,275	0,9304	0,942	0

These values permit us to plot the graphs to of time period for the two structures as seen in figure 3.79.

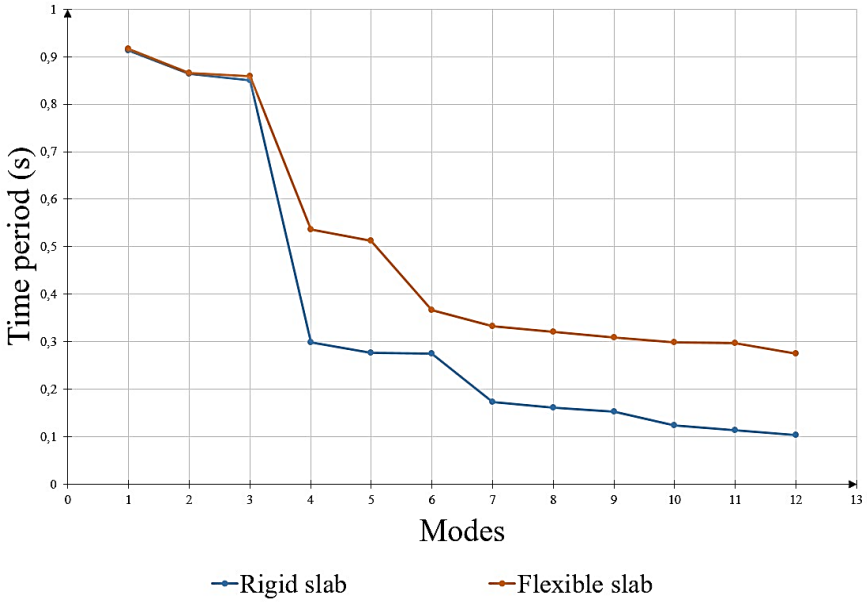

Figure 3.79. Period of vibration of structures with rigid and flexible slab

As expected, the results of the analysis presented in table 3.16 and illustrated in figure 3.79 indicate that the model with the flexible slab condition has higher periods of vibration, especially as from mode 3. This due to the fact that the flexible slab will generally increase the overall flexibility of the structure and thus its period of vibration. It can also be observed that for the mass participation ratios, the model with rigid slab condition reaches 90% of mass participation at mode 6 in the x-direction and at mode 4 in the y-direction whereas, for the structure flexible slab condition, the mass participation ratio reaches 90% in the x-direction at mode 12 and in the y-direction at mode 9. The percentage increase of the periods between the model with rigid slab and the model with flexible slab is of less than 1% for mode 1 to 3. From modes 4 to 12, the percentage increase ranges from 44% to 62%. This shows how the in-plane rigidity of the slab affects the natural period of vibration of the structure.

3.6.3. Maximum story displacement

The results of the 3D numerical predictions for the maximum story displacements of the structure with the rigid slab condition and flexible slab condition are evaluated in the x and y directions. The values of the lateral displacements at each storey along the x-axis are presented in table 3.17 and plotted in the figure 3.80.

Table 3.17. Maximum story displacement for the different slabs along the x-axis

	Elevation	**Displacement (mm) along x-axis**	
	m	Rigid slab	Flexible slab
Foundation	0	0	0
Storey1	3,5	38,989	39,821
Storey2	7	96,191	97,196
Storey3	10,5	148,463	150,073
Storey4	14	188,834	190,753
Storey5	17,5	213,681	215,352
Storey6	21	223,498	224,948

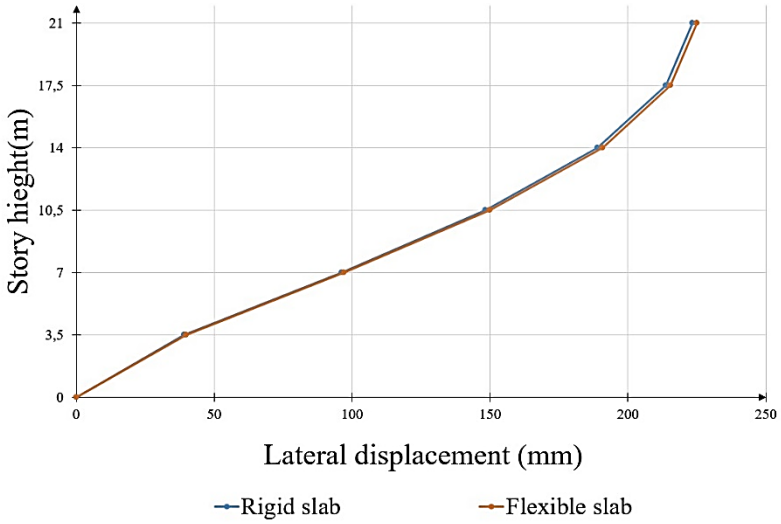

Figure 3.80. Lateral storey displacement along the x-axis

From the values in table 3.17 and illustrated in figure 3.80, it is observed that along the x-axis the largest value of lateral displacement belongs to the model with the flexible slab. This due to the fact that the flexible slab permits in-plane deformations when subjected to lateral loads meanwhile the rigid slab does not. The maximum lateral displacement is of 223.5 mm for the rigid slab model and 224.95 mm for the flexible slab model. This corresponds to an increase of the maximum lateral displacement of 0.65% from the rigid slab model to the flexible slab model.

The values of the lateral displacements for each story along the y-axis are presented in table 3.18 and plotted in the figure 3.81.

Table 3.18. Maximum story displacement for the different slabs along the y-axis

	Elevation	Displacement (mm) along y-axis	
	m	Rigid slab	Flexible slab
Foundation	0	0	0
Storey1	3,5	47,502	49,134
Storey2	7	107,098	110,448
Storey3	10,5	160,486	165,155
Storey4	14	202,553	208,053
Storey5	17,5	229,782	235,42
Storey6	21	241,258	248,889

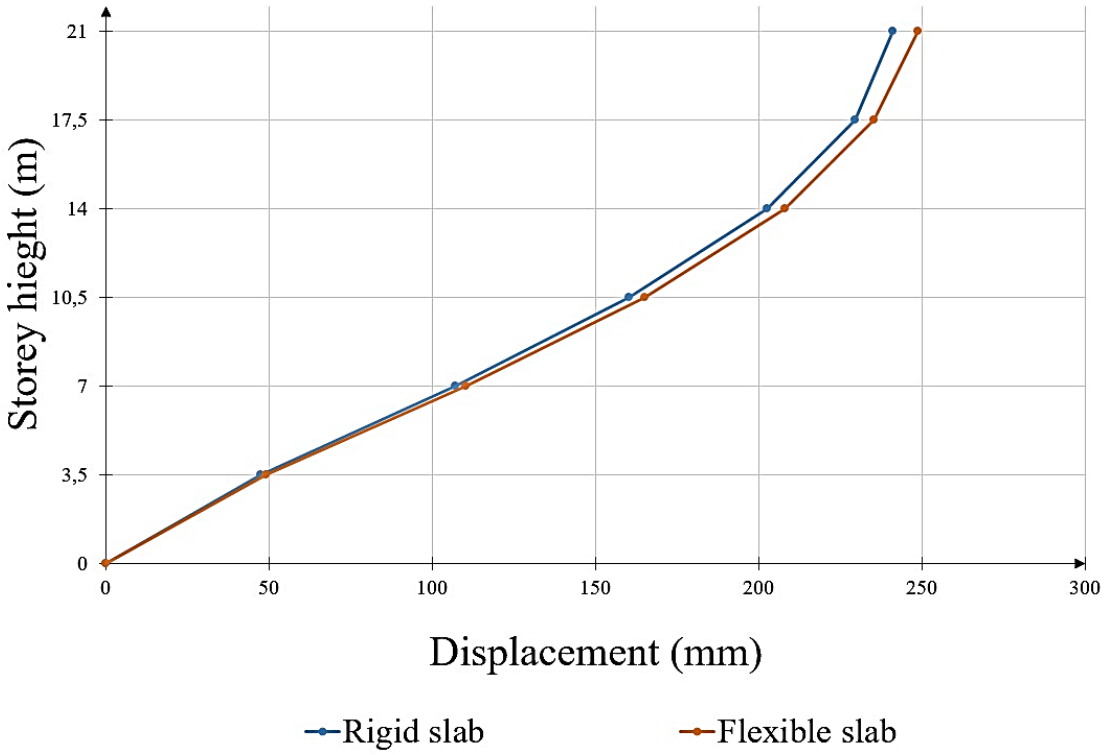

Figure 3.81. Lateral storey displacement along the y-axis

In the y-direction as in x-direction, the largest value of lateral displacement belongs to the model with the flexible slab. The maximum lateral displacement in for the rigid slab model is 241.25 mm and 248.9 mm for the flexible slab model. This corresponds to an increase of the maximum lateral displacement of 3% from the rigid slab model to the flexible slab model.

From the above results it is observed that the effect of the in-plane slab flexibility on maximum lateral displacement of the structure is greater along the y-axis and both structures with the rigid and flexible slab condition undergo greater lateral displacement along the y-axis.

3.6.4. Inter-story drift

The inter-storey drifts are defined as the difference between the lateral deflections of two adjacent stories divided by the height of that storey represented as a percentage. The maximum story displacements for the different models presented in tables 3.18 permits to obtain the maximum inter-story drift for the different models along x-axis presented in table 3.19. Figures 3.82 graphically illustrate the result in tables 3.19 compared to the Eurocode limit.

Table 3.19. Inter-story drift ratio for the different slabs along the x-axis

	Elevation	**Inter-storey drift ratio (%) along X**	
	m	Rigid slab	Flexible slab
Storey1	3,5	1,11	1,14
Storey2	7	1,65	1,70
Storey3	10,5	1,51	1,54
Storey4	14	1,17	1,18
Storey5	17,5	0,73	0,75
Storey6	21	0,29	0,34

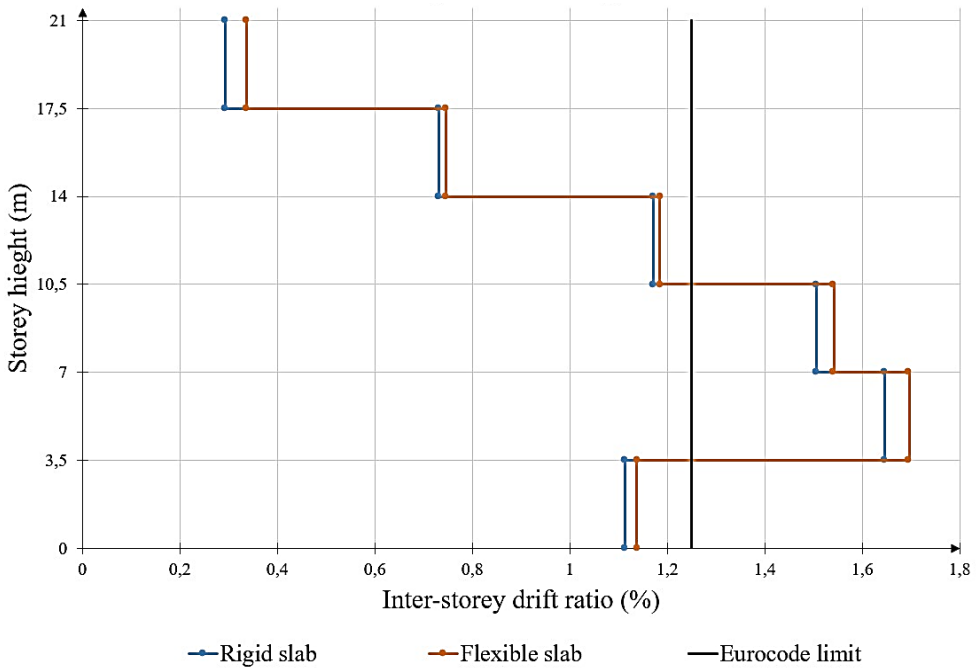

Figure 3.82. Inter-story drift ratio for the different slabs along the x-axis with Eurocode limit

From the figure 3.82, slab flexibility tends to increase the inter-storey drifts of the superstructure. The inter-storey drift of storey 2 and 3 along the x-axis exceeds 1.25 % for the rigid and flexible slab models which is the limit prescribed by the Eurocode standard. This means that the associated damage due to high inter storey drift will occur at these levels for the two models. It can be observed that in general, the structure with the flexible slab has greater inter-storey drifts. For instance, at the height 7m the maximum drift of the rigid slab model is

1.65%, while the corresponding values for the flexible slab model is 1.72%. The structure with the flexible slab gives the largest value of inter-storey drift due to the fact that building it undergoes greater deflections compared to the structure with rigid slab, as seen previously.

Table 3.20. Inter-story drift ratio for the different slabs along the y-axis

	Elevation	**Inter-storey drift ratio (%) along Y**	
	m	Rigid slab	Flexible slab
Storey1	3,5	1,36	1,40
Storey2	7	1,71	1,76
Storey3	10,5	1,54	1,58
Storey4	14	1,23	1,27
Storey5	17,5	0,81	0,86
Storey6	21	0,34	0,41

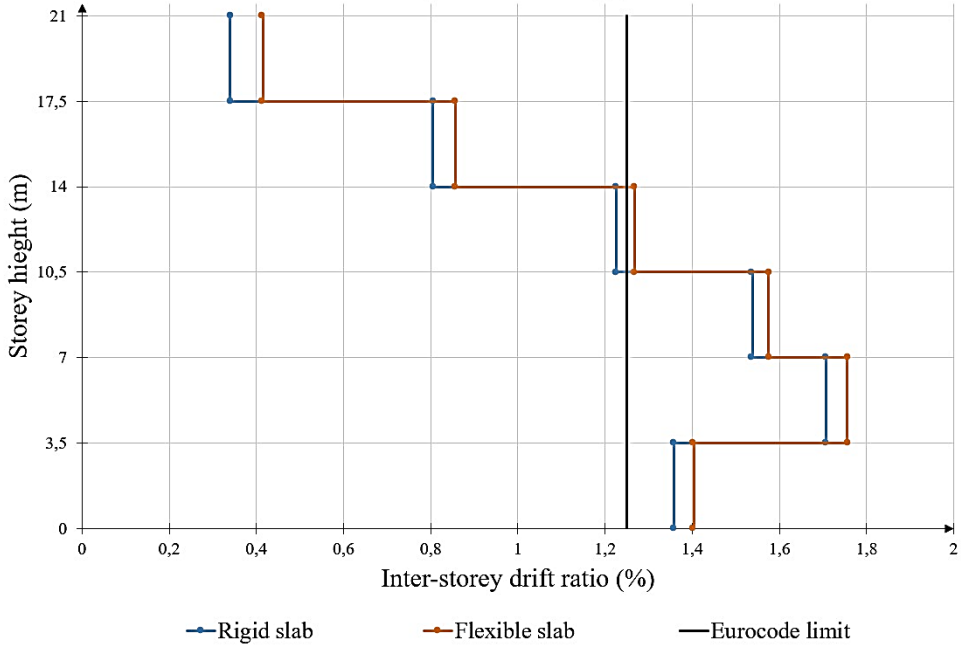

Figure 3.83. Inter-story drift ratio for the different slabs along the y-axis with Eurocode limit

Along y-axis, the inter-storey drift of four storeys in the flexible slab model exceed the Eurocode formulation where as in the rigid slab model only three storeys exceed the Eurocode limitations. This shows again that the structure with the flexible slabs undergoes greater inter-storey drifts compared to the structure with rigid slabs. It is also observed that, the inter-story drifts of the structure are greater along the y-axis than along the x-axis both for the rigid and flexible slab model.

The high values of inter-story drift exceeding the Eurocode limit is due to the fact that there is no mass concentration in our structure. In other to solve this problem a shear wall can be designed and introduced in the structure thereby creating a concentration of mass.

3.6.5. Base shear

The Base shear experienced on the rigid and flexible slab models along the x-axis are presented in table 3.21 and plotted in figure 3.84.

Table 3.21. Base shears for the rigid and flexible slab models along the x-axis

	Base shear (kN) along the X-axis
Rigid slab	11 457,27
Flexible slab	11 426,66

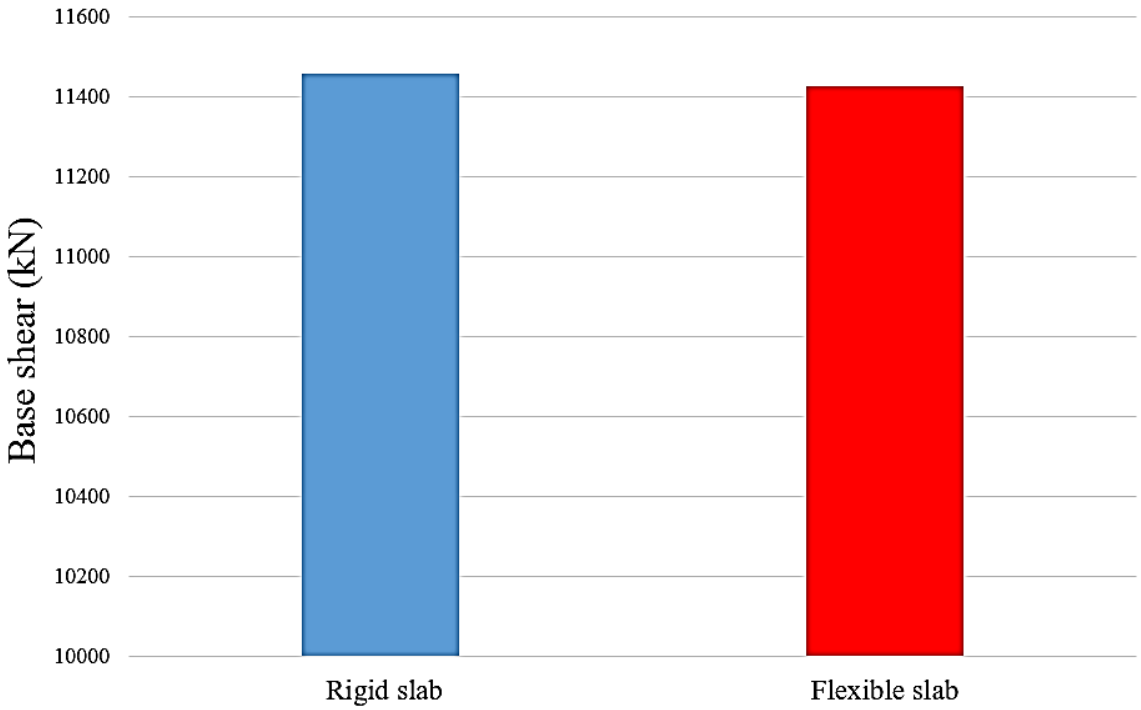

Figure 3.84. Base shears for the rigid and flexible slab models along the x-axis

From figure 3.84 it is observed that the Base shear for the structure with rigid slab and the structure with the flexible slab are practically equal with the storey shears of the rigid slab model being slightly greater. The base shear for the rigid slab model is 11457.27 kN. In the case of the flexible slab model, the base shear is 11426.66 kN which compared to the rigid slab model corresponds to a percentage reduction of 0.3%.

The base shear experienced at each level of the structures along the y-axis are presented in table 3.22 and plotted in figure 3.85.

Table 3.22. Story shears for the different slabs along the y-axis

	Base shear (kN) along the Y-axis
Rigid slab	11 021,60
Flexible slab	10 932,84

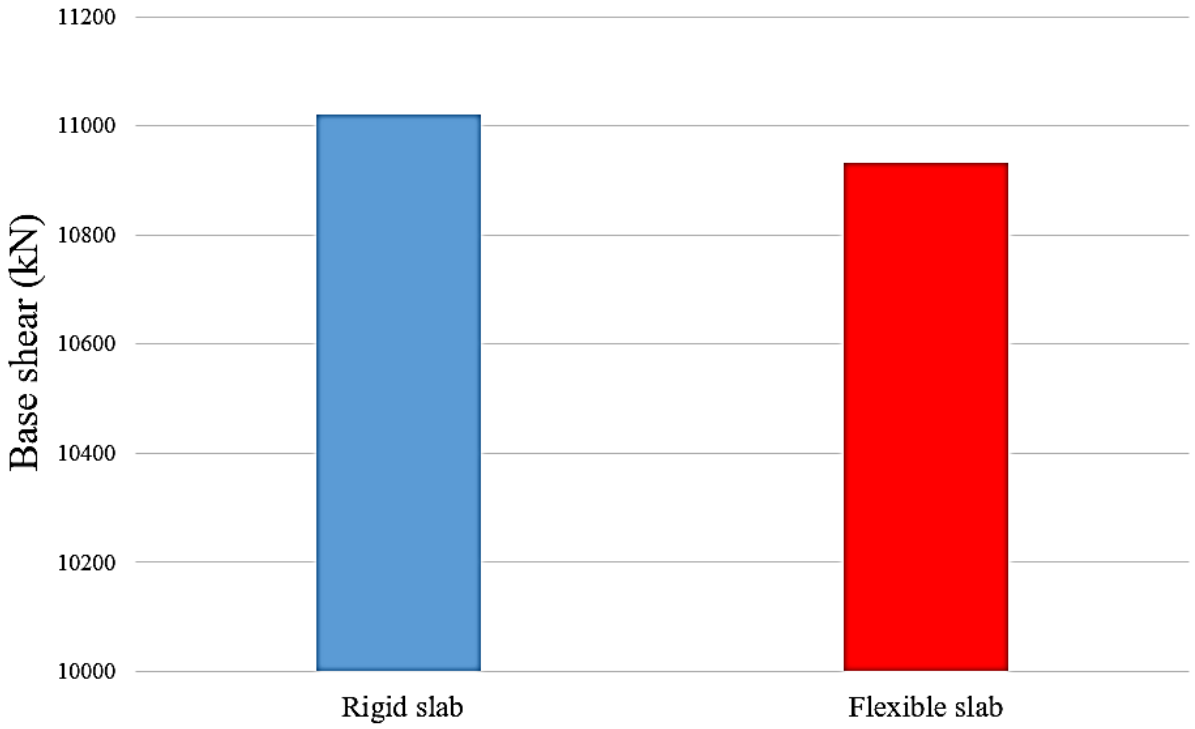

Figure 3.85. Story shears for the different slabs along the y-axis

Along the y-axis, it is observed from figure 3.83 that the base shears for the structure with rigid slab are greater than those of the structure with the flexible slab. The base shear for the rigid slab model is 11021,60 kN. In the case of the flexible slab model, the base shear is 10932,84 kN which compared to the rigid slab model corresponds to a percentage reduction of 0.8%.

Comparing the base shears acting along the x and y-axes of the building, it is seen that the base shears acting along the x-axis for both rigid and flexible slab models are greater than the base shears along the y-axis. The effect of slab flexibility on the base shear is greater along the y-axis compared to the x-axis since the percentage decrease in story shears is greater along the y-axis.

3.6.6. Torsional moment

The torsional effect generated by the seismic action is due to the irregularity of the building. The torsional effect causes a torsional moment which acts at each story and is calculated using equation 2.78 in section 2.9.5. The position of the center of mass and center of rigidity and the structural eccentricities for both structures with rigid and flexible slab model are presented in table 3.23.

Table 3.23. Center of mass and center of rigidity at each story of the structure

	XCM	YCM	XCR	YCR	$e_{o,x}$	$e_{o,y}$
	m	m	m	m	m	m
Story 6	14,50	7,42	14,5	7,0195	0,000	0,397
Story 5	14,49	7,23	14,5	7,0195	-0,014	0,214
Story 4	14,49	7,23	14,5	7,0195	-0,014	0,214
Story 3	14,49	7,23	14,5	7,0195	-0,014	0,214
Story 2	14,49	7,23	14,5	7,0195	-0,014	0,214
Story 1	14,49	7,23	14,5	7,0195	-0,014	0,214

Where:

XCM: is the position of the center of mass along the x-axis

YCM: is the position of the center of mass along the y-axis

XCR: is the position of the center of rigidity along the x-axis

YCR: is the position of the center of rigidity along the y-axis

$e_{o,x}$: is the structural eccentricity in the along the x-axis

$e_{o,y}$: is the structural eccentricity in the along the y-axis

The total eccentricities e_x and e_y used are the sum of the accidental eccentricities (e_a) and the structural eccentricities (e_s) along the x and y axes respectively. The accidental eccentricity is calculated using equation 3.12

$$e_{ai} = \pm 0.05 L_i \tag{3.12}$$

With:

e_{ai}: is the accidental eccentricity of the storey mass i

L_i: is the dimension of the slab perpendicular to the direction of the seismic action

The total eccentricity is the given by the sum e_{ai} and e_{si} for each story mass. The equation 2.78 to determine the torsional moment at each storey becomes;

$$M_{ai} = (\pm 0.05 L_i + e_{si}) \times F_i \tag{3.13}$$

The accidental eccentricity considered is the one giving the maximum total eccentricity so as to have the highest torsional moment. Table 3.24 presents the maximum torsional moments acting at each storey for the structure with the rigid slab condition and Table 3.25 presents the torsional moments acting at each storey for the structure with the flexible slab condition.

Table 3.24. Torsional moments for the rigid slab model

	e_x	e_y	Story force X	Story force Y	Torsional X	Torsional Y
	m	m	kN	kN	kN-m	kN-m
Story 6	0,685	1,857	2815,44	2689,49	1970,8	3426,4
Story 5	-0,7	1,274	2690,85	2560,73	1883,6	3262,4
Story 4	-0,7	1,274	2378,81	2258,61	1665,2	2877,5
Story 3	-0,7	1,274	1870,24	1789,28	1309,2	2279,5
Story 2	-0,7	1,274	1211,89	1193,96	848,3	1521,1
Story 1	-0,7	1,274	490,05	529,54	343,0	983,3

Table 3.25. Torsional moments for the flexible slab model

	e_x	e_y	Story force X	Story force Y	Torsional X	Torsional Y
	m	m	kN	kN	kN-m	kN-m
Story 6	0,685	1,857	2833,20	2774,66	1983,2	3534,9
Story 5	-0,7	1,274	2712,26	2624,49	1898,6	3343,6
Story 4	-0,7	1,274	2402,36	2319,37	1681,7	2954,9
Story 3	-0,7	1,274	1890,90	1841,11	1323,6	2345,6
Story 2	-0,7	1,274	1224,49	1230,75	857,1	1568,0
Story 1	-0,7	1,274	501,38	547,71	351,0	1017,1

From tables 3.24 and 3.25, it is observed that the structure has a greater eccentricity along the y-axis. This therefore causes the torsional moments along the y-axis to be greater than those along the x-axis. The torsional moments for the rigid slab model are greater than the torsional moments for the flexible slab due to the fact that, the story forces of being greater for the rigid slab condition than for the flexible slab condition.

3.6.7. Effect of Soil structure interaction

In section 3.4.2 we observed that soil structure interaction had an effect on the solicitations of the structure under vertical loads. After observing the dynamic response of the two models with fixed base, we are going to see how the consideration of soil structure interaction affects the dynamic response of the structure. The results are going to be observed in terms of time period, story displacement, and story shears.

3.6.7.1. Time period

Considering soil structure interaction, table 3.26 provides the vibration periods and the mass participation ratios of the building models with the different slab conditions.

Table 3.26. Periods of vibration and mass participation ratios for rigid and flexible slab model with SSI

	Rigid slab				Flexible slab			
Mode	**Period**	**Mass participation ratio**			**Period**	**Mass participation ratio**		
-	sec	X	Y	Z	sec	X	Y	Z
1	1.044	0	0.8025	0	1.046	0	0.8018	0
2	0.957	0.0956	0.8034	0	0.961	0.0684	0.8029	0
3	0.938	0.7976	0.8035	0	0.94	0.7986	0.8029	0
4	0.325	0.7976	0.8983	0	0.396	0.7986	0.8035	0
5	0.303	0.7986	0.8985	0	0.392	0.7986	0.8035	0
6	0.297	0.8914	0.8985	0	0.329	0.7986	0.892	0
7	0.185	0.8914	0.9213	0	0.324	0.8	0.892	0
8	0.172	0.8917	0.9214	0	0.306	0.8004	0.892	0
9	0.166	0.922	0.9214	0	0.299	0.888	0.892	0
10	0.131	0.922	0.9288	0	0.291	0.888	0.8947	0
11	0.126	0.9227	0.9288	0	0.284	0.8906	0.8947	0
12	0.12	0.9232	0.9288	0	0.277	0.8906	0.8971	0

From table 3.26 it is observed that, the period of vibration for the rigid and flexible slab models with SSI are greater than those for the models with fixed base. In the same way as the models with fixed base, the period of vibrations of the flexible slab model are greater than for the rigid slab model when considering SSI. The difference between the period of vibration of the two models with SSI increases as from mode 4 in the same way as for the fixed base model.

So one can conclude that SSI has an effect on the period of vibration of the structure but does not change the difference in the effect of the rigid and flexible slab on the period of vibration of the structure.

3.6.7.2. Story displacements

The story displacements is observed along the x and y axis. The values of the lateral displacements at each storey along the x-axis are presented in table 3.27.

Table 3.27. Maximum story displacements for the rigid and flexible slab models along the x and y axes for structure with SSI

	Elevation	**Displacement (mm) along x-axis**		**Displacement (mm) along y-axis**	
	m	Rigid slab	Flexible slab	Rigid slab	Flexible slab
Foundation	0	0	0	0	0
Storey1	3,5	62.365	65.71	78.346	80.149
Storey2	7	122.135	122.378	145.018	140.95
Storey3	10,5	174.43	174.905	202.873	199.357
Storey4	14	214.458	215.41	248.957	245.845
Storey5	17,5	239.667	240.918	280.629	279.304
Storey6	21	251.256	252.185	297.254	299.774

From the values of table 3.27 it is observed that the structure with the flexible slab undergoes greater displacements along the x and y axes. Comparing these values to those obtained with the fixed base structure, we see that the structure with SSI has greater lateral displacements for the for the rigid and flexible slab models and in both directions. In the same way as for the fixed base models, the storey displacements along the y-axis are greater than those along the x-axis for the rigid and flexible slab model with SSI.

The greater values of displacement for the models with SSI is due to the fact that the SSI increases the overall flexibility of the structure. The results of the storey displacements for the rigid and flexible slab models with SSI and with the fixed base are illustrated in the figures 3.86 and figure 3.87. Figure 3.86 shows the results along the x-axis and figure 3.87 the results along the y-axis. These figures give a better visualisation of the difference between the results.

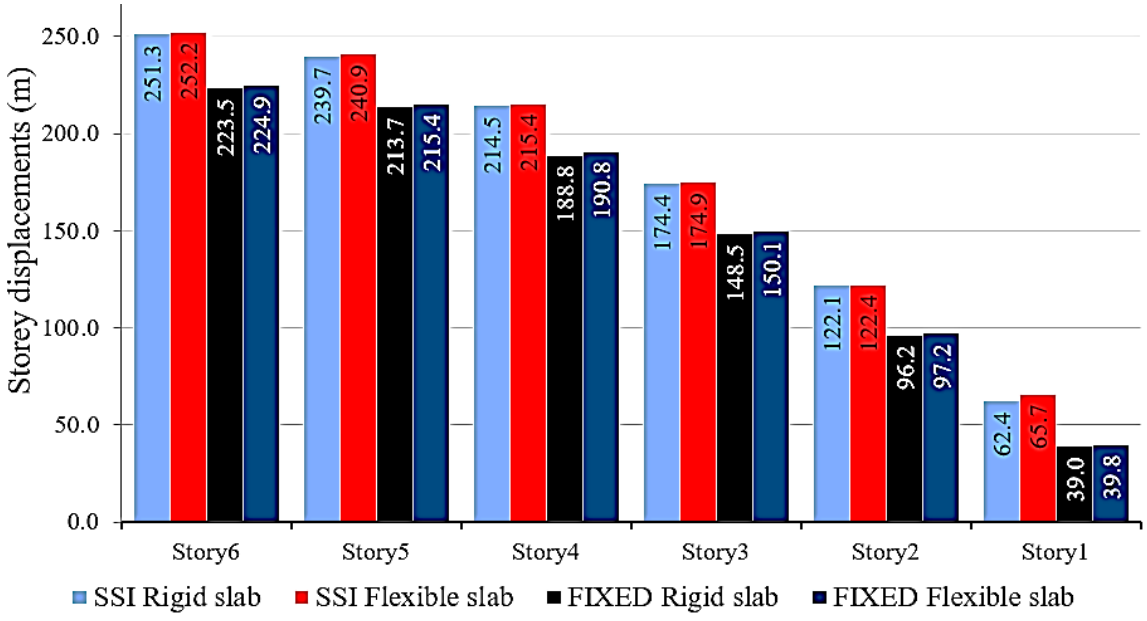

Figure 3.86. Storey displacements for the rigid and flexible slab models with SSI and with fixed base along the x-axis

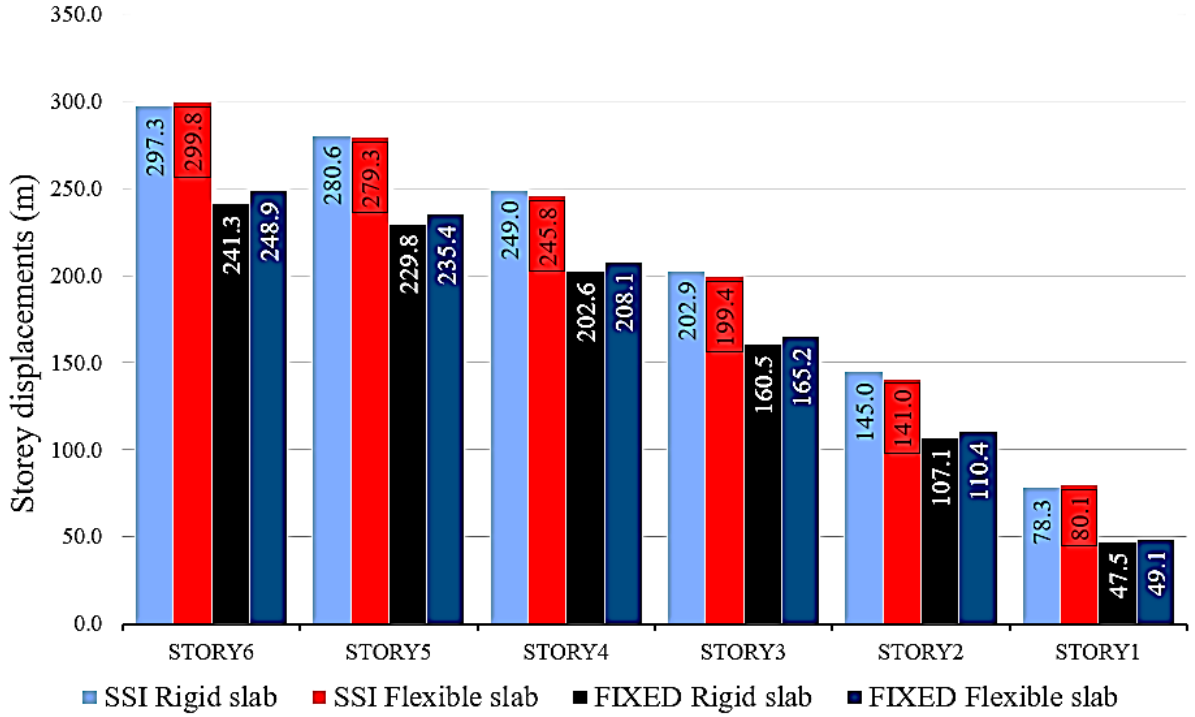

Figure 3.87. Storey displacements for the rigid and flexible slab models with SSI and with fixed base along the x-axis

3.6.7.3. Base shear

The base shear experienced at the base of the structures along the x and y axes are presented in table 3.28.

Table 3.28. Base shear along the x and y axes for the rigid and flexible slab models with SSI

	Storey shear (KN) along the X-axis	Storey shear (KN) along the Y-axis
Rigid slab	-11388.66	-10353.82
Flexible slab	-11366.38	-10306.06

From table 3.28 it is observed that along the x and y axes, the base shear in the rigid slab models are greater than those in the flexible slab model as was the case for the models with fixed base. As for the models with fixed base, the difference between the effects (base shears) of the rigid slab and the flexible slabs are very small and the storey shears along the x-axis are greater than those along the y-axis for the rigid and flexible slab models with SSI.

Comparing the results obtained for the fixed base model to the results obtained for the models with SSI, it is observed that the base shears are generally greater for the model with the fixed base. The above explanations are illustrated in figures 3.87 and 3.88 showing the results of the storey shears for the rigid and flexible slab models with SSI and with the fixed base. Figure 3.88 shows the results along the x-axis and figure 3.89 the results along the y-axis.

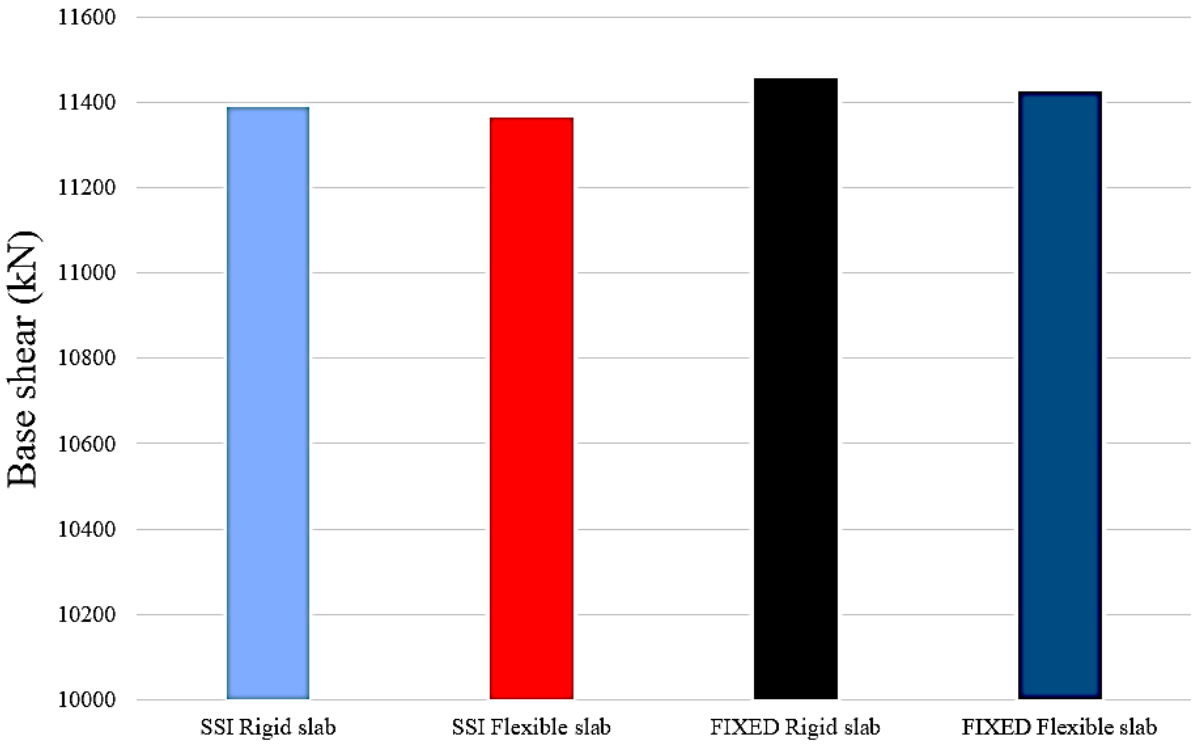

Figure 3.88. Base shear for the rigid and flexible slab models with SSI and with fixed base along the x-axis

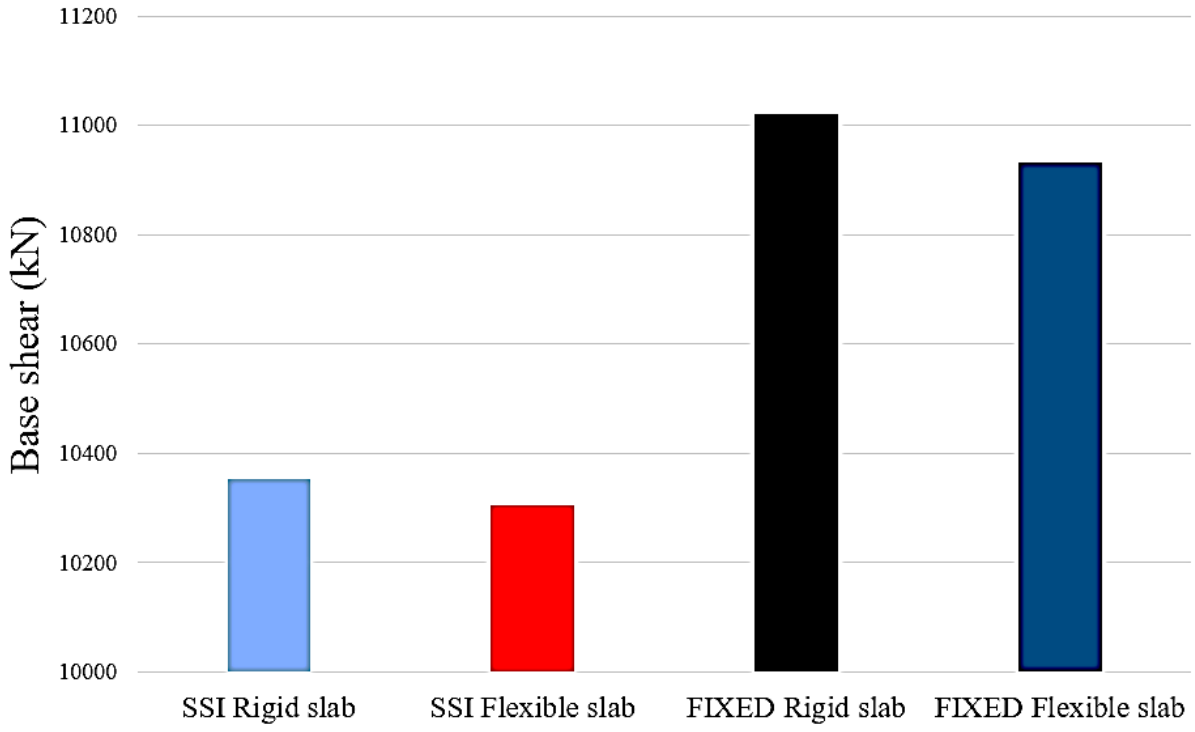

Figure 3.89. Base shear for the rigid and flexible slab models with SSI and with fixed base along the y-axis

Conclusion

The aim of this chapter was to present the case study, to perform the analysis and the design of the structural elements and to compare its seismic behaviour considering rigid and flexible slabs. Starting with the design of the two most used types of slabs in Cameron, the two-way slab supported by beams of thickness 18cm was able to support the loads of the building in the same as the hollow core slab of thickness 20cm. Considering the structure with the hollow core slab, a section of 40 cm height and 20 cm width is obtained for beams and a section of 30 cm by 40 cm for the one the most solicited column at the basement level. In other to introduce SSI a preliminary design of the footing was done and we obtained two footing sections (1.5 x 2.0 and 1.8 x 2.4).

The analysis of the building is first done with fixed base. At the end, we found that the rigid slab assumption underestimates the building periods, the maximum lateral displacement and the inter-storey drift compared to the flexible slab condition although the differences are small and may not cause significant damage to the structure. For base shear and torsional moment, the effects are greater for the rigid slab condition compared to the flexible slab condition. Moreover, for both conditions, the effects are always greater along the y-axis.

The analysis of the building considering SSI revealed that for the for the rigid and flexible slab models, there was an increase in the period of vibration, and the story displacement where as for the story shears there was a reduction. In the same way as the fixed base models, the models with SSI the effects of the story displacement and story shear are greater along the y-axis compared to the x-axis

GENERAL CONCLUSION

The purpose of this work was to carry out analyses to show the effects of rigid and flexible slabs, on the structural behaviour of an irregular buildings. This study concentrated on the seismic response of the models since seismic loads are the most devastating for irregular structures. The study started with a literature review on slabs, slab rigidity, tall buildings and irregular buildings principally. This was followed by the methodology of the static design and dynamic analysis of the case study. Following this methodology, an irregular five storey building located at Mimboman Yaoundé was studied. The static analysis was performed in SAP 2000 version 22, with which two slabs (hollow block and two-way slab), one beam and one column were designed. Considering the building with a hollow block slab, the structure was modelled in ETABS version 18 where the rigid and flexible slab condition were affected to the structure which gave a total of two models for a comparative study. The results obtained from the analysis revealed that: The considering slab flexibility reduces the vibration periods of the building compared to the rigid slab assumption. It was seen that flexible slab model had higher vibration periods compared to the rigid slab model, meaning that the flexible will cause a reduction in the intensity of the seismic force acting on the building. Increase slab flexibility increases the lateral storey displacements and therefore the maximum lateral displacement of the building. This is due to the fact that, under action of lateral loads flexible slabs undergo in-plane deformation increasing the total displacement while rigid sabs undergo little or no in-plane deformation. The inter-story drift follows the same pattern as the lateral displacement with the flexible slab model having higher values than the rigid slab. It was observed that the all the base shears for the flexible slab model are less than those of the rigid slab model demonstrating that the increase in slab flexibility reduces the story shear of the structure. As for the base shear, the torsional moment acting at each storeys for the flexible slab model are less than those of the rigid slab model. It can be concluded that the slab flexibility has an effect on the seismic response of buildings. For buildings with moment resisting frames as vertical lateral load resisting systems as is the case here, the difference in the effects of rigid and flexible slabs is quite small. So, for buildings with moment resisting frames the rigid slab assumption may not be accurate but since the difference in the effect of flexible slab condition compared to the rigid slab condition is quite small, there will not be significant damages on the structure if the slab behaves as a flexible slab instead of rigid. As perspective, the effect of rigid and non-rigid slabs can be studied on structures with shear walls or braced systems as vertical-lateral load resisting systems.

BIBLIOGRAPHY

BOOKS

Bowles, J. E. (1996). *Foundation analysis and design.* The McGraw-Hill Companies, Inc.

Comité Européen de Normalisation. (2002). Eurocode 0: Basis of structural design. Norm EN 1990. Brussels: Comité Européen de Normalisation.

Comité Européen de Normalisation. (2002). Eurocode 1: Actions on structure. Norm EN 1991. Brussels: Comité Européen de Normalisation.

Comité Européen de Normalisation. (2005). Eurocode 2: Design of concrete structures. Norm NF EN 1992. Brussels: Comité Européen de Normalisation.

Comité Européen de Normalisation. (2005). Eurocode 3: Design of concrete structures. Norm NF EN 1992. Brussels: Comité Européen de Normalisation.

Comité Européen de Normalisation. (2005). Eurocode 8: Design of concrete structures. Norm NF EN 1992. Brussels: Comité Européen de Normalisation.

Eurocode 2 Commentary. (2017).

Gonz, J. (2017). *Structural Design Of Concrete Structures*.

May. Hsu, T. T. C., & Mo, Y. L. (N.D.). *Unified Theory Of*

Concrete. *Reinforced Concrete Design*. (N.D.).

Standard, E. (2002). *En 1990*.

Taranath, B. S. (2013). Tall Building Design: Steel, Concrete, and Composite Systems.In *Aquatic Procedia* (Vol. 1).

Yoo, C. H., & Lee, S. C. (N.D.). *Stability Of Principles And Applications*.

ARTICLES

Ahmed, D., & Asiz, A. (2017). *Structural Modeling and Design of Tall Buildings Composed of Ultra- lightweight floor systems Structural modeling and design of tall buildings composed of ultra- lightweight floor systems*. *September 2013*.

Antony, R. R., & Pillai, P. R. S. (2016). *Effect of Vertical Irregularities on Seismic Performance of Rc Buildings*. *7*(10), 198–207.

Badami, S., & Suresh, M. R. (2014). *A Study on Behavior of Structural Systems for Tall Buildings Subjected To Lateral Loads*. *3*(7), 989–994.

Bhatt, M. R., Jha, S., & Pradhan, P. M. (2019). *Study on the Effect of Mass and Stiffness Irregularities on Fundamental Period of Infilled RC Framed Buildings*. *April*.

C, P. P., E, P. G. P. M., & G, P. S. H. (2017). *Evaluation Of Roof Diaphragm Effects On Seismic Behaviour Of Rc Evaluation Of Roof Diaphragm Effects On Seismic Behaviour Of Rc Buildings*. *10*(December2020), 2010–2019. https://doi.org/10.13140/RG.2.2.33703.37280

Conference, W., October, E. E., Earth, G., & Constructions, I. (2008). *Influence of plan irregularity of buildings*. *1982*.

El-habbal, I. M. (2011). *Types of Slabs*. *Ii*.

Elsherbeny, H. A. (2016). *Behavior of Reinforced Concrete Flexible Floor Diaphragms under Seismic Loads By Eng . Hesham Ahmed El Sherbeny B . Sc . in Civil Eng . 1992 A Thesis Submitted to the Faculty of Engineering at Cairo University in Partial Fulfillment of Requirements for the Degree of in*. *April*. https://doi.org/10.13140/RG.2.1.1995.3046

Fouad, K., & Ali, Z. (n.d.). *Strucural Analyses With Flexiblility Effect Of The Floor Slabs*.

Fu, F. (2019). *Advanced Modelling Techniques in Structural Design*. *201805975002*, 2–3. https://doi.org/10.1002/9781118825440.ch3

Georgoussis, G. K., & Mamoua, A. (2018). The effect of mass eccentricity on the torsional response of building structures. *Structural Engineering and Mechanics*, *67*(6), 671–682. https://doi.org/10.12989/sem.2018.67.6.671

İlerisoy, Z. Y. (2019). *Discussion of the Structural Irregularities in the Plan for Architectural Design within the Scope of Earthquake Codes*. *50*(1), 50–62.

Magarpatil, H. R. (2017). *Evaluation of Seismic Response Modification Factor for Asymmetric Structures*. *7*(6), 87–94.

Mandal, A., & Nigam, M. K. (2018). *E-R E-R E-R E-R*. *1*(10), 46–54.

Moeni, M., & Rafezy, B. (2011). Investigation into the Floor Diaphragms Flexibility in Reinforced Concrete Structures and Code Provision. *Global Journal of Research In Engineering*, *11(1)*(1), 25–35.

Nassani, D. E., & Ali, K. (2020). *Lateral Load Resisting Systems in High-Rise Reinforced Concrete Buildings Lateral Load Resisting Systems in High-Rise Reinforced Concrete Buildings Yüksek Katlı Betonarme Binalarda Yanal Yük Dayanım Sistemleri*. *December*. https://doi.org/10.31590/ejosat.808269

Naveen, G. M., & Chaya, S. (2016). *" STUDY ON REGULAR AND IRREGULAR BUILDING STRUCTURES DURING AN EARTHQUAKE ."* 42–48.

Nazifkerdar, A. (2020). *Investigation of Rigid Floor Diaphragm Effects in Reinforced Concrete Structures*. *June*.

Of, C., Tall, F., & In, B. (n.d.). *Lateral load design of tall buildings*.

Planchers, F. D. E. S., Planchers, L. E. S., Creux, A. C., Planchers, L. E. S., Beton,E.N., Metalliques, L. E. S. P., & Alveoles, L. E. S. P. (n.d.). *CHAPITRE 1 : PLANCHERS.2*(Figure 2), 1–26.

Shah, K., & Vyas, P. (2017). *Effects Of Vertical Geometric And Mass Irregularities In Structure*. *1*, 87–92.

Stiffness of Concrete Slabs. (n.d.). *4*.

Titiksh, A. (2018). Effects of Irregularities on the Seismic Response. *Asian Journal of Civil Engineering (Bhrc)*, *18*(8).

Varadharajan, S., Sehgal, V. K., & Saini, B. (2013). *Review of different Structural irregularities in buildings*. *39*(5), 538–563.

Wahyuni, A. S., Vimonsatit, V., & Nikraz, H. (2013). *Effective stiffness of reinforced concrete section with lightweight blocks infill*. 381–384.

THESIS

Djeukoua Nathou. G. L. (2018). *Comparative analysis of seismic protection system. (MasterThesis).* National Advanced School of Public Works.

Bile Bile Abessolo. (2019). *FEM analysis applied to the study of joints in RC structures. (Master Thesis).* National Advanced School of Public Works.

Biloa Bidjanga. *Numerical numbering of composite structures: case of timber-concrete slab. (Master Thesis).* National Advanced School of Public Works.

Moustapha Houseini. (2019). *Influence of foundation type on the seismic response of buildings considering soil-structure interaction. (Master Thesis).* National Advanced School of Public Works.

WEBOGRAPHY

Wikipedia.org. (2020, january 19). effetcts https://civilread.com

ANNEX

Tables for the methodology

Table A1. Categories of use of the building (EC 1 Part 1)

Category	Specific Use	Example
A	Areas for domestic and residential activities	Rooms in residential buildings and houses; bedrooms and wards in hospitals; bedrooms in hotels and hostels kitchens and toilets.
B	Office areas	
C	Areas where people may congregate (with the exception of areas defined under category A, B, and D[1)])	**C1**: Areas with tables, etc. e.g. areas in schools, cafés, restaurants, dining halls, reading rooms, receptions. **C2**: Areas with fixed seats, e.g. areas in churches, theatres or cinemas, conference rooms, lecture halls, assembly halls, waiting rooms, railway waiting rooms. **C3:** Areas without obstacles for moving people, e.g. areas in museums, exhibition rooms, etc. and access areas in public and administration buildings, hotels, hospitals, railway station forecourts. **C4**: Areas with possible physical activities, e.g. dance halls, gymnastic rooms, stages. **C5**: Areas susceptible to large crowds, e.g. in buildings for public events like concert halls, sports halls including stands, terraces and access areas and railway platforms.
D	Shopping areas	**D1:** Areas in general retail shops **D2**: Areas in department stores
[1)] Attention is drawn to 6.3.1.1(2), in particular for C4 and C5. See EN 1990 when dynamic effects need to be considered. For Category E, see Table 6.3		
NOTE 1 Depending on their anticipated uses, areas likely to be categorised as C2, C3, C4 may be categorised as C5 by decision of the client and/or National annex. NOTE 2 The National annex may provide sub categories to A, B, C1 to C5, D1 and D2 NOTE 3 See 6.3.2 for storage or industrial activity		

Table A2. Imposed loads on floors, balconies and stairs in buildings (EC 1 Part 1)

Categories of loaded areas	q_k [kN/m²]	Q_k [kN]
Category A		
- Floors	1,5 to2,0	2,0 to 3,0
- Stairs	2,0 to4,0	2,0 to 4,0
- Balconies	2,5 to 4,0	2,0 to 3,0
Category B	2,0 to 3,0	1,5 to 4,5
Category C		
- C1	2,0 to 3,0	3,0 to 4,0
- C2	3,0 to 4,0	2,5 to 7,0 (4,0)
- C3	3,0 to 5,0	4,0 to 7,0
- C4	4,5 to 5,0	3,5 to 7,0
- C5	5,0 to 7,5	3,5 to 4,5
category D		
- D1	4,0 to 5,0	3,5 to 7,0 (4,0)
- D2	4,0 to 5,0	3,5 to 7,0

Table A3. Ground types description (EC 8 Part 1)

Ground type	Description of stratigraphic profile	Parameters		
		$v_{s,30}$ (m/s)	N_{SPT} (blows/30cm)	c_u (kPa)
A	Rock or other rock-like geological formation, including at most 5 m of weaker material at the surface.	> 800	–	–
B	Deposits of very dense sand, gravel, or very stiff clay, at least several tens of metres in thickness, characterised by a gradual increase of mechanical properties with depth.	360 – 800	> 50	> 250
C	Deep deposits of dense or medium-dense sand, gravel or stiff clay with thickness from several tens to many hundreds of metres.	180 – 360	15 - 50	70 - 250
D	Deposits of loose-to-medium cohesionless soil (with or without some soft cohesive layers), or of predominantly soft-to-firm cohesive soil.	< 180	< 15	< 70
E	A soil profile consisting of a surface alluvium layer with v_s values of type C or D and thickness varying between about 5 m and 20 m, underlain by stiffer material with v_s > 800 m/s.			
S_1	Deposits consisting, or containing a layer at least 10 m thick, of soft clays/silts with a high plasticity index (PI > 40) and high water content	< 100 (indicative)	–	10 - 20
S_2	Deposits of liquefiable soils, of sensitive clays, or any other soil profile not included in types A – E or S_1			

Table A4. Importance classes for buildings (EN 1998-1 2004)

Importance Class	Buildings	Recommended value
I	Buildings of minor importance for public safety, eg. agricultural buildings, etc.	0.8
II	Ordinary buildings, not belonging in the other categories	1
III	Building whose seismic resistance is of importance in view of the consequences associated with a collapse, eg. Schools, assembly house, cultural institutions, etc.	1.2
IV	Buildings whose integrity during earthquakes is of vital importance for civil protection, eg. Hospitals, fire station, power plants, etc.	1.4

Table A5. Values of φ for calculating ΨEi (EC 8 Part 1)

Type of variable action	Storey	φ
Categories A-C*	Roof	1,0
	Storeys with correlated occupancies	0,8
	Independently occupied storeys	0,5
Categories D-F* and Archives		1,0

Table A6. Recommended values of Ψ factors for buildings (EC8 Part 1)

Action	ψ_0	ψ_1	ψ_2
Imposed loads in buildings, category (see EN 1991-1-1)			
Category A : domestic, residential areas	0,7	0,5	0,3
Category B : office areas	0,7	0,5	0,3
Category C : congregation areas	0,7	0,7	0,6
Category D : shopping areas	0,7	0,7	0,6
Category E : storage areas	1,0	0,9	0,8
Category F : traffic area, vehicle weight ≤ 30kN	0,7	0,7	0,6
Category G : traffic area, 30kN < vehicle weight ≤ 160kN	0,7	0,5	0,3
Category H : roofs	0	0	0
Snow loads on buildings (see EN 1991-1-3)*			
Finland, Iceland, Norway, Sweden	0,70	0,50	0,20
Remainder of CEN Member States, for sites located at altitude H > 1000 m a.s.l.	0,70	0,50	0,20
Remainder of CEN Member States, for sites located at altitude H ≤ 1000 m a.s.l.	0,50	0,20	0
Wind loads on buildings (see EN 1991-1-4)	0,6	0,2	0
Temperature (non-fire) in buildings (see EN 1991-1-5)	0,6	0,5	0
NOTE The ψ values may be set by the National annex. * For countries not mentioned below, see relevant local conditions.			

Table A7. Indicative design working life (EC 0)

Design working life category	Indicative design working life (years)	Examples
1	10	Temporary structures (1)
2	10 to 25	Replaceable structural parts, e.g. gantry girders, bearings
3	15 to 30	Agricultural and similar structures
4	50	Building structures and other common structures
5	100	Monumental building structures, bridges, and other civil engineering structures
(1) Structures or parts of structures that can be dismantled with a view to being re-used should not be considered as temporary.		

Table A8.Values of Minimum cover, $C_{min,dur}$, requirements with regard to durability for reinforcement steel (EC2)

Environmental Requirement for $c_{min,dur}$ (mm)							
Structural Class	**Exposure Class according to Table 4.1**						
	X0	XC1	XC2 / XC3	XC4	XD1 / XS1	XD2 / XS2	XD3 / XS3
S1	10	10	10	15	20	25	30
S2	10	10	15	20	25	30	35
S3	10	10	20	25	30	35	40
S4	10	15	25	30	35	40	45
S5	15	20	30	35	40	45	50
S6	20	25	35	40	45	50	55

Table A9. Values of the factor K uses in deflection verification

Structural System	*K*	Concrete highly stressed $\rho = 1,5\%$	Concrete lightly stressed $\rho = 0,5\%$
Simply supported beam, one- or two-way spanning simply supported slab	1,0	14	20
End span of continuous beam or one-way continuous slab or two-way spanning slab continuous over one long side	1,3	18	26
Interior span of beam or one-way or two-way spanning slab	1,5	20	30
Slab supported on columns without beams (flat slab) (based on longer span)	1,2	17	24
Cantilever	0,4	6	8

Note 1: The values given have been chosen to be generally conservative and calculation may frequently show that thinner members are possible.
Note 2: For 2-way spanning slabs, the check should be carried out on the basis of the shorter span. For flat slabs the longer span should be taken.
Note 3: The limits given for flat slabs correspond to a less severe limitation than a mid-span deflection of span/250 relative to the columns. Experience has shown this to be satisfactory.

Table A10. Values of subgrade modulus for different soil types (Forni, sd)

	Nature du sol	*C* (t/m³)
1	terrain légèrement tourbeux et marécageux	500- 1 000
2	terrain essentiellement tourbeux et marécageux	1 000- 1 500
3	sable fin	1 000- 1 500
4	remblais d'humus, sable et gravier	1 000- 2 000
5	sol argileux détrempé	2 000- 3 000
6	sol argileux humide	4 000- 5 000
7	sol argileux sec	6 000- 8 000
8	sol argileux très sec	10 000
9	terrain compacté contenant de l'humus du sable et peu de pierres	8 000-10 000
10	même nature que ci-dessus avec beaucoup de pierres	10 000-12 000
11	gravier fin et beaucoup de sable fin	8 000-10 000
12	gravier moyen et sable fin	10 000-12 000
13	gravier moyen et sable grossier	12 000-15 000
14	gros gravier et sable grossier	15 000-20 000
15	gros gravier et peu de sable	15 000-20 000
16	gros gravier et peu de sable mais très compacté	20 000-25 000